US Army Corps of Engineers

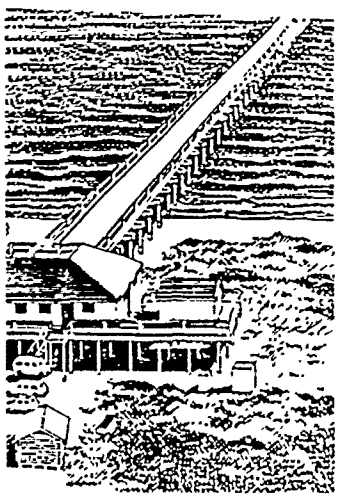

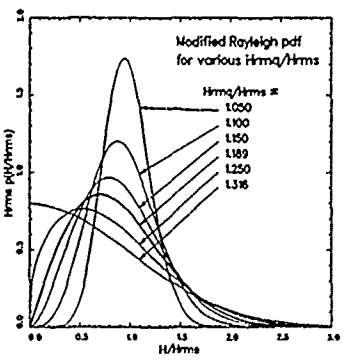

COASTAL ENGINEERING RESEARCH CENTER

TECHNICAL REPORT CERC-91-6

USE OF THEORETICAL WAVE HEIGHT DISTRIBUTIONS IN DIRECTIONAL SEAS

by

Charles E. Long

Coastal Engineering Research Center

DEPARTMENT OF THE ARMY
Waterways Experiment Station, Corps of Engineers
3909 Halls Ferry Road, Vicksburg, Mississippi 39180-6199

US ARMY ENGINEER WATERWAYS EXPERIMENT STATION

August 1991

Final Report

Prepared for DEPARTMENT OF THE ARMY
US Army Corps of Engineers
Washington, DC 20314-1000

Under Civil Works Research Work Unit 32484

Destroy this report when no longer needed. Do not return it to the originator.

The findings in this report are not to be construed as an official Department of the Army position unless so designated by other authorized documents.

The contents of this report are not to be used for advertising, publication, or promotional purposes. Citation of trade names does not constitute an official endorsement or approval of the use of such commercial products.

REPORT DOCUMENTATION PAGE

Form Approved
OMB No. 0704-0188

1. AGENCY USE ONLY *(Leave blank)*	2. REPORT DATE	3. REPORT TYPE AND DATES COVERED
	August 1991	Final report

4. TITLE AND SUBTITLE
Use of Theoretical Wave Height Distributions in Directional Seas

5. FUNDING NUMBERS
Civil Works Research Work Unit 32484

6. AUTHOR(S)
Charles E. Long

7. PERFORMING ORGANIZATION NAME(S) AND ADDRESS(ES)
USAE Waterways Experiment Station
Coastal Engineering Research Center
3909 Halls Ferry Road
Vicksburg, MS 39180-6199

8. PERFORMING ORGANIZATION REPORT NUMBER
Technical Report CERC-91-6

9. SPONSORING/MONITORING AGENCY NAME(S) AND ADDRESS(ES)
US Army Corps of Engineers
Washington, DC 20314-1000

10. SPONSORING/MONITORING AGENCY REPORT NUMBER

11. SUPPLEMENTARY NOTES
Available from National Technical Information Service, 5285 Port Royal Road, Springfield, VA 22161

12a. DISTRIBUTION/AVAILABILITY STATEMENT
Approved for public release; distribution unlimited

12b. DISTRIBUTION CODE

13. ABSTRACT *(Maximum 200 words)*

Knowledge of total water levels, of which the heights of wind waves are an important part, is critical to the successful design of coastal shore protection projects. In this report, a preliminary examination is made of the behavior of two wave height distribution models using a small but diverse set of test data. Data are derived from a Waverider buoy deployed near the 8-m-depth contour about 1 km offshore the Coastal Engineering Research Center's Field Research Facility near Duck, NC. Data are classified by directional characteristics derived from a high-resolution, linear array, directional wave gage also located near the 8-m contour and just north of the Waverider buoy.

The two models are the Rayleigh probability function and the Beta-Rayleigh probability function, introduced to address the problem of wave heights in shallow water. The Beta-Rayleigh model was used in three forms: a deepwater asymptotic form, the formally derived form, and a finice-depth form

(Continued)

14. SUBJECT TERMS		15. NUMBER OF PAGES
Probability models Wave heights	Wind waves	107
		16. PRICE CODE

17. SECURITY CLASSIFICATION OF REPORT	18. SECURITY CLASSIFICATION OF THIS PAGE	19. SECURITY CLASSIFICATION OF ABSTRACT	20. LIMITATION OF ABSTRACT
UNCLASSIFIED	UNCLASSIFIED		

13. (Concluded).

in which the governing parameters are estimated from the spectrally based characteristic wave height and peak period. Models were tested under the constraints that they be computed exactly as published and with no allowance to adjust parameters to reduce differences with observations.

In comparisons of overall wave height distributions, average wave height and averages of the highest one-third, one-tenth, one-twentieth, and one-hundredth waves, the deepwater Beta-Rayleigh model performed best but just slightly better than the formal, shallow-water form. The Rayleigh model was found to overpredict slightly the wave heights on the high-wave tail of the distribution, as has been observed before. The estimated Beta-Rayleigh model performed worst, primarily due to a high sensitivity of the formulation to differences of order 10 percent in estimated parameters. All models were comparable in estimating maximum wave height, given the sampling uncertainty of measured maximum wave height from a single record. No particular sensitivity of measured wave height distributions to sea state directional character was detected; the primary influence seemed to be overall energy level and the character of frequency distributions of energy.

In spite of the stringent requirements of the tests, all models performed remarkably well. Some recommendations for additional research include: effects of filtering a time series on estimates of observed wave heights, effects of different breaking wave height models on behavior of the Beta-Rayleigh model, and the need to improve formulae relating frequency domain parameters to wave height distribution parameters.

PREFACE

The study reported herein was authorized by Headquarters, US Army Corps of Engineers (HQUSACE), Coastal Engineering Area of Civil Works Research and Development. Work was performed under Civil Works Research Work Unit 32484, "Directionality of Waves in Shallow Water," Coastal Flooding Program, at the Coastal Engineering Research Center (CERC) of the US Army Engineer Waterways Experiment Station (WES). Technical Monitors were Messrs. John H. Lockhart, Jr.; John G. Housley; James E. Crews; and Robert H. Campbell, HQUSACE. Dr. C. Linwood Vincent was the CERC Program Manager

The study was conducted by Dr. Charles E. Long at the WES\CERC Field Research Facility (FRF) in Duck, NC, in response to questions concerning the ease of application and accuracy of results of various wave height distribution models, especially in light of the recent ability to observe detailed directional characteristics of shallow-water sea states at the FRF.

The report was prepared under the direct supervision of Mr. William A. Birkemeier, Chief, FRF, and Mr. Thomas W. Richardson, Chief, Engineering Development Division, and under the general supervision of Mr. Charles C. Calhoun, Jr., and Dr. James R. Houston, Assistant Chief and Chief, CERC, respectively.

The high-quality data used in this report would not have been possible without the physical maintenance of the Waverider and linear array gages by the FRF dive team, consisting of Messrs. Birkemeier, Michael W. Leffler, H. Carl Miller, Eugene W. Bichner, and Brian L. Scarborough; calibration maintenance by Messrs. Kent K. Hathaway (currently) and William E. Grogg (formerly) of the FRF; and data acquisition, monitoring, and storage by Mr. Clifford F. Baron of the FRF. This report was edited by Ms. Lee T. Byrne, Information Technology Laboratory, WES.

Commander and Director of WES during publication of this report was COL Larry B. Fulton, EN. Dr. Robert W. Whalin was Technical Director.

CONTENTS

USE OF THEORETICAL WAVE HEIGHT DISTRIBUTIONS IN DIRECTIONAL SEAS

PART I: INTRODUCTION

1. Knowledge of water levels, especially the extreme water levels that occur during high energy events (such as storms and hurricanes), is critical to the successful design of coastal shore protection projects. Nearshore, oceanic water levels can vary because of processes such as tides, storm surges, and ocean surface waves in the so-called wind-wave frequency band (roughly 0.04 to 0.35 Hz). Wind waves do significant amounts of work on the coastal boundary. Water levels resulting from large wind waves contribute to the extremes of beach and structural runup and to the potential for overtopping and subsequent flooding behind coastal defenses.

2. A reasonably successful method of describing water levels in a way that coordinates well with coastal engineering design is statistical. That is, a probability is assigned to water levels induced by wind waves in a given sea state (which is itself a statistical description of the coastal environment over times long compared with typical wind-wave periods but short compared with tidal periods and storm durations). From a collection of these (derived either empirically from historic data or in conjunction with a well-designed mathematical model), a probability of extreme water levels expected over the life of a structure can be computed. The structure can then be designed to tolerate these extreme conditions and, logically, all lesser conditions.

3. Clearly, an important facet in this procedure is the definition used for the probability of wave-induced water levels. A frequently used function is the *wave height distribution*. In the form of a *probability density function* (pdf*), this gives the probability that a randomly chosen wave height will fall within a small range about a specified wave height. Here, a *wave height* is defined as the vertical separation of a wave crest and its following

---

* For convenience, symbols and abbreviations are listed in the Notation (Appendix E).

trough as observed at a fixed horizontal location*. Once a pdf is specified, the rules of statistical theory allow many important properties of a wave field (in a particular sea state) to be estimated. These include mean wave height, root-mean-square (RMS) wave height, average height of a certain fraction of the highest waves, and the expected largest wave height.

4. The most efficient way to specify a wave height distribution is with a mathematical model of the appropriate pdf. Models can be used to relate conditions from different coastal sites (by classifying large numbers of observations or sea states with a few parameters), can usually be readily exercised to make a particular computation (as compared with searching through large numbers of observations), and can be incorporated in broader models (which include effects of storms and tides) that describe waves in a probabilistic way. The search is then to find a mathematical model of wave height distributions sufficiently accurate for consideration in coastal structural design.

5. One of the earliest and most widely used models is the *Rayleigh pdf*, introduced by Longuet-Higgins (1952). It was derived based on the assumptions that the sea surface is composed of a large number of linear wave components arising from a narrow band of frequencies. It is attractive because it is derived rationally and has only one parameter, the RMS wave height. Once this parameter is set, all other properties of the wave height distribution are fixed. A comparison of this model with a large set of observations is described in the Shore Protection Manual (SPM) (1984). Unfortunately, that tome recommends modifying both the number of waves and the RMS wave height from a wave record in order to minimize differences between the model and data. The SPM (1984) indicates that once these adjustments are made, the model still differs from the observations by 10 to 15 percent in the low-probability but high-wave-height tail of the distribution that is important for estimating extreme conditions. This result suggests that the data, the model, or both are not representative of real ocean conditions to within the above-indicated percentage.

6. In defense of the Rayleigh distribution, Longuet-Higgins (1980) cites favorable comparisons of that distribution with data presented by Earle (1975). He goes on to indicate how the model agrees quite favorably with data

---

* Determined from a time series record by up-crossing analysis.

presented by Forristall (1978) when some effects of finite wave heights are taken into consideration. The crux of that discussion was that Forristall's data were normalized by the zeroth moment of the sea-surface spectrum and not the RMS wave height. In linear wave theory, there is a theoretical relationship between the two. This relationship is changed slightly under the nonlinear conditions considered by Longuet-Higgins (1980).

7. This variation suggests an important consideration in the application of a theoretical wave height distribution to data that may have been processed so as to determine one set of parameters, but not the RMS wave height (or any other parameter), which would be used directly in a wave height distribution model. Such a situation could occur with a wave gage that had internal data processing capability and computed and stored only the smoothed wave frequency spectrum but not the RMS wave height (a time domain parameter). The adequacy of a model is subject then to two tests: first is the adequacy of the basic model when primary model parameters are used and second is the adequacy of relationships between primary and measured parameters.

8. The finite wave heights addressed by Longuet-Higgins (1980) could arise during the shoaling of low-amplitude, deepwater waves approaching a coast. Because waves tend to steepen on shoaling, such waves would tend to evolve larger amplitudes relative to their wavelengths than in deep water and thereby be more subject to nonlinear effects. A further consequence of shoaling is the eventual breaking of waves in shallow water. This is an important phenomenon for two reasons. First, it changes the wave height distribution because the largest waves break and so are eliminated from the distribution. Second, the region in which this occurs is also the region most frequently involved in coastal engineering activity. It is therefore most important to have an accurate wave height distribution model that is valid in shallow water.

9. The arguments presented by Longuet-Higgins (1980) indicated that the Rayleigh distribution is valid under mildly nonlinear conditions when the RMS wave height is used as the controlling parameter. Thornton and Guza (1983) extended the hypothesis to include highly nonlinear, actively breaking wave conditions in very shallow water. They tested this hypothesis using data from a number of sensors in water depths as shallow as 1 m in the breaker zone at Torrey Pines Beach, California. They found the model to yield very good estimates of wave height statistics, albeit with a very slight overprediction

of the wave population in the high-wave tail. This is somewhat like the result given in the SPM (1984), although under a much broader range of dynamics.

10. These results suggest that the Rayleigh pdf is a very good estimator of the properties of wave height distributions under a very broad variety of nearshore conditions. There are two potential problems with this model, however. One is its tendency to have different values on the high-wave tail than have been observed in at least two experiments. As mentioned, this tendency can be important in the estimation of extreme statistics. The second problem is related to this in that the Rayleigh model is a continuous function; i.e., there is a very small but finite probability of a wave of gigantic height in water of any depth. This hypothetical situation is not physically meaningful in shallow water where waves are known to break. Again, this is a property of the tail of the distribution that can affect estimates of extreme statistics.

11. A number of proposed models take into account a limiting height for waves in shallow water. Thornton and Guza (1983) review four models which, in varying degrees of complexity, simply truncate the basic Rayleigh pdf above some wave height identified as the breaking wave height. These models are by Collins (1970), Battjes (1972), Kuo and Kuo (1974), and Goda (1975). Although these models have the proper intent of including the effect of a limiting wave height, they do so at the expense of the shape of the high-wave tail, which is discontinuous (i.e., not smooth) in all cases. This property must have an adverse effect on estimates of extreme statistics.

12. In a somewhat more elegant approach to this problem, Hughes and Borgman (1987) have described a model derived more nearly from first principles. That is, they assumed that the wave field is composed of a large number of linear wave components from a relatively narrow range of frequencies (just as in the derivation of the Rayleigh distribution), subject to the constraints that the envelope of wave extrema not exceed a limiting value and that the resulting pdf is analytic within its constraining limits. They named the resulting function the *Beta-Rayleigh pdf* because the leading coefficient contains a Beta function (see Abramowitz and Stegun 1970) and because the function degenerates to a Rayleigh pdf under certain conditions. The mathematical description of this model is presented in Part II.

13. Hughes and Borgman (1987) tested this model against a somewhat limited data set involving photographically recorded wave staffs placed in depths as shallow as 0.5 m at Duck, NC, site of the Field Research Facility (FRF) of the US Army Engineer Waterways Experiment Station, Coastal Engineering Research Center (CERC). They found good agreement of the model with these data. However, the data sets were somewhat limited, containing only 60 to 70 waves per observation, so the statistical verity of their test is somewhat suspect. To augment their tests, additional tests have been performed using longer term data from another instrument at the FRF. The data used in these tests are described in Part III, and test results are presented in Part IV of this report.

14. As will be seen in Part II, the Beta-Rayleigh pdf has a fundamental form that degenerates to a simpler form in the case of deep water and degenerates further to a Rayleigh pdf if the wave distribution parameters have a certain relationship to each other. In an auxiliary model, Hughes and Borgman (1987) describe the governing wave height distribution parameters (time domain properties) in terms of spectral parameters (frequency domain properties) so that the model can be applied if only spectral parameters are known. Spectral parameters are often the output of numerical wave transformation models (and so relates to the question of using secondary parameters to replace primary parameters, as discussed previously). Hence, there are four different forms of the model that can be tested. Because one of the forms is the Rayleigh pdf, it is also tested in the process.

15. As part of any model test, the conditions should be sufficiently varied that model strengths or flaws become apparent. In the tests reported here, advantage was taken of the high-resolution directional wave climatology that exists at the FRF (Long and Oltman-Shay, in preparation) to isolate a small but diverse set of conditions which include small and large directional spread, unimodal and bimodal energy distributions, a range of frequency spreads, and a range of total energy levels before, during, and after a storm.

16. The test consists of comparing observed wave height distributions with each of the four model forms. Because this is a test of the applicability of these models, the test is constrained to use the models exactly as published and to use observed parameters as they are found. That is (SPM procedure notwithstanding), there is to be no fitting of model parameters to improve the comparisons. The intent here is to determine where, if at all,

there may be problems with any of these models in straight application. It should be noted that the number of test cases is small; the results given here should not be considered comprehensive but rather indicative of model viability.

PART II: MODEL DEFINITIONS

Basic Statistical Relationships

17. The models to be tested are all defined as probability density functions which will be denoted by the symbol $p(H)$ in general and where subscripts after the p will distinguish the different models. The variable H is a specified wave height. The function $p(H)$ has units of inverse length such that, when multiplied by an incremental range of height dH, the resulting expression $p(H)\,dH$ is dimensionless and gives the probability that a randomly chosen wave height (denoted by $\hat{H}$) lies between the heights H and $H + dH$. This can be written as

$$p(H)\,dH = \text{Prob}[H < \hat{H} < (H + dH)] \tag{1}$$

where Prob means *the probability that.*

18. If a number of terms like Equation 1 are summed together over the range between some specified height H_1 and another height H_2, the integral takes on the meaning

$$\int_{H_1}^{H_2} p(x)\,dx = \text{Prob}[H_1 < \hat{H} < H_2] \tag{2}$$

where x is a dummy integration variable. In particular, the *cumulative probability function* $P(H)$ is given by

$$P(H) = \int_0^H p(x)\,dx$$

$$= \text{Prob}[\hat{H} < H] \tag{3}$$

and means the probability that a randomly chosen wave height is less than the specific height H. Note that $P(\infty) = 1$ because all wave heights are less than infinitely high. The complement of the cumulative probability, called

the *exceedence probability* $Q(H)$, is simply the probability that a random wave height is greater than the specified height H. The exceedence probability can be computed from either

$$Q(H) = 1 - P(H)$$

$$= \text{Prob}[\hat{H} > H] \tag{4}$$

if $P(H)$ is known, or from

$$Q(H) = \int_H^\infty p(x)\, dx \tag{5}$$

where $Q(0) = 1$; i.e., any wave exceeds zero height.

19. Using the theory of statistics, other properties of a wave height distribution can be found. For instance, the *mode*, or most probable wave height, is determined from the maximum of $p(H)$. The *mean*, or average wave height, is determined from the integral of the product $H\, p(H)$ over all possible wave heights. In the test descriptions that follow, formulae will be given for the statistical properties used. The essential point here is that all are derived from a pdf.

Rayleigh Probability Density

20. As described by Longuet-Higgins (1952), the Rayleigh pdf is defined by

$$p_R(H) = \frac{2H}{H_{rms}^2}\, e^{-(H/H_{rms})^2} \tag{6}$$

where the subscript R identifies the pdf as Rayleigh. The symbol H_{rms} is the *root-mean-square wave height*. It is a parameter of the pdf and must be specified separately from the pdf. It can be computed from a set of observed wave heights by the expression

$$H_{rms} = \left[\frac{1}{N} \sum_{n=1}^{N} H_n^2\right]^{1/2} \tag{7}$$

where N is the number of observed waves and H_n is the height of the n^{th} wave.

21. The pdf given by Equation 6 has dimensions of inverse length. It is convenient to transform it to a dimensionless form so it can be compared with other density functions. The only scaling parameter is H_{rms} ; so, if the pdf is multiplied by H_{rms} and all wave heights are divided by H_{rms} , a dimensionless form of the Rayleigh pdf is

$$H_{rms}\ p_R\left(\frac{H}{H_{rms}}\right) = 2\ \frac{H}{H_{rms}}\ e^{-(H/H_{rms})^2} \tag{8}$$

A sketch of the shape of this function is shown as the bold curve in the upper panel of Figure 1.

22. Because of its simple mathematical definition, the Rayleigh cumulative probability function in dimensionless form $P_R(H/H_{rms})$ can be found by integrating Equation 8 with respect to H/H_{rms} over the limits from zero to H/H_{rms} . The result is simply

$$P_R\left(\frac{H}{H_{rms}}\right) = e^{-(H/H_{rms})^2} \tag{9}$$

and, from Equation 4, the corresponding Rayleigh exceedence probability is

$$Q_R\left(\frac{H}{H_{rms}}\right) = 1 - e^{-(H/H_{rms})^2} \tag{10}$$

23. In other computations using the Rayleigh pdf, such as the computation of moments involving the integration of the product of the pdf with wave height raised to some power, there is no simple analytic integral. In such cases, numerical integration can be performed using the simple trapezoid rule with increments of $\Delta H/H_{rms}$ equal to 0.001 . Where an integration to infinity is required, it has been found that a value of $H/H_{rms} = 6$ is sufficient for the purposes of this report. Comparison of such results agrees to at least the three decimal places reported by Longuet-Higgins (1952). It is noted that all integrals of the probability functions described below must be

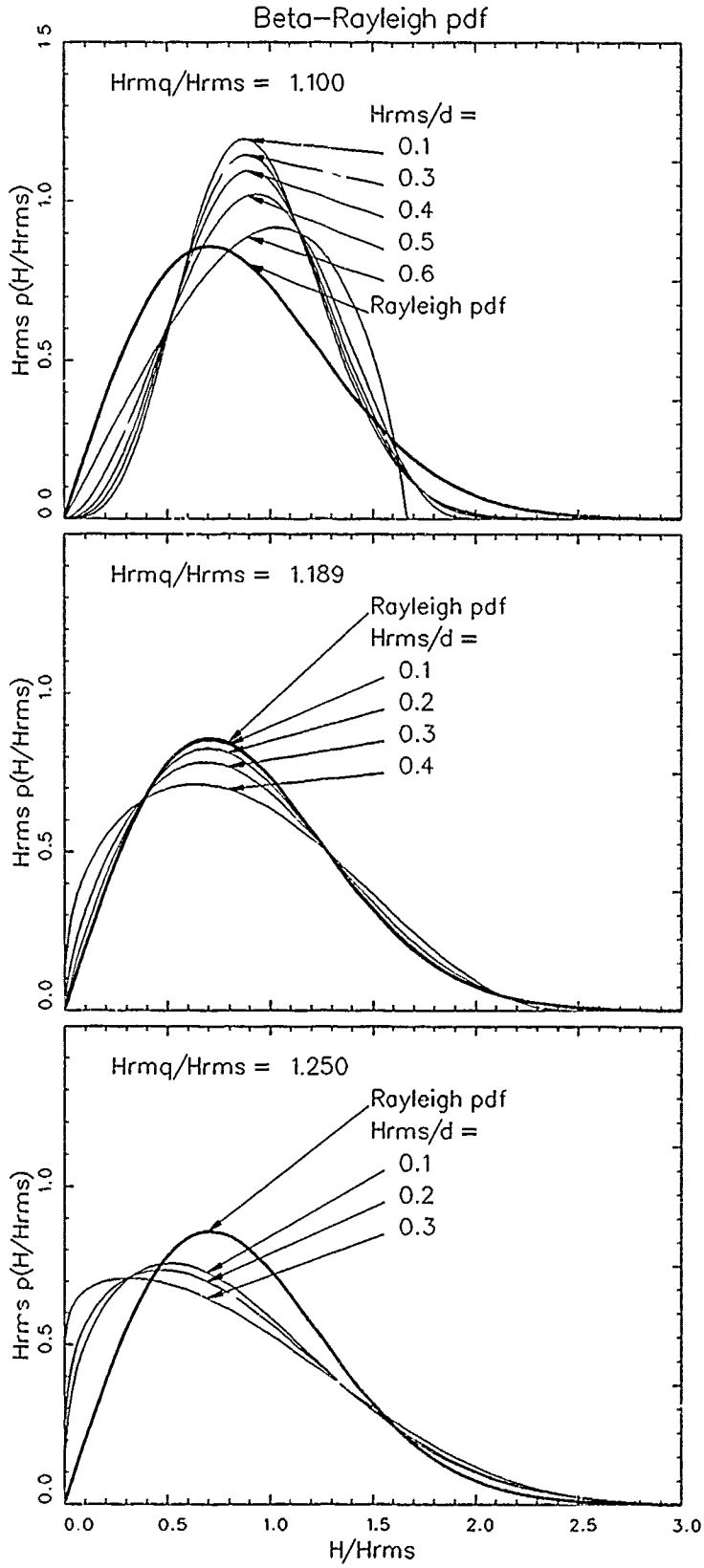

Figure 1. Examples of Beta-Rayleigh probability densities at various parameter settings

done numerically. In some of the algorithms employed by this author, it was found that small differences between large numbers were to be accumulated such that precision to at least 10 places was necessary to avoid rounding errors. Such precision is available on most mainframe computers.

Beta-Rayleigh Distribution

24. The Beta-Rayleigh pdf introduced by Hughes and Borgman (1987) has, as one of three parameters, a dependence on breaking wave height which places an absolute limit on the extreme wave height. They recommended that, as an elementary initial model, the breaking wave height be set equal to water depth d. As a result, the equation used in this report for the Beta-Rayleigh pdf is the basic definition given by Hughes and Borgman (1987) with the substitution of depth d for breaking wave height. In dimensionless form, this is

$$H_{rms}\, p_{BR}\left(\frac{H}{H_{rms}}\right) = \begin{cases} 2\,\dfrac{\Gamma(a+b)}{\Gamma(a)\Gamma(b)}\left(\dfrac{H_{rms}}{d}\right)^{2a}\left(\dfrac{H}{H_{rms}}\right)^{2a-1}\left[1-\left(\dfrac{H_{rms}}{d}\right)^{2}\left(\dfrac{H}{H_{rms}}\right)^{2}\right]^{b-1} & \text{for } H < d \\ 0 & \text{for } H > d \end{cases} \tag{11}$$

where Γ is the gamma function (see Abramowitz and Stegun 1970), the parameters a and b are given by

$$a = \left(\frac{H_{rms}}{d}\right)^{2}\left[\frac{(H_{rms}/d)^{2} - (H_{rmq}/d)^{4}}{(H_{rmq}/d)^{4} - (H_{rms}/d)^{4}}\right] \tag{12}$$

$$b = \left[1 - \left(\frac{H_{rms}}{d}\right)^{2}\right]\left[\frac{(H_{rms}/d)^{2} - (H_{rmq}/d)^{4}}{(H_{rmq}/d)^{4} - (H_{rms}/d)^{4}}\right] \tag{13}$$

and the symbol H_{rmq} stands for *root-mean-quad wave height*. It is a basic parameter of this pdf and can be determined from a set of N observed wave heights H_n from the expression

$$H_{rmq} = \left[\frac{1}{N}\sum_{n=1}^{N} H_n^4\right]^{1/4} \tag{14}$$

It should be noted that Hughes and Borgman (1987) defined H_{rmq} using a square root instead of a fourth root on the right side of Equation 14. This seems quite confusing because it results in a symbol that looks as if it should have dimensions of length when it actually has dimensions of length squared. The notation has been changed in the present report to avoid this confusion. The H_{rmq} of Equation 14 has dimensions of length as one would expect. This is only a modification of notation, not of the basic model. The effect is that one would use the square root of their H_{rmq} in the definitions above (Equations 12 and 13) for the parameters a and b .

25. Examination of the defining Equations 11, 12, 13, and 14 shows that the shape of the Beta-Rayleigh pdf is determined by three parameters: H_{rms} , H_{rmq} , and d . When the wave height and the pdf are both made dimensionless with H_{rms} , the resulting shape is dictated by two dimensionless groups of these parameters: H_{rms}/d and H_{rmq}/d . The second of these can also be written as $(H_{rmq}/H_{rms})(H_{rms}/d)$ so that an equivalent set of two dimensionless groups is H_{rms}/d and H_{rmq}/H_{rms} .

26. Figure 1 illustrates some of the variety of shapes that can be assumed by the Beta-Rayleigh pdf for various values of these two dimensionless groups. Each subplot is distinguished by a value of H_{rmq}/H_{rms} . Note that this ratio can never be less than one. If it equals one, then $H_{rmq} = H_{rms}$ and all wave heights must be equal to each other and to H_{rms} . Hence, one would expect the pdf to become spikelike for values of H/H_{rms} near 1.0 . This tendency is seen in the upper panel of Figure 1. A Rayleigh pdf (the bold curve) is also plotted for comparison. In this case, the Beta-Rayleigh pdf tends to a lower probability of small waves and an increased probability of waves having heights near H_{rms} .

27. In the middle panel of Figure 1, the ratio H_{rmq}/H_{rms} is given the value $2^{1/4}$ (≈ 1.189). This number has significance because it is the ratio of H_{rmq}/H_{rms} that occurs for a pure Rayleigh pdf. Here it can be seen that as depth increases relative to the wave height scale, i.e., H_{rms}/d becomes small, the Beta-Rayleigh pdf becomes asymptotic to the Rayleigh distribution. As the wave height scale becomes an appreciable fraction of the depth, the highest waves and those near the peak of the Rayleigh curve are much reduced in probability. The largest gain in probability occurs for small waves. This trend continues in the lower panel of Figure 1 where the ratio H_{rmq}/H_{rms} is greater than in the middle panel of Figure 1. This suggests a greater

disparity between large and small waves, so the pdf tends to flatten. To decay properly at large H/H_{rms}, the flattening effect must further increase the probability of small waves.

Deepwater Asymptote

28. The Beta-Rayleigh pdf is completely defined in the limit as the depth goes to infinity (in the form of the equation used here where depth has replaced the breaking wave height). The form given for this by Hughes and Borgman (1987) can be expressed nondimensionally as

$$H_{rms}\, p_{MR}\left(\frac{H}{H_{rms}}\right) = \frac{2\alpha^{\alpha}}{\Gamma(\alpha)} \left(\frac{H}{H_{rms}}\right)^{2\alpha-1} e^{-\alpha(H/H_{rms})^2} \tag{15}$$

where α is the asymptotic form of parameter a (from Equation 12) as $d \to \infty$ and is given by

$$\alpha = \frac{1}{\left(\frac{H_{rmq}}{H_{rms}}\right)^4 - 1} \tag{16}$$

The subscript MR on the pdf of Equation 15 stands for Modified Rayleigh. Hughes and Borgman (1987) refer to this pdf as a "generalized Rayleigh," which suggests that the Rayleigh pdf is a degenerate form of Equation 15 alone. While it is true that Equation 15 degenerates to the Rayleigh form, there are many other mathematical expressions which can also degenerate to the Rayleigh form, so it does not seem quite accurate to suggest that Equation 15 is the general expression. The word "modified" is used here instead.

29. Examination of Equations 15 and 16 shows that the shape of the dimensionless function is governed completely by one parameter. In Equation 15, this is α, which is uniquely determined by the ratio H_{rmq}/H_{rms} by virtue of Equation 16. This is like the Beta-Rayleigh pdf except that now there is no dependence on d.

30. Figure 2 illustrates some of the distributions possible with the Modified Rayleigh pdf for select values of the parameter H_{rmq}/H_{rms}. The bold curve is the Rayleigh pdf, which occurs when $H_{rmq}/H_{rms} = 2^{1/4}$ (≈ 1.189) and for which $\alpha = 1$. As H_{rmq}/H_{rms} takes on smaller values and approaches its

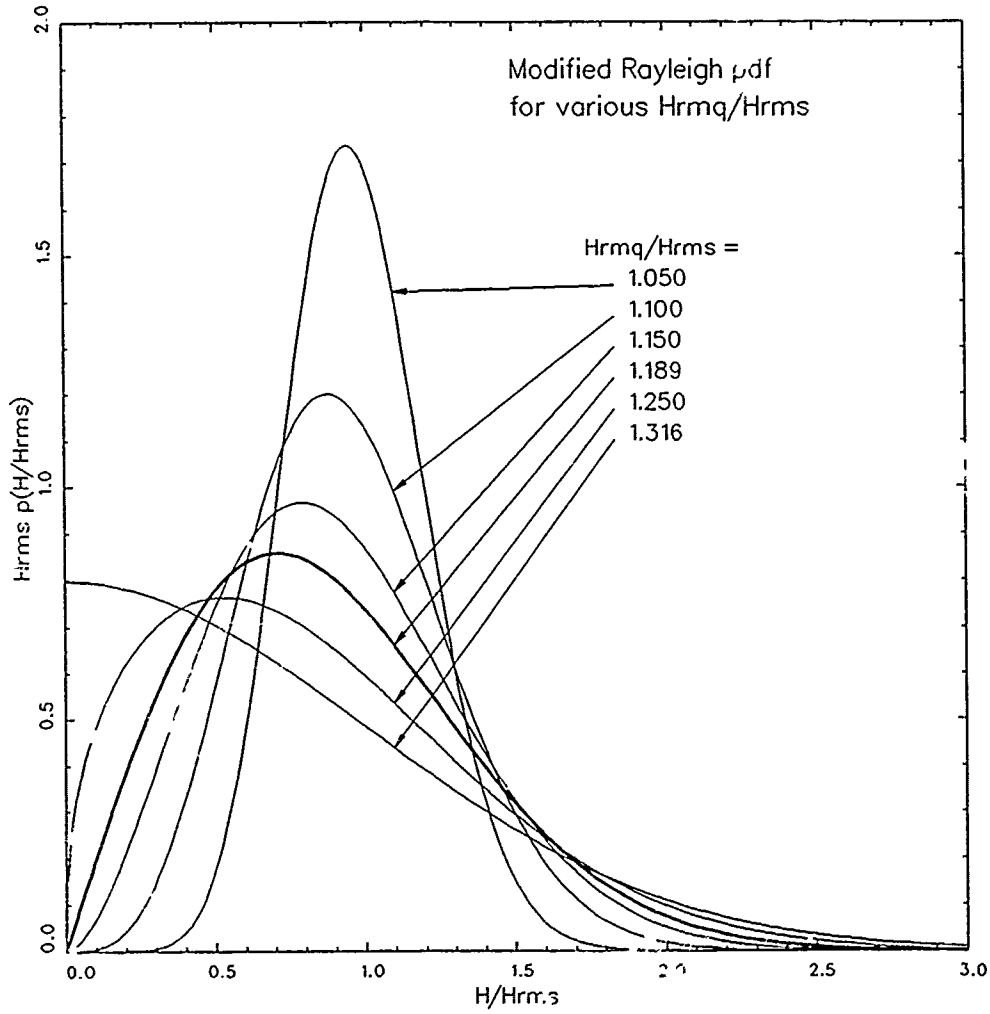

Figure 2. Examples of the modified Rayleigh probability density function

lower limiting value of unity, the pdf takes on modal values (peaks) that become nearer to $H/H_{rms} = 1$ and has reduced probabilities for low and high wave heights. This is the same behavior as mentioned previously for the Beta-Rayleigh pdf. At the limit of $H_{rmq}/H_{rms} \rightarrow 1$, the pdf becomes a spikelike function with all wave heights properly being made equal to H_{rms}.

31. As H_{rmq}/H_{rms} exceeds $2^{1/4}$, one would expect a greater disparity between large and small waves so that the distribution tends to become broader. As shown in Figure 2, there is an increase in the probability of low waves and high waves with a corresponding reduction in the probability of intermediate waves in this case. The model forces an upper limit on the ratio

H_{rmq}/H_{rms} to be less than $3^{1/4}$. At values equal to or greater than this, α becomes less than or equal to 1/2, at which point the exponent $2\alpha - 1$ in Equation 15 becomes zero or goes negative. The pdf then has a singularity at the origin, meaning the most probable wave is of zero height, a condition that does not seem realistic. The physical significance of this is not clear. If measurements indicate this limit is exceeded, the model must be rejected. This is unlikely, however, because most of the tests discussed in the introduction indicate that ocean wave height distributions are very nearly Rayleigh. This means that an improved model is not expected to be very different from Rayleigh and, in this case, that the ratio H_{rmq}/H_{rms} is not likely to be very different from $2^{1/4}$.

32. This asymptotic version of the Beta-Rayleigh model is included in the present tests as a separate model for several reasons. It is less complex, having only two governing parameters (H_{rms} and H_{rmq}) instead of the three (H_{rms}, H_{rmq} and d) of the more complete Beta-Rayleigh model. In the same sense, it has more freedom of shape than the fundamental Rayleigh pdf (which depends only on H_{rms}) and so might characterize observations better. This is not assured in the present test, however, because model parameters are set by measurements and not allowed to vary as might be done in a curve-fitting exercise. To be considered an improved model, a new theoretical curve must in fact agree better with observations. By eliminating depth dependence from and comparing the results with the full model, differences in the two versions can be clarified, and the possibility that the modified Rayleigh pdf provides comparable or better results than the Beta-Rayleigh pdf can be examined.

Parameter Estimation Model

33. The final version of the Beta-Rayleigh pdf to be tested here is one in which the parameters H_{rms} and H_{rmq} are estimated from measured, frequency-domain (i.e., spectral) parameters. This is done to see if the essential properties of a wave height distribution can be found knowing only processed spectral properties from the same sea state. Hughes and Borgman (1987) propose a preliminary set of relationships which depend on the spectrum-based characteristic wave height H_{mo}, spectral peak period T_p, and water depth d.

34. The conventional definitions of these parameters apply. That is,

$$H_{mo} = 4\ m_0^{1/2} \tag{17}$$

where m_0 is the spectral zeroth moment and where the more general spectral moment n is defined by

$$m_n = \int_{f_1}^{f_2} f^n\ S(f)\ df \tag{18}$$

where

S = sea-surface variance spectral density

f = frequency

f_1 = low frequency bound of spectral definition

f_2 = high frequency bound of spectral definition

The f_1 and f_2 frequencies are zero and infinity, respectively, in theory, but in practice are bound to less diverse values. In practice, a typical value for f_1 is about 0.04 Hz and for f_2 is about 0.35 Hz. Spectral peak period is found from $T_p = 1/f_p$ where f_p is spectral peak frequency, i.e., the frequency of the maximum of $S(f)$.

35. Based on data and results of a study by Thompson and Vincent (1985), Hughes and Borgman (1987) suggested

$$H_{rms,e} = \frac{H_{mo}}{2^{1/2}}\ e^{0.00089(d/gT_p^2)^{-0.834}} \tag{19}$$

and

$$H_{rmq,e} = \frac{H_{mo}}{2^{1/4}}\ e^{0.000049(d/gT_p^2)^{-1.208}} \tag{20}$$

where $H_{rms,e}$ is the estimated value of H_{rms} , g is gravitational acceleration, and $H_{rmq,e}$ is the estimated value of H_{rmq} . Equation 20 has been modified from that published by Hughes and Borgman (1987) to take into account the difference in definitions of H_{rmq} .

36. In applying this form of the model in the tests that follow, the estimated parameters $H_{rms,e}$ and $H_{rmq,e}$ are used everywhere that the corresponding true parameters H_{rms} and H_{rmq} would be used. This is important

because the Beta-Rayleigh pdf, as given by Equations 11, 12, and 13, is in dimensionless form with H_{rms} the normalizing parameter for the pdf and the wave heights. When the pdf or any of its derived quantities are made dimensional to compare with observations or results from other models, the scaling parameter for this version of the model is $H_{rms,e}$. Any differences between the estimated and measured parameters are then properly carried to all levels of computation and will appear in the test results.

Model Summary

37. The four probability density function models tested here consist of:

a. The Rayleigh pdf defined by Equation 8 and having H_{rms} as its single parameter.

b. The modified Rayleigh pdf defined by Equations 15 and 16, having H_{rms} and H_{rmq} as its two parameters.

c. The Beta-Rayleigh pdf defined by Equations 11, 12, and 13, having H_{rms} , H_{rmq} , and d as its three parameters.

d. The Beta-Rayleigh pdf defined by Equations 11, 12, 13, 19, and 20 with H_{mo} , T_p , and d as its three varying parameters and g its fixed (in value) fourth parameter.

Because the last two models are both Beta-Rayleigh forms, they will be distinguished in tables and graphs by listing their governing parameters. Hence, one will be referenced as Beta-Rayleigh (H_{rms} , H_{rmq} , d) and the other as Beta-Rayleigh (H_{mo} , T_p , d).

PART III: TEST DATA

Instrumentation

38. Data for the tests reported herein were taken from the measurements archive of CERC's FRF in Duck, NC. A general description of the site and the facility is given by Birkemeier et al. (1985).

39. Data from two instruments are used. One instrument is a high-resolution, linear array, directional wave gage. It consists of nine, bottom-mounted pressure sensors placed straight along a constant isobath line. It provides detailed estimates of the frequency-direction spectra of ocean-surface wind waves. A detailed description of this gage is given by Long and Oltman-Shay (in preparation). The other instrument is an ocean-surface-following buoy instrumented with vertically sensitive accelerometers. Accelerometer signals are integrated twice to provide a measure of sea-surface displacement. Called a Waverider by its manufacturer, this buoy provided the basic wave height information used in the present tests.

40. Figure 3 shows the positions of the two gages relative to each other and to the FRF research pier. Both gages are roughly 1 km offshore where the water depth is nominally 8 m. Note that this water depth is greater than the very shallow conditions sampled by other investigators as mentioned in the introduction. Active depth-induced wave breaking happens at this depth only during extreme conditions. On the other hand, this depth is considered either to be intermediate or shallow for all wind waves of interest. Hence, the effects of finite depth should become apparent. The idea is to test the different wave height distribution models in shallow water but outside the commonly defined breaker zone to determine their efficacy in that application.

41. In addition to the above test criterion, the Waverider was chosen from a set of alternative sea-surface displacement gages for two reasons. One was its proximity to the linear array directional wave gage. This lent some validity to the assumption that both gages were sampling the same wave field.

42. The other was the relative purity of its signal. The bottom-mounted pressure gages of the linear array could have been used to measure wave height distributions. However, they would be subject to errors in

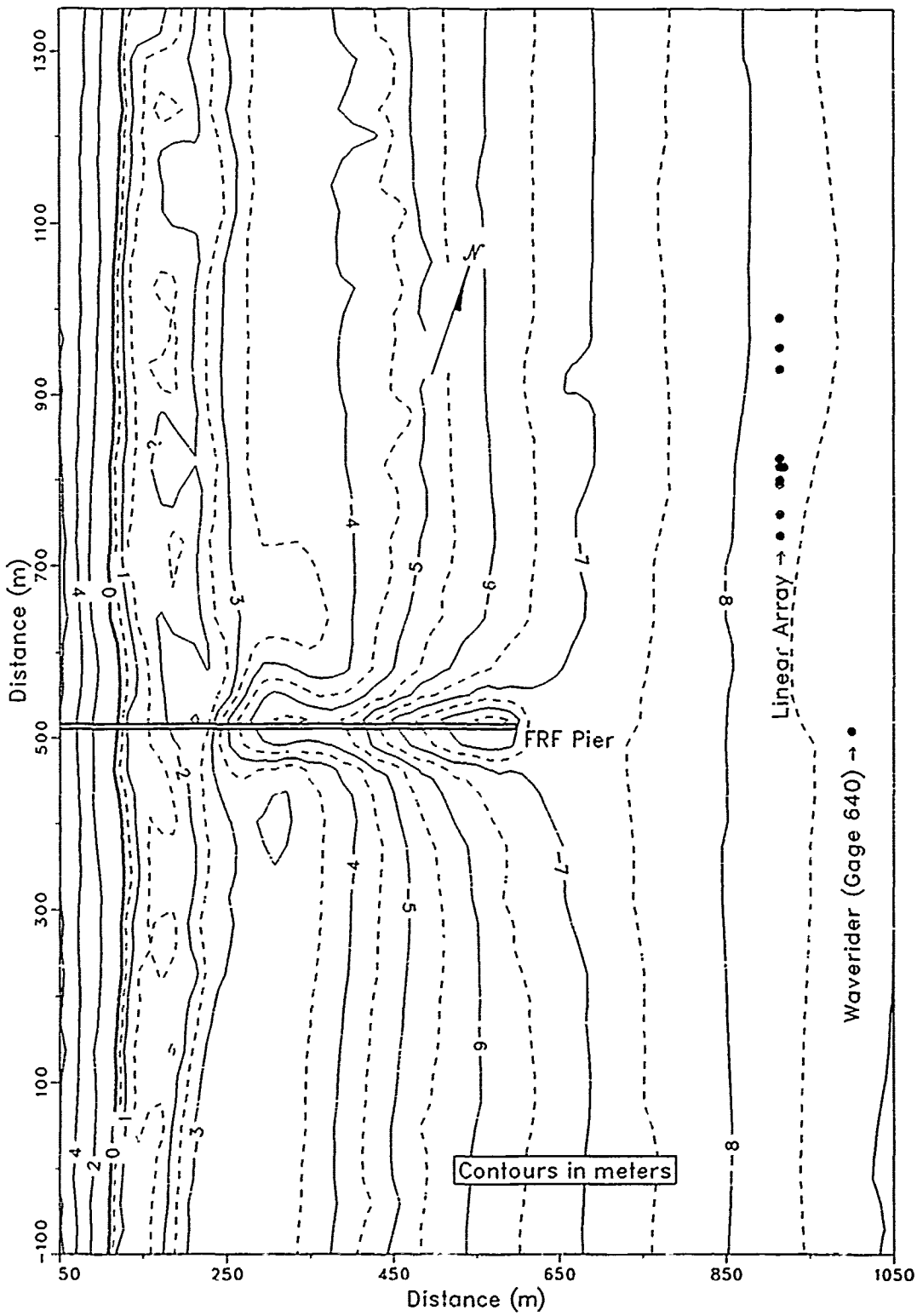

Figure 3. Field Research Facility bathymetry and location map for Waverider buoy (gage 640) and linear array directional wave gage

individual wave height measurements incurred by using the linear wave pressure response function in high wave conditions where the assumption of linearity is suspect. In addition, contributions by high-frequency waves would be effectively filtered from the signal by the water column so that wave height estimates would further be degraded. The Waverider does not have these problems. It is a surface-following buoy with a reasonably flat frequency response from about 0.06 Hz to about 0.50 Hz. It has a rather sharp roll-off below 0.06 Hz and so does not respond well to tides, storm surge periods or infra-gravity waves. As a result, its signal does not have to be detrended to find a stable datum about which to estimate wave heights. The buoy has a buoyancy resonance at a frequency of about 0.8 Hz, but this is beyond the frequency of most wind waves of interest. The manufacturer claims a minimum sea-surface displacement resolution of 0.02 m and an accuracy of ±3 percent of the signal in the flat-response portion of the spectrum.

Data Processing

43. For each of the test observations, both gages were sampled at 2 Hz for time series of 16,384 points, a duration of about 2 hr, 16 min. Time series from each of the linear array pressure gages were Fourier transformed (as an average of the transforms of 15, windowed, half-overlapping, 2,048-point segments, smoothed over 10 adjacent bands for a final resolution frequency bandwidth of about 0.01 Hz and spectral density estimates with about 150 degrees of freedom) and converted to sea-surface displacement spectra using the linear wave theory pressure response function. These results were used to estimate cross-spectral densities between every unique pair of gages for wave frequencies in the range from 0.05 to 0.32 Hz. Wave energy directional distributions were determined from cross-spectral data using the iterative maximum likelihood estimation method described by Long and Oltman-Shay (in preparation).

44. Waverider data were analyzed in four steps. First, the signal mean was removed from the time series that was considered to be a single segment of 16,384 data points. This was necessary because of an electronic bias imposed by one of the land-based signal amplifiers. The buoy itself had no mean displacement from sea-surface mean level, defined as an average over any time period longer than the buoy's low-frequency response cutoff. In the second

step, the demeaned signal was Fourier transformed to determine a raw frequency spectrum of the sea-surface variance and a set of Waverider spectral parameters (described below). The analyzed record was so long that no windowing was done; variance leakage between adjacent frequency bands would be very small. The raw spectrum was averaged over 64 bands to create a smoothed spectral density estimate with 128 degrees of freedom. Third, the raw Fourier transform was truncated at frequencies commonly considered to bound ocean wind waves, and a new set of spectral parameters was computed based on the filtered spectrum Here the low-frequency cutoff was 0.04 Hz, and the high-frequency bound was 0.35 Hz. Fourth, the filtered Fourier transform was inverted (back transformed) to provide a filtered time series. This time series was analyzed by the zero up-crossing method to isolate a set of wave heights to be used for model comparisons.

45. As noted by Thornton and Guza (1983), there is a certain amount of subjectivity in selecting pass-band limits for a filtered time series. Clearly, the filtered signal will be different as the limits change, having more or less contribution from high- and low-frequency parts of the raw signal. Curiously, this should make no difference to the statistical wave height distribution models considered here. All rely on the assumptions of a large number of wave components in random phase from a narrow range of frequencies. If these conditions are met, it must be presumed that the height distribution parameters (H_{rms} for the Rayleigh pdf and, additionally, H_{rmq} for the other three models) adjust internally to compensate for the effects of changing frequency content. The validity of this assumption was not tested here because the present task is limited to evaluation of signals that have been filtered at commonly defined cutoff frequencies. However, a test of this assumption is important and should be done in future work.

Sea State Characteristics

46. Figure 4 illustrates a frequency-direction spectrum as determined from the linear array directional wave gage. Note that direction θ is the direction measured counterclockwise from shore normal. It represents the angle from which waves are coming for an observer looking seaward. A positive angle means a wave train is arriving from the observer's left or from the northeast quadrant at the FRF.

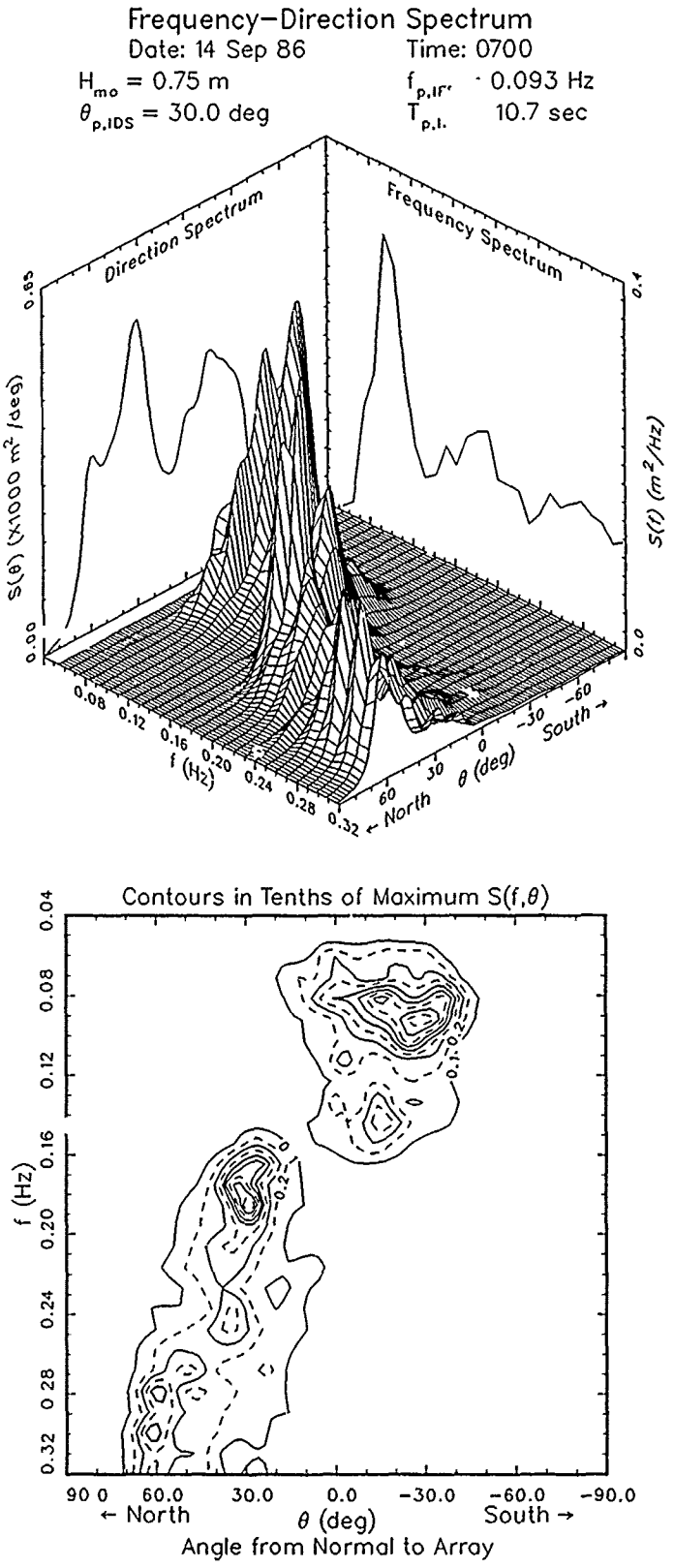

Figure 4. Frequency-direction spectrum for test Case 1

47. The panel labeled "frequency spectrum" in the upper part of Figure 4 shows the sum over all directions of the variance (energy) at each frequency. It is the variance spectrum that one would measure with any conventional, nondirectional gage. The area under this spectrum gives an estimate of the energy based wave height H_{mo} defined by Equations 17 and 18. The frequency of the maximum spectral density is the peak frequency $f_{p,IFS}$ (meaning frequency at the peak of the integrated frequency spectrum), the inverse of which gives the peak period $T_{p,IFS}$.

48. The panel labeled "direction spectrum" in the upper part of Figure 4 is the sum over all frequencies of the wave variance at each direction. Two parameters are deduced from this curve. The direction at the maximum of the direction spectrum is the peak direction $\theta_{p,IDS}$ (meaning direction at the peak of the integrated direction spectrum). A measure of the angular spread of wave energy is given by the angle subtending the central half of the area under the direction spectrum $\Delta\theta_{IDS}$, found by dividing the area into four equal parts and finding the difference between the angles that bound the middle two parts.

49. The five parameters just discussed give some indication of the frequency and direction characteristics of the sea state. They do not provide a complete description, however. This can be seen by examining the lower part of Figure 4, which is a contour plot of the frequency-direction spectrum. This figure illustrates regions in frequency and direction where there are heavy concentrations of energy. Shown are two (and possibly three) modes in the energy distribution. Counting the number, size, and location of these modes begins to make a rather lengthy list of parameters. Hence, the test data are characterized here by the five frequency and direction parameters, which are listed in Table 1, and the graphs which illustrate the frequency-direction spectra. Figure 4 is one test case. Figures for the remaining test cases are shown in Appendix A.

50. Figure 5 illustrates the frequency spectrum of the Waverider signal from the same time span that Figure 4 was derived. The spectrum is shown in two guises. The upper frame of Figure 5 shows the smoothed frequency spectrum in linear coordinates and contains a list of parameters derived from the full (unfiltered) Waverider spectrum. The lower frame shows the smoothed spectrum (as the bold line) as well as the raw spectrum in semilogarithmic coordinates.

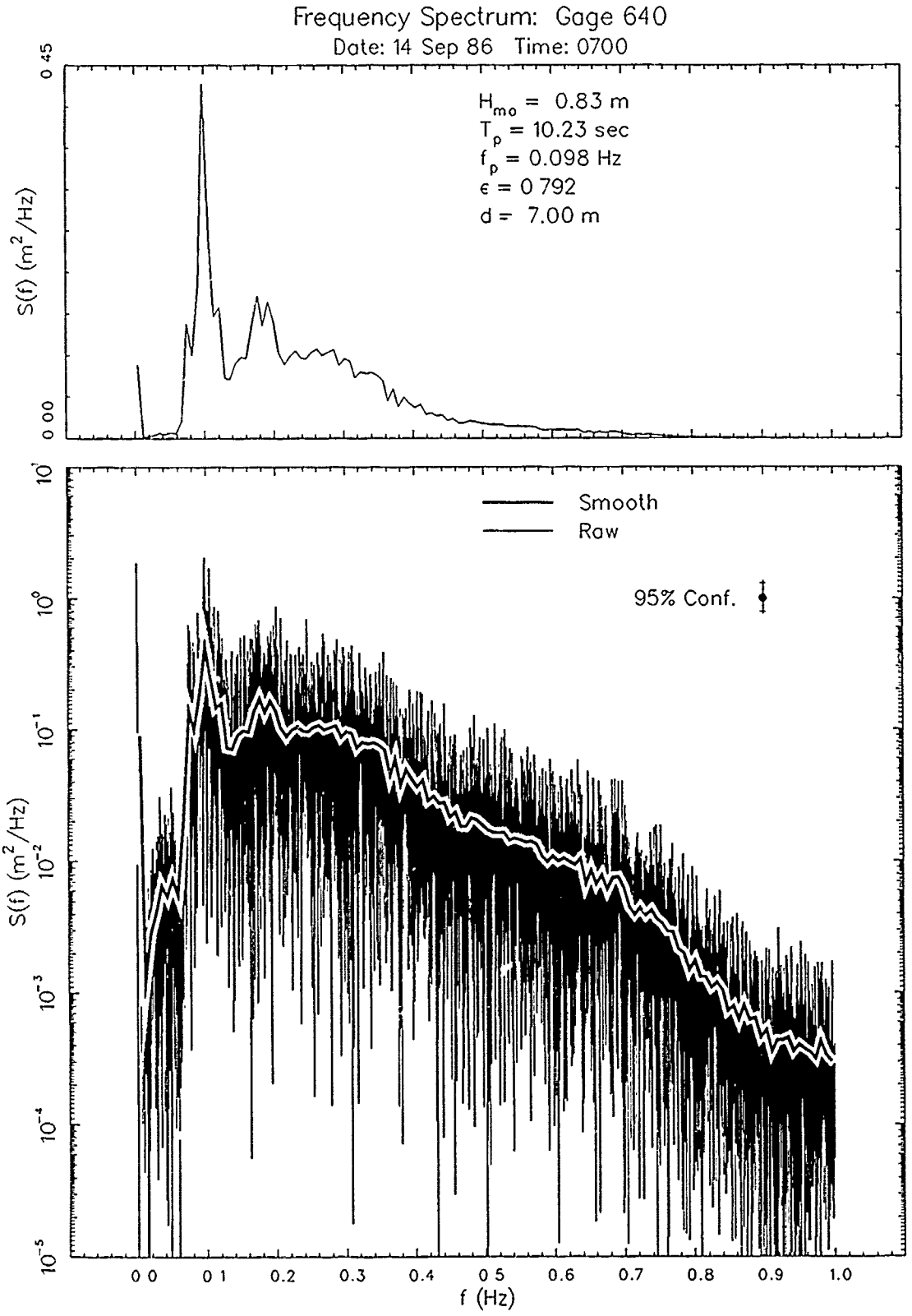

Figure 5. Waverider frequency spectrum in linear (upper panel) and log-linear (lower panel) coordinates for test Case 1

This form of display emphasizes the low energy part of the spectrum and makes clearer what is being eliminated by filtering the signal.

51. The parameters H_{mo} , T_p , and f_p in Figure 5 can be compared with the corresponding linear array parameters in Table 1 to see if there are important differences. For instance, H_{mo} is higher in Figure 5, suggesting that some energy was lost from analysis by clipping the spectrum at 0.35 Hz. Note that the shapes of the frequency spectra within the pass band from Figures 4 and 5 should (ideally) be identical and are, in fact, very similar qualitatively.

52. The parameter ϵ shown in Figure 5 is a measure of the broadness of the frequency spectrum as defined by Cartwright and Longuet-Higgins (1956). It is defined by

$$\epsilon = 1 - \frac{m_2^2}{m_0 m_4} \tag{21}$$

where the moments m_n are defined by Equation 18. A small ϵ indicates a narrow spectrum, and an ϵ near 1 indicates a broad spectrum. In Figure 5, ϵ is computed using the full spectrum from 0 to 1 Hz. In Table 1, a value is listed for ϵ based on the filtered spectrum (bounded by 0.04 and 0.35 Hz). Comparison of ϵ from Figure 5 with that from Table 1 suggests that filtering the spectrum does, in fact, make it narrower by this definition because the parameter drops from 0.792 for the full spectrum to 0.618 after filtering.

53. For completeness, plots of the Waverider spectra for the other test cases are included in Appendix B. The small spike at very low frequency which appears in several of the plots is evidently due to a cyclic drift in some electronic component of the Waverider or the data acquisition system. It is removed upon filtering the signal, and tests indicate that including it does not substantially alter the resulting wave height data.

Test Cases

54. To keep this investigation brief, a set of 11 test cases was isolated for analysis. Integral frequency and direction parameters are listed for these cases in Table 1. The primary criteria for selection were a range of directional spreads $\Delta\theta_{IDS}$ and a range of wave energies as indicated by

Table 1

Parameters of Test Data

			Frequency Domain (Source: Linear Array)							Time Domain (Source: Waverider)			
Case	Date	Time	d m	$f_{p,IFS}$ Hz	$T_{p,IFS}$ sec	$\theta_{p,IDS}$ deg	$\Delta\theta_{IDS}$ deg	ϵ	H_{mo} m	H_{rms} m	H_{rmq} m	$H_{rms,e}$ m	$H_{rmq,e}$ m
1	14 Sep 1986	0700	7.00	0.093	10.72	30.0	54.5	0.618	0.75	0.48	0.56	0.55	0.64
2	21 Sep 1986	1800	7.36	0.083	11.98	-14.0	27.8	0.759	0.52	0.33	0.40	0.37	0.42
3	15 Feb 1987	0100	7.23	0.181	5.52	14.0	48.7	0.564	0.73	0.44	0.51	0.48	0.56
4	16 Feb 1987	0100	7.35	0.191	5.24	26.0	40.6	0.489	1.70	1.03	1.20	1.09	1.28
5	16 Feb 1987	1900	8.26	0.152	6.58	12.0	48.6	0.523	2.18	1.42	1.67	1.51	1.76
6	16 Feb 1987	2200	8.14	0.142	7.04	16.0	48.6	0.563	2.64	1.71	2.02	1.81	2.11
7	17 Feb 1987	1600	7.53	0.103	9.71	-8.0	41.3	0.669	3.14	2.21	2.64	2.43	2.78
8	17 Feb 1987	1900	8.20	0.093	10.72	-8.0	45.9	0.659	2.95	1.96	2.32	2.13	2.46
9	18 Feb 1987	0100	7.67	0.093	10.72	6.0	43.8	0.687	2.44	1.64	1.94	1.82	2.08
10	18 Feb 1987	0700	8.06	0.093	10.72	-10.0	44.8	0.656	2.19	1.40	1.66	1.54	1.77
11	19 Feb 1987	1900	7.73	0.152	6.58	14.0	43.5	0.573	1.30	0.63	0.74	0.68	0.79

H_{mo} . Case 1 is an example of broad directional spread given the range of directional spreads of 20 to 60 deg normal for this site as reported by Long and Oltman-Shay (in preparation). Case 2 is an example of narrow directional spread. Both of the first two cases are of relatively low energy. Cases 3 to 11 are from a sequence of measurements before, during, and after a large storm in February 1987. Although large energy is achieved in this series (H_{mo} equal to 3.1 m in 7.5-m water depth), there is little variation in directional spread. This is consistent with the findings of Long and Oltman-Shay (in preparation), who showed that directional spreads are most commonly in the range 30 to 50 deg in high energy situations.

55. Table 1 also shows the basic governing parameters of the wave height distribution models. The parameters H_{rms} and H_{rmq} are deduced from the set of zero up-crossing wave heights by Equations 7 and 14, respectively. Parameters $H_{rms,e}$ and $H_{rmq,e}$ were found from Equations 19 and 20, respectively, using parameters H_{mo} and T_p deduced from the filtered spectra of the Waverider data rather than from the directional wave gage. It was felt that parameters for a second-order model should come from the same gage as the data used to test the model, so the Waverider H_{mo} and T_p were used in the Beta-Rayleigh model relying on those parameters. They are not listed in Table 1 because they are all within a few percentages of the corresponding parameters found from the linear array. They are given in the headers of the plotted results below, however, so the reader may verify this.

56. Curiously, the spectral width parameter ϵ does not vary a great deal over the present variety of test cases. It goes from about 0.49 to about 0.76, not a very broad range given the expected properties of the height distributions of such spectra discussed by Cartwright and Longuet-Higgins (1956). This may be a fortuitous consequence of using a small batch of test cases, a result of filtering the spectra (compare the ϵ of Table 1, based on filtered spectra, with those based on unfiltered spectra and listed in Waverider spectral plots) or, as suggested by Goda (1975), a property of spectra with a tendency to behave as f^{-5} at frequencies higher than f_p. In any case, the current tests do not stress the limits of this parameter very much.

57. On the other hand, the ratio H_{rms}/d varies by almost an order of magnitude. This is a parameter that is quite important in the formal Beta-Rayleigh pdf of Equations 11, 12, and 13 when it achieves any value of order 1. From the variables listed in Table 1, it becomes as large as about 0.3. The smallest value it assumes in the present set of tests is about 0.04. This is a sufficient range to determine if the effects of finite depth give an advantage to the Beta-Rayleigh pdf over the Rayleigh pdf in shallow water.

PART IV: TEST RESULTS

58. The four models were tested in three different ways. One test is a comparison of the exceedence probability defined by Equation 5 for the models with that deduced from the wave height data. The second test examines the ability of the four models to estimate the average of a given fraction of the highest waves. The third test compares observed and model predictions of the maximum wave height.

Wave Height Distributions

59. The most straightforward test is that which uses the model definitions directly. Because they are probability density functions, the data must be interpreted in the form of probability densities. The most common way to do this is to form a histogram from the data. If the set of N observed wave heights H_n are all normalized by H_{rms} as determined through Equation 7, the number J_u that fall in the range $u\,\Delta H/H_{rms}$ and $(u+1)\,\Delta H/H_{rms}$ can be divided by N to compute the fraction (or estimated probability) of this occurrence. In this definition, u is the index of a bin in a discrete histogram and J_u is the population of that bin. When the fraction J_u/N is divided by ΔH (an incremental wave height range arbitrarily chosen by the investigator), and multiplied by H_{rms} to make the result dimensionless, the result is an estimate of the normalized pdf for that data set.

60. An example of such a computation is shown in the upper panel of Figure 6 as the stepped curve representing the estimated pdf for test Case 1. The wave height range bins were chosen to be $\Delta H = 0.05\ H_{rms}$ as a trade-off between resolution on the abscissa and number of contributions to the bins with low densities. Superimposed on the histogram are curves representing each of the four models being tested. At the top of the figure are listed the parameters used in specifying the model curves. With the exception of depth d, which was obtained from the linear array, all parameters are determined from the Waverider time series, filtered through the frequency pass band shown.

61. What is evident in Figure 6 is that differences between the models for a given H/H_{rms} are of the same order as the scatter of the histogram

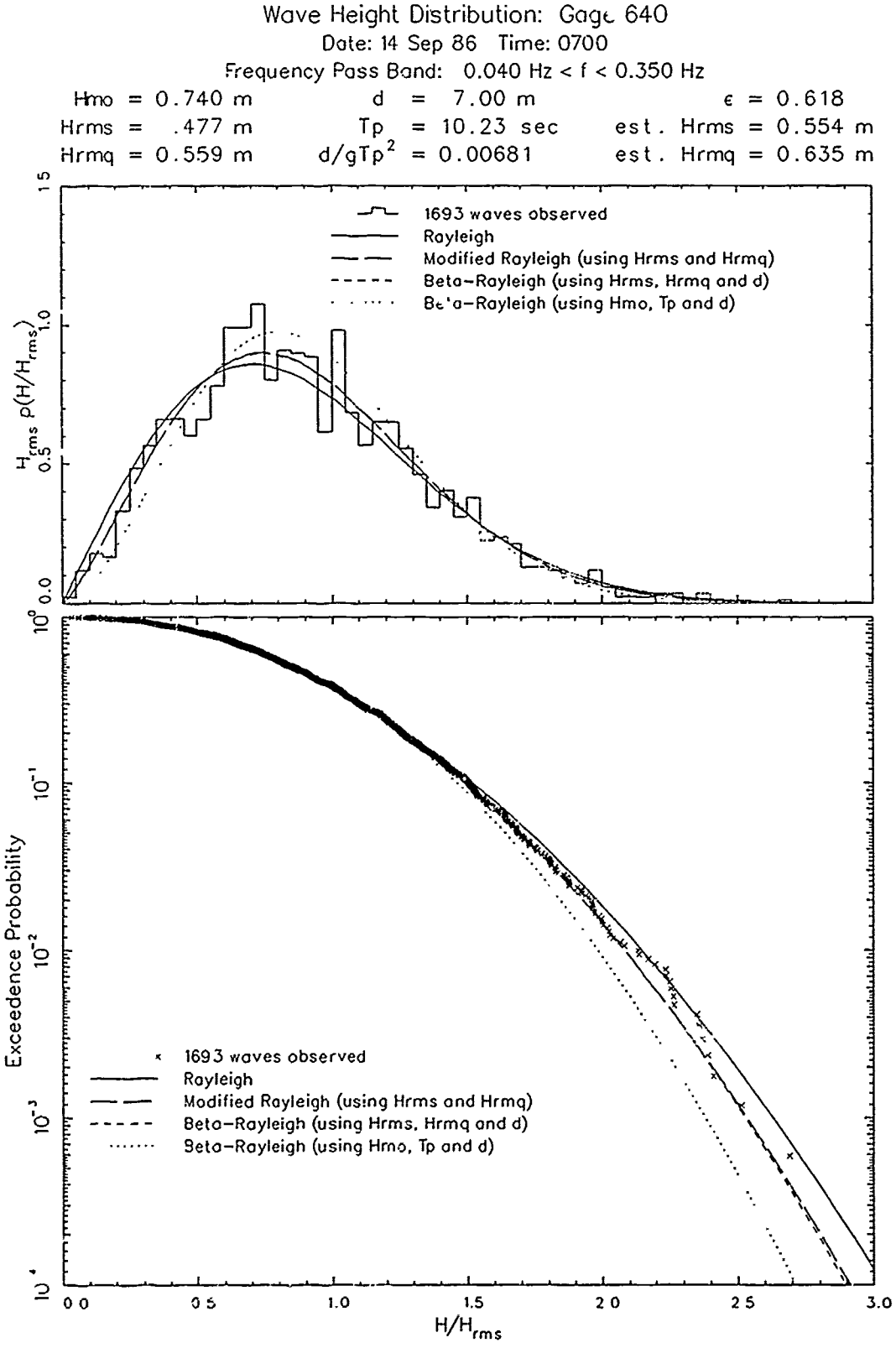

Figure 6. Comparison of observed and modeled probability densities (upper panel) and exceedence probabilities (lower panel) for test Case 1

points about what one would imagine is a smooth curve representing the data. Computing, for example, RMS differences between the histogram and the model curves would not be conclusive because the histogram is not well resolved (even with the 1,693 waves observed in this case). This is especially true in the tail of the distribution, at high H/H_{rms}, where important differences in the model curves exist. One could improve the smoothness of the histogram by increasing ΔH, but then the histogram bins become so wide that substantial variations in model values can occur across one bin. It then becomes difficult to decide where within a bin to evaluate the model for comparison with the one data point represented by that bin. Hence, even though the histogram method was employed by Hughes and Borgman (1987) and Thornton and Guza (1983) to argue for model validation, the method is rejected here. The histogram is presented for illustration only.

62. A less subjective and not much more complicated model test is to use the integral of a model pdf in the form of a cumulative probability or an exceedence probability in a comparison with corresponding data estimates. If a set of N observed, normalized wave heights H_n/H_{rms} are ordered from smallest to largest, the probability that any of the wave heights is less than the height of wave n is simply $n/(N+1)$. This procedure provides an estimate from the data of the cumulative probability distribution. The data estimate of exceedence probability $Q_d(H_n/H_{rms})$ is 1 minus the cumulative distribution at height n and is given by

$$Q_d\left(\frac{H_n}{H_{rms}}\right) = 1 - \frac{n}{N+1} \tag{22}$$

It should be noted that this method differs from the method given in the SPM (1984) in that estimates are computed here with $N + 1$ vice N. As explained by Dr. L. F. Borgman of the University of Wyoming in a lecture at CERC on 13 May 1986, use of N by itself suggests that, for the N^{th} measured wave, one has a height which cannot be exceeded. This is true for the observation set but highly unlikely for the much larger population of waves of which the measurements are but a small sample. Use of $N + 1$ provides a much better estimate of the cumulative probability of the N^{th} wave in this larger population.

63. Model estimates of the exceedence probability are found by using a defining model pdf in Equation 5, as adapted to nondimensional coordinates. The resulting exceedence probability takes the generic form

$$Q\left(\frac{H}{H_{rms}}\right) = \int_{H/H_{rms}}^{\infty} H_{rms}\ p\left(\frac{H}{H_{rms}}\right)\ d\left(\frac{H}{H_{rms}}\right) \tag{23}$$

In application, this integral can be evaluated numerically using the method described in Part II. By interpolating the discrete numerical results to find the model H/H_{rms} corresponding to data estimates $Q_d(H_n/H_{rms})$, one can compare values of wave height for the data-specified exceedence probabilities.

64. The lower panel of Figure 6 shows data estimates of exceedence probability (symbols) along with model estimates (patterned lines) for test Case 1. A semilogarithmic coordinate system has been used to expand the high-wave tail region of the distribution for easier visual comparison. The qualitative result is quite interesting. Where the model curves can be distinguished, the data appear to follow very closely both the modified and formal Beta-Rayleigh curves. These almost coincide because H_{rms} is small relative to the water depth so the formal Beta-Rayleigh curve is approaching the deepwater asymptote. This means the shapes of these curves are governed more by the ratio of H_{rmq} to H_{rms} than directly by water depth.

65. The Rayleigh curve appears to lie above the data in Figure 6. This means that, for a given H/H_{rms} , the Rayleigh model gives a higher probability of exceedence (or, conversely, for a given probability of exceedence, a higher wave height is indicated). This is qualitatively consistent with observations by other investigators, as discussed in the introduction, that the Rayleigh model tends to overpredict the higher waves. In terms of magnitude of exceedence probability, the overprediction is not large on the scale of the graph as a whole, being about two parts per thousand (compared with one) at $H/H_{rms} \approx 2.0$, but is significant relative to the local probability, being about 20 percent at the same H/H_{rms} . Conversely, for a fixed exceedence probability, the overprediction of wave height by the Rayleigh model is small, being roughly 3 percent at the higher wave heights.

66. The estimated Beta-Rayleigh model appears to underestimate the observations and the other models. It is roughly 10 percent lower than the Rayleigh model and about 6 percent lower than both the data and the formal

Beta-Rayleigh curve at the larger wave heights. The reason for this deviation can only be that $H_{rms,e}$ and $H_{rmq,e}$ are different from H_{rmq} and H_{rms}, respectively, because it is the shift in governing parameters that distinguishes the two models. Comparison of estimated and measured root-mean-square and root-mean-quad wave heights (listed at the top of Figure 6) shows that the estimated values are both about 10 percent higher than the measured values. The magnitude of this deviation is consistent with deviations about the estimation curves (Equations 19 and 20) shown by Hughes and Borgman (1987). Evidently, the Beta-Rayleigh model is somewhat sensitive to the values of the parameters used. This is especially true on the deepwater asymptote where the shape governing parameter H_{rmq}/H_{rms} is restricted to values between 1.0 and about 1.3 (see Figure 2 and related discussion). A 10-percent deviation on either side of the middle of this range exceeds this range. This suggests that great care must be exercised in estimating H_{rms} and H_{rmq}.

67. It is noted that all of the curves in Figure 6 are actually quite good approximations of the data. It just appears that the formal Beta-Rayleigh and the modified Rayleigh are slightly better than the other two. This pattern is consistent in all of the test cases. Graphs like Figure 6 for the remaining test cases are given in Appendix C.

68. Of particular interest is the model comparison at high energy. Cases 5 to 10 all have H_{mo} in excess of 2 m and H_{rms}/d in the range 0.17 to 0.29, large enough to distinguish the shapes of the modified Rayleigh and the formal Beta-Rayleigh models. In qualitative description, the tendency for the Rayleigh model to overpredict the data still exists, but is generally only between 0 and 2 percent high. The modified Rayleigh curve appears to agree best with the data and also appears to be quite close in shape to the Rayleigh curve. Where the modified Rayleigh model deviates from the Rayleigh curve, the deviation is generally toward the data. The formal Beta-Rayleigh model indicates smaller extreme wave heights at the same probability than either the Rayleigh or modified Rayleigh models. It appears in these tests to deviate from the modified Rayleigh curve only for $H/H_{rms} > 2.0$, a region in which the scatter of the data increases. There appears to be a tendency for the formal Beta-Rayleigh model to underpredict the data and to be less than the modified Rayleigh curve, though these differences are rather slight. The estimated Beta-Rayleigh model is consistently lower than the data and all the other models at the larger wave heights.

69. In an attempt to quantify these differences in a simple way, the RMS difference in H/H_{rms} between the data and each model for exceedences at all data points was computed. Results are shown in Table 2. If the number in each column is multiplied by 100, the result is the RMS difference as a percentage of the parameter H_{rms} for each test case. The average normalized RMS difference for each model is shown on the bottom row.

70. Curiously, the modified Rayleigh model is as good as, if not a lot better than, all the other models. Its maximum deviation, about 0.025, is less than the mean deviation of the Rayleigh model. It has about the same RMS deviation as the formal Beta-Rayleigh model in all cases except for two of the highest energy cases (6 and 7) where it has somewhat less deviation from the data. This is important because the depth dependence of the Beta-Rayleigh model is at or near maximum in these two cases and it appears that the depth-independent model yields a better result. This suggests that it may be necessary to do additional work on the model for the case of shallow water waves in incipient-breaking conditions, i.e., at or just outside the seaward edge of the breaker zone. Note that the dominantly varying parameters in this sequence are the total energy and related wave height scales. Neither directional nor frequency spread parameters show a strong variation. The frequency and frequency-direction spectra do not show any significant

Table 2

Root Mean Square Difference of Measured Data and Models of Cumulative Wave Height Distribution

			Model Name and Parameter Set			
Case	Date	Time	Rayleigh H_{rms}	Modified Rayleigh H_{rms}, H_{rmq}	Beta-Rayleigh H_{rms}, H_{rmq}, d	Beta-Rayleigh H_{mo}, T_p, d
1	14 Sep 86	0700	0.0286	0.0092	0.0098	0.0408
2	21 Sep 86	1800	0.0201	0.0223	0.0220	0.0812
3	15 Feb 87	0100	0.0333	0.0162	0.0167	0.0291
4	16 Feb 87	0100	0.0333	0.0105	0.0115	0.0142
5	16 Feb 87	1900	0.0278	0.0153	0.0171	0.0184
6	16 Feb 87	2200	0.0285	0.0242	0.0312	0.0324
7	17 Feb 87	1600	0.0240	0.0191	0.0321	0.0785
8	17 Feb 87	1900	0.0205	0.0228	0.0185	0.0507
9	18 Feb 87	0100	0.0167	0.0186	0.0153	0.0703
10	18 Feb 87	0700	0.0235	0.0247	0.0228	0.0623
11	19 Feb 87	1900	0.0312	0.0132	0.0130	0.0218
		Mean	0.0261	0.0178	0.0191	0.0454

deviations of shape. Hence, it is unlikely that any of these parameters correlates well with deviations of the Beta-Rayleigh curve from the data.

71. In order of increasing deviation, the classic Rayleigh model is third and the estimated Beta-Rayleigh is fourth. The Rayleigh curve is rather consistently different by about 2 to 3 percent of H_{rms} over most cases. The estimated Beta-Rayleigh is, overall, quite a bit worse than the other models. It does about as well as its parent model in test Cases 4, 5, and 6, but more typically has deviations of two to four times those of the modified Rayleigh model.

Wave Height Averages

72. The RMS deviations listed in Table 2 are strongly weighted by waves with heights between 0.5 and 1.0 times H_{rms} because, by the definitions of the probability densities, this is where most of the waves occur. To evaluate the models over different regions of probability space, it might be interesting to isolate some part of the tail region and compute the RMS differences of data and models over this domain. On the other hand, there are some common wave height statistics that will, in effect, allow such comparisons to be made indirectly. These are the averages of the highest fraction of waves where the fraction r is allowed to vary from some small value to unity. One of the most commonly cited parameters of this group is the average of the highest one-third of the waves in a given sea state. Here, this will be given the symbol $H^{(1/3)}$ following the notation of Longuet-Higgins (1952) (the SPM (1984) and some other references use the symbol $H_{1/3}$, instead), with the general form being a function of r and written as $H^{(r)}$. For small values of the fraction r, the computations will be confined to the high-wave tail of the distribution. Comparability of data and models can then be evaluated indirectly over any arbitrary part of the high-wave domain, at least where there are sufficient data to compute a stable average.

73. Following the derivation given by Longuet-Higgins (1952), the fraction r of waves that are larger than a given value of H/H_{rms} is the exceedence probability for that H/H_{rms}. From basic statistics, the average value of waves higher than a given H/H_{rms} is the integral from that H/H_{rms} to infinity of the normalized heights weighted by the probability density

function and divided by the area over the same limits under the weighting function (i.e., the pdf). Hence, the general forms for r and $H^{(r)}/H_{rms}$ are

$$r = \int_{H/H_{rms}}^{\infty} \left[H_{rms}\ p\left(\frac{H}{H_{rms}}\right)\right]\ d\left(\frac{H}{H_{rms}}\right) \tag{24}$$

$$\frac{H^{(r)}}{H_{rms}} = \frac{1}{r} \int_{H/H_{rms}}^{\infty} \left(\frac{H}{H_{rms}}\right)\left[H_{rms}\ p\left(\frac{H}{H_{rms}}\right)\right]\ d\left(\frac{H}{H_{rms}}\right) \tag{25}$$

where the terms in square brackets are to be the dimensionless pdf models under consideration and the integrations are performed numerically as described in Part II.

74. For a set of N measured, normalized, ordered wave heights H_n/H_{rms}, the computation for a discrete, monotonically increasing fraction r_j where j is the index is given by

$$r_j = \frac{j}{N} \tag{26}$$

$$\frac{H^{(r_j)}}{H_{rms}} = \frac{1}{j} \sum_{i=1}^{j} \frac{H_{N-i+1}}{H_{rms}} \tag{27}$$

When both data and models of $H^{(r)}/H_{rms}$ have been computed, the resulting arrays can be interpolated for particular values of the fraction r.

75. Figure 7 shows the function $H^{(r)}/H_{rms}$ for the four models (using the model pdf formulae in Equations 24 and 25) and the data estimate, Equations 26 and 27, for test Case 1 and for $r > 10^{-4}$. Model parameters are iterated at the top of the figure. A semilogarithmic scale has been used to expand the small-fraction region.

76. Results indicated by Figure 7 are similar to those indicated by Figure 6. The modified Rayleigh and formal Beta-Rayleigh models are not very different, again because depth is large relative to H_{rms}. The Rayleigh curve indicates a larger mean wave height for a given fraction r than the formal Beta-Rayleigh and the modified Rayleigh curves. It is also larger than the data indicate for most values of r, consistent with its tendency to overpredict wave heights. The estimated Beta-Rayleigh curve underestimates the observed mean normalized wave heights for all fractions. Similar general

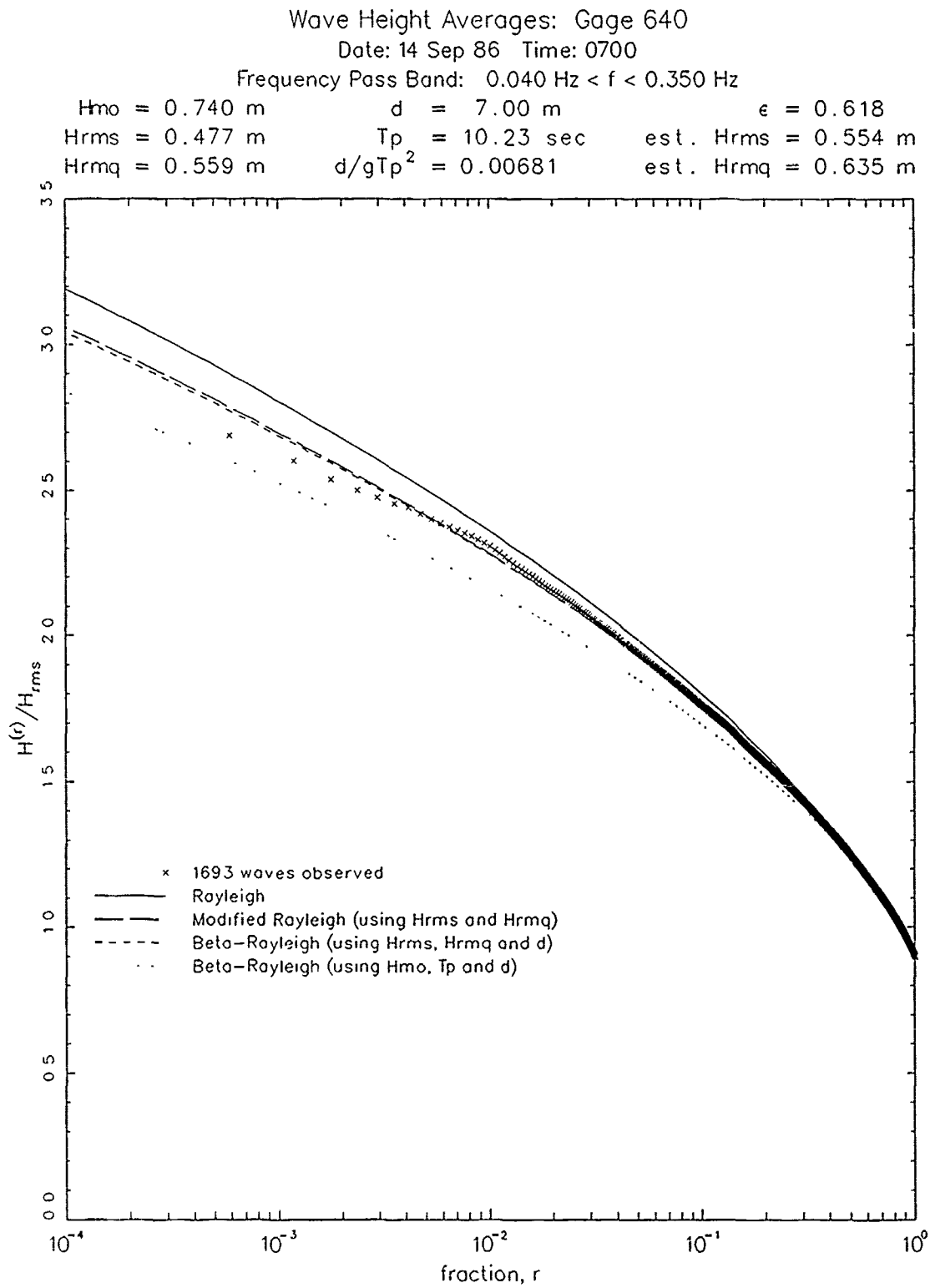

Figure 7. Observed and modeled averages of the highest fraction r of wave heights for test Case 1

patterns can be seen in wave height average curves for the other test cases, which are shown in Appendix D.

77. The wave height average values appear to vary more smoothly in Figure 7 than do the source wave heights in Figure 6. This smoothness is an artifact of averaging and, for the larger wave heights, give the impression that deviations of data and model curves are a result of modeling errors. While this is possible, it is more likely that such deviations are due to poor sampling of the largest wave heights. There are very few of these in any given sample (there is only one largest wave height) so that confidence intervals are somewhat broad. Consideration of deviations of the largest wave height is given in the next section of this report. The point here is that reasonable model comparisons are difficult when the possible sampling error is as large as the range of values predicted by the set of test models.

78. A crude idea of the sampling problem can be obtained by scanning the graphs in Appendix D and Figure 7 to see how much the low-fraction part of the data varies relative to the set of model curves. For the small and intermediate wave heights, there are enough samples for much more stable estimates of the averages. If the errors in the largest wave heights are random and not biased, then averages through a relatively small number of the largest waves will tend to converge rather rapidly to the true population average. Hence, it can be expected that data in Figure 7 near $H^{(1/100)}/H_{rms}$ are more reliable than data near $H^{(1/1000)}/H_{rms}$ so that, in subsequent model comparisons, data at very small r are not used.

79. Model tests are conducted by finding the dimensional model estimates of wave height averages for five values of r and comparing these to measured averages at the same r, interpolating the discrete data curves where necessary. Specific averages are $H^{(1/1)}$ (the average of all waves), $H^{(1/3)}$ (the conventional time domain characteristic wave height), $H^{(1/10)}$, $H^{(1/20)}$, and $H^{(1/100)}$, where this last height is expected to be reliably estimated from data because of the large number of waves (of order 1,000) in each time series. All dimensionless model computations are made dimensional with the observed H_{rms} except for the estimated Beta-Rayleigh model. This must use $H_{rms,e}$ because one of the test criteria is that only H_{mo}, T_p, and d are known for this model.

80. Table 3 lists the average heights thus found for each test case and for each r. The percent difference of each model estimate from the data is

also listed in Table 3. As a gross measure of model behavior, the mean (over 11 test cases) of the absolute values of percent differences is given at the bottom of each difference column. Figures 8 to 12 are correlograms of observations and model results for the same five values of r . Correlation

Table 3

Percent Difference of Measured Data and Model Prediction of Average of Highest Fraction r of Height Distribution

				Model Name and Parameter Set							
				Rayleigh (H_{rms})		Modified Rayleigh (H_{rms},H_{rmq})		Beta-Rayleigh (H_{rms},H_{rmq},d)		Beta-Rayleigh (H_{mo},T_p,d)	
Case	Date	Time	Obs. $H_m^{(r)}$	$H_m^{(r)}$	diff. %	$H_m^{(r)}$	diff. %	$H_m^{(r)}$	diff. %	$H_m^{(r)}$	diff. %
						Case (a) r = 1/1					
1	14 Sep 86	0700	0.43	0.42	-1.39	0.43	-0.09	0.43	-0.13	0.51	18.04
2	21 Sep 86	1800	0.30	0.30	0.28	0.30	0.55	0.30	0.53	0.34	14.71
3	15 Feb 87	0100	0.39	0.39	-1.51	0.39	-0.27	0.39	-0.30	0.44	11.48
4	16 Feb 87	0100	0.93	0.91	-1.58	0.93	0.05	0.92	-0.11	0.98	5.95
5	16 Feb 87	1900	1.28	1.26	-1.13	1.28	0.10	1.27	-0.16	1.35	6.15
6	16 Feb 87	2200	1.53	1.52	-0.77	1.52	-0.22	1.52	-0.66	1.63	6.69
7	17 Feb 87	1600	1.94	1.95	0.74	1.94	0.18	1.92	-0.94	2.21	14.07
8	17 Feb 87	1900	1.74	1.74	0.08	1.74	0.55	1.73	-0.07	1.93	11.26
9	18 Feb 87	0100	1.45	1.45	0.26	1.46	0.52	1.45	0.03	1.66	14.51
10	18 Feb 87	0700	1.24	1.24	0.09	1.24	0.43	1.24	0.12	1.40	13.12
11	19 Feb 87	1900	0.57	0.56	-1.46	0.57	0.09	0.57	0.04	0.62	8.67
	Mean |%|				0.84		0.27		0.28		11.33
						Case (b) r = 1/3					
1	14 Sep 86	0700	0.67	0.68	1.32	0.67	0.15	0.67	0.19	0.76	14.02
2	21 Sep 86	1800	0.48	0.47	-0.71	0.47	-0.93	0.47	-0.91	0.51	6.20
3	15 Feb 87	0100	0.61	0.62	1.72	0.61	0.60	0.61	0.64	0.67	9.56
4	16 Feb 87	0100	1.43	1.46	1.66	1.43	0.17	1.44	0.36	1.53	7.15
5	16 Feb 87	1900	1.98	2.01	1.53	1.99	0.44	2.00	0.74	2.10	6.12
6	16 Feb 87	2200	2.38	2.42	1.58	2.41	1.10	2.42	1.59	2.53	6.30
7	17 Feb 87	1600	3.13	3.12	-0.21	3.14	0.25	3.17	1.38	3.36	7.38
8	17 Feb 87	1900	2.78	2.78	-0.28	2.76	-0.65	2.78	-0.01	2.96	6.50
9	18 Feb 87	0100	2.32	2.32	0.14	2.31	-0.08	2.33	0.44	2.50	7.94
10	18 Feb 87	0700	1.97	1.98	0.41	1.97	0.12	1.98	0.46	2.13	7.75
11	19 Feb 87	1900	0.89	0.90	1.15	0.88	-0.26	0.88	-0.19	0.95	6.88
	Mean |%|				0.97		0.43		0.63		7.80
						Case (c) r = 1/10					
1	14 Sep 86	0700	0.84	0.86	2.28	0.84	-0.06	0.84	-0.05	0.94	11.74
2	21 Sep 86	1800	0.60	0.60	0.87	0.60	0.43	0.60	0.43	0.62	4.54
3	15 Feb 87	0100	0.77	0.79	1.83	0.77	-0.40	0.77	-0.39	0.83	7.09
4	16 Feb 87	0100	1.81	1.85	2.40	1.80	-0.54	1.80	-0.53	1.92	6.46
5	16 Feb 87	1900	2.50	2.56	2.54	2.51	0.35	2.51	0.37	2.63	5.23
6	16 Feb 87	2200	3.03	3.08	1.41	3.05	0.45	3.05	0.50	3.15	3.87
7	17 Feb 87	1600	4.01	3.97	-0.98	4.01	-0.06	4.01	0.08	4.10	2.19
8	17 Feb 87	1900	3.47	3.53	1.75	3.50	0.97	3.50	1.04	3.66	5.41
9	18 Feb 87	0100	2.95	2.95	0.03	2.94	-0.40	2.94	-0.34	3.07	4.04
10	18 Feb 87	0700	2.50	2.52	0.66	2.50	0.08	2.50	0.13	2.62	4.84
11	19 Feb 87	1900	1.11	1.14	2.88	1.11	0.06	1.11	0.07	1.18	6.43
	Mean |%|				1.60		0.34		0.36		5.62

(Continued)

Table 3 (Concluded)

Case	Date	Time	Obs. $H^{(r)}$ m	Model Name and Parameter Set: Rayleigh (H_{rms}) $H^{(r)}$ m	Rayleigh (H_{rms}) diff. %	Modified Rayleigh (H_{rms}, H_{rmq}) $H^{(r)}$ m	Modified Rayleigh (H_{rms}, H_{rmq}) diff. %	Beta-Rayleigh (H_{rms}, H_{rmq}, d) $H^{(r)}$ m	Beta-Rayleigh (H_{rms}, H_{rmq}, d) diff. %	Beta-Rayleigh (H_{mo}, T_p, d) $H^{(r)}$ m	Beta-Rayleigh (H_{mo}, T_p, d) diff %
					Case (d) r = 1/20						
1	14 Sep 86	0700	0.93	0.95	2.43	0.92	-0.32	0.92	-0.36	1.0[illegible]	10.67
2	21 Sep 86	1800	0.65	0.66	2.00	0.66	1.47	0.66	1.45	0.68	4.50
3	15 Feb 87	0100	0.86	0.87	1.17	0.85	-1.43	0.85	-1.46	0.91	5.46
4	16 Feb 87	0100	1.98	2.04	3.34	1.97	-0.15	1.97	-0.32	2.11	6.76
5	16 Feb 87	1900	2.75	2.82	2.80	2.75	0.21	2.75	-0.05	2.87	4.59
6	16 Feb 87	2200	3.37	3.40	0.84	3.36	-0.29	3.34	-0.70	3.44	2.19
7	17 Feb 87	1600	4.48	4.38	-2.36	4.43	-1.28	4.39	-2.22	4.43	-1.33
8	17 Feb 87	1900	3.82	3 89	1.81	3.86	0.90	3.84	0.33	3.97	3.92
9	18 Feb 87	0100	3.26	3.25	-0.27	3.24	-0.78	3.22	-1.20	3.33	2.09
10	18 Feb 87	0700	2.76	2.78	0.49	2.76	-0.19	2.75	-0.45	2.86	3.34
11	19 Feb 87	1900	1.22	1.26	2.78	1.22	-0.53	1.22	-0.59	1.29	5.48
	Mean |%|				1.84		0.69		0.83		4.57
					Case (e) r = 1/100						
1	14 Sep 86	0700	1.10	1.13	2.29	1.09	-1.09	1.09	-1.25	1.19	8.56
2	21 Sep 86	1800	0.77	0.79	2.85	0.78	2.19	0.78	2.11	0.79	3.45
3	15 Feb 87	0100	1.00	1.03	3.13	1.00	-0.14	1.00	-0.26	1.06	5.97
4	16 Feb 87	0100	2.29	2.43	5.84	2.33	1.44	2.31	0.75	2.48	7.98
5	16 Feb 87	1900	3.28	3.36	2.19	3.25	-0.98	3.22	-2.05	3.36	2.18
6	16 Feb 87	2200	4.11	4.03	-1.95	3.98	-3.31	3.91	-4.98	4.00	-2.88
7	17 Feb 87	1600	5.24	5.20	-0.59	5.28	0.77	5.07	-3.24	5.03	-3.94
8	17 Feb 87	1900	4.54	4.62	1.94	4.57	0.81	4.47	-1.53	4.58	0.87
9	18 Feb 87	0100	3.79	3.86	1.89	3.84	1.24	3.77	-0.60	3.84	1.14
10	18 Feb 87	0700	3.21	3.30	2.84	3.27	1.98	3.23	0.80	3.31	3.27
11	19 Feb 87	1900	1.39	1.49	7.23	1.44	2.97	1.43	2.74	1.51	8.58
	Mean |%				2.98		1.54		1.85		4.44

coefficients of the observations with each model are given at the top of each correlation plot.

81. Information in Table 3 is consistent with findings from the overall RMS difference comparison of the last section. The modified Rayleigh and formal Beta-Rayleigh models are almost indistinguishable for the four largest values of r , having differences from the data typically less than 1 percent. In the same range of r , the Rayleigh model is worse but only slightly so, with some of the larger differences between 2 and 3 percent. The estimated Beta-Rayleigh has the greatest deviations, with differences of 5 to 15 percent not uncommon.

82. There does not appear to be any particular deviation or trend in the comparisons related to frequency or directional spread parameters. Cases 1, 2, 3, and 11 are all relatively low energy cases with diverse spectral structure, yet the Rayleigh, modified Rayleigh, and formal Beta-Rayleigh

models all do very well in estimating characteristic heights. It should be pointed out that, for the two largest values of r, model and data differences for these three models are generally comparable to or less than instrument accuracy (± 0.02 m), so the percentages given are mostly within measurement noise.

83. The most stringent test here is for the smallest fraction, $r = 1/100$, and for the largest characteristic wave heights, test Cases 4 to 10. Examination of that part of Table 3 indicates less diversity among the models. The modified Rayleigh continues to do best with a typical difference of 1 percent and a maximum difference of 3.3 percent. The other three models seem about the same with typical differences of about 2 percent and maximum differences of 5 to 8 percent. There is a tendency for the formal Beta-Rayleigh to have results consistently lower than observations (most of the signs are negative at the highest energies), a trait not seen in the modified Rayleigh model results. It is possible that the effects of finite depth as employed in the formal Beta-Rayleigh model (breaking wave height equals water depth) affects the high-wave tail region of that model in a way that causes this bias. This should be investigated further because it could also be statistical variation due to a small set of test cases.

84. The correlation plots of Figures 8 to 12 illustrate the data of Table 3. The correlation coefficients are all quite high, being in excess of 0.999 for all models and all fractions except for the estimated Beta-Rayleigh model at the largest and smallest r, where correlation coefficients of about 0.998 occur in both cases. Note that the correlation coefficient gives a measure of how well a set of coordinate points is represented by a straight line but not necessarily a line of slope 1.0. The difference percentages in Table 3 are a better measure of that type of deviation.

85. The modified Rayleigh and the formal Beta-Rayleigh models have the highest correlation coefficients with the data for all r. Their correlation coefficients are almost indistinguishable. The Rayleigh model follows these two in all cases except for the smallest r, where the estimated Beta-Rayleigh is better correlated with the data. This ordering of the models is consistent with prior discussion.

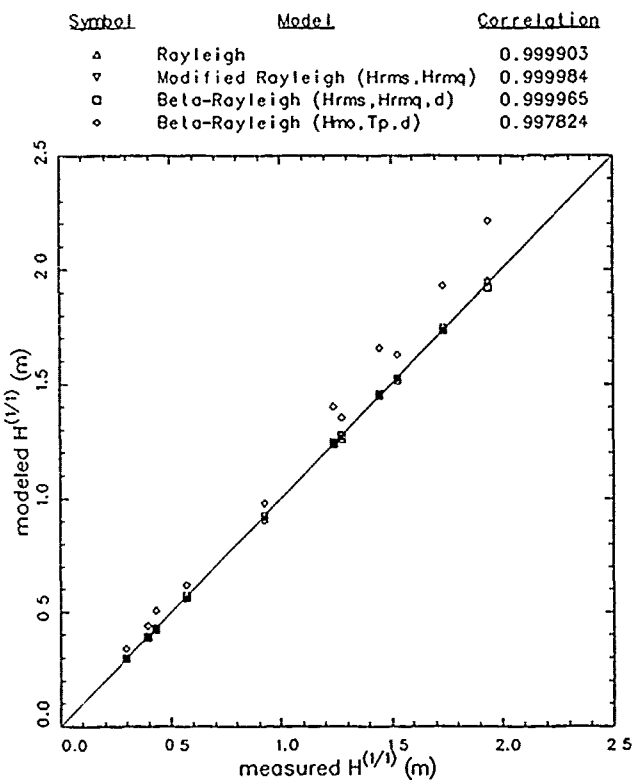

Figure 8. Correlation plot of observed and modeled $H^{(1/1)}$

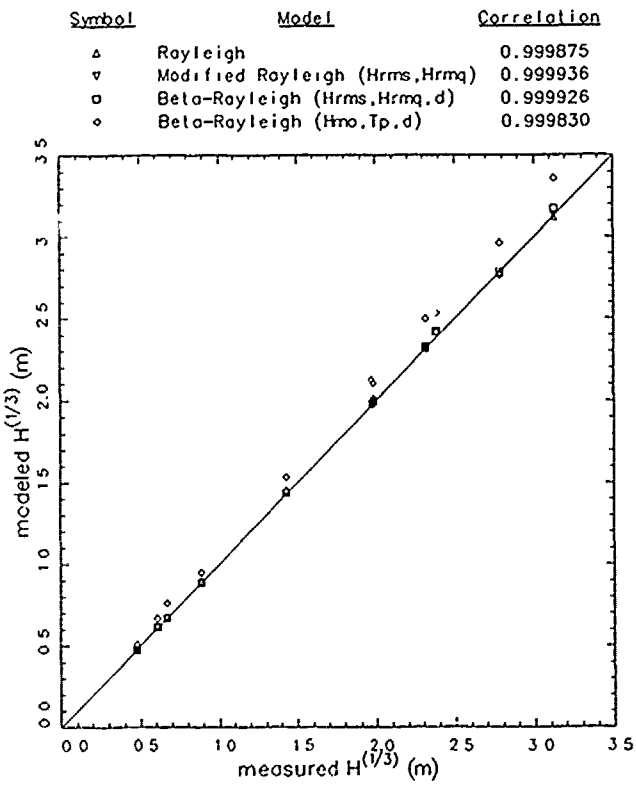

Figure 9. Correlation plot of observed and modeled $H^{(1/3)}$

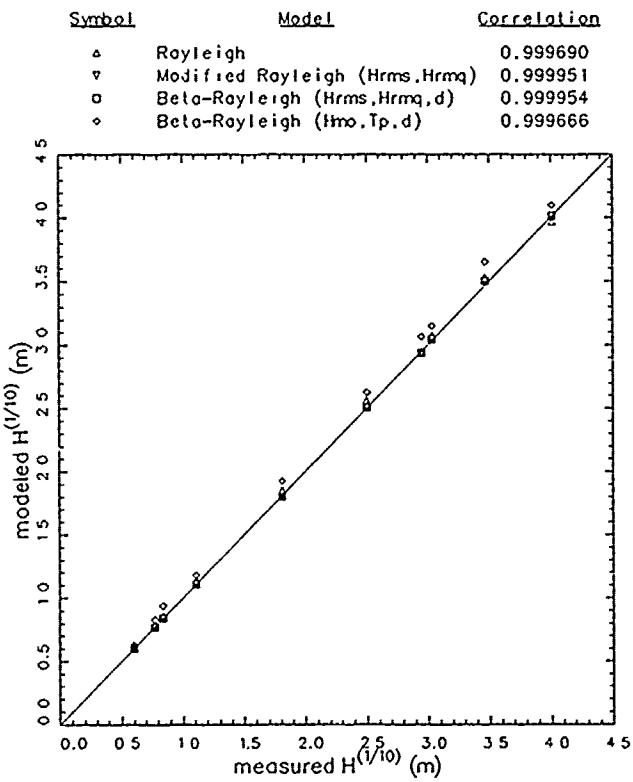

Figure 10. Correlation plot of observed and modeled $H^{(1/10)}$

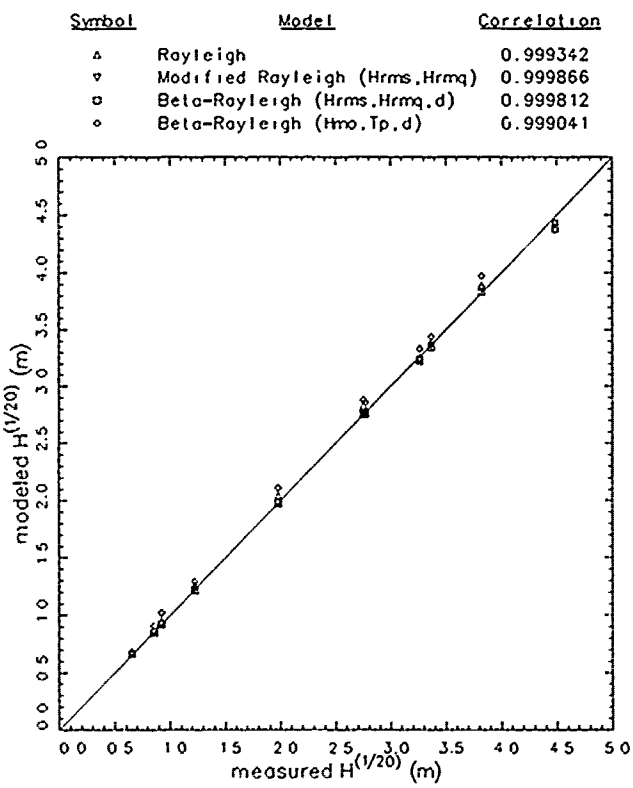

Figure 11. Correlation plot of observed and modeled $H^{(1/20)}$

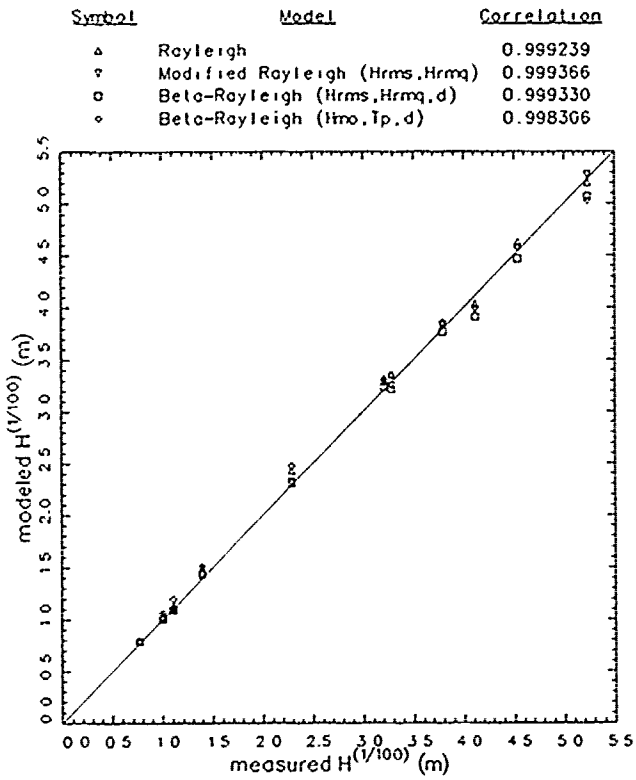

Figure 12. Correlation plot of observed and modeled $H^{(1/100)}$

Maximum Wave Height

86. Estimation of the maximum wave height that may occur in a wave field is clearly important since it can be used to set an upper limit for considerations of run-up or overtopping in engineering design. In the papers by Longuet-Higgins (1952) and Thornton and Guza (1983), some consideration is given to expected values of the maximum wave height in a field of N waves but only cursory discussion of the range of values one might find given a single sample of maximum wave height. This is important because it is not always possible to obtain more than one wave record from a given site and sea state. Hence, it is useful to have some idea of the confidence interval one can place on an observed maximum wave height assuming that one knows the governing probability law. In this report, a crude confidence measure is computed based on the pdf models being tested. It is used to argue that the models cannot be distinguished by their estimates of the maximum wave height and that all the model estimates of maximum wave height are reasonable.

87. Longuet-Higgins (1952) gives the derivation of the probability density function for the maximum wave height in a sample governed by a Rayleigh pdf. The same derivation would apply for a sample governed by any well-behaved pdf. Letting $p_{max}(H/H_{rms})$ symbolize the probability density that the maximum wave height H_{max} normalized by H_{rms} lies in some small range dH/H_{rms} near H/H_{rms}, the expression given by Longuet-Higgins (1952) can be written in dimensionless form as

$$H_{rms}\ p_{max}\left(\frac{H}{H_{rms}}\right) = N\ P\left(\frac{H}{H_{rms}}\right)^{N-1}\left[H_{rms}\ p\left(\frac{H}{H_{rms}}\right)\right] \tag{28}$$

where

N = number of wave heights in an observed time series

$P(H/H_{rms})$ = cumulative distribution function of Equation 3

$p(H/H_{rms})$ = governing probability density function

88. Because Equation 28 governs the distribution of H_{max}/H_{rms}, the expected value of the maximum wave height can be found from

$$E\left[\frac{H_{max}}{H_{rms}}\right] = \int_0^\infty \left(\frac{H}{H_{rms}}\right)\left[H_{rms}\ p_{max}\left(\frac{H}{H_{rms}}\right)\right] d\left(\frac{H}{H_{rms}}\right) \tag{29}$$

as shown by Longuet-Higgins (1952), and as follows from basic statistical operations. One can also find the variance of H_{max}, here called $\sigma^2[H_{max}/H_{rms}]$, using Equation 28 and standard statistical operations. This takes the form

$$\sigma^2\left[\frac{H_{max}}{H_{rms}}\right] = \int_0^\infty \left(\frac{H}{H_{rms}}\right)^2\left[H_{rms}\ p_{max}\left(\frac{H}{H_{rms}}\right)\right] d\left(\frac{H}{H_{rms}}\right) - E\left[\frac{H_{max}}{H_{rms}}\right]^2 \tag{30}$$

The standard deviation of the maximum wave height is the square root of Equation 30, or $\sigma[H_{max}/H_{rms}]$.

89. The above statistics can be computed for the models being tested by substitution of each model pdf in the above set of equations. Dimensional forms for the expected value and standard deviation are found by multiplying the dimensionless results by H_{rms} for all models except the estimated

Beta-Rayleigh, which must use $H_{rms,e}$. The general form for the expected maximum wave height is then $E[H_{max}] = H_{rms}\ E[H_{max}/H_{rms}]$ and similarly $\sigma[H_{max}] = H_{rms}\ \sigma[H_{max}/H_{rms}]$.

90. Table 4 shows the results of such computations for each test case and each model. The percentage difference of the expected from the observed maximum wave height is shown. Also shown is the standard deviation as a percentage of the expected H_{max} . This latter quantity is important because it shows the amount of scatter one would expect from a large ensemble of samples of the same sea state, of which each observed maximum wave height in Table 4 is just one. That is, one may not get the expected H_{max} in a single random sample, but one might more reasonably expect to be within one standard deviation of the expected H_{max} . Table 4 indicates that with the numbers of

Table 4

Comparison of Measured Maximum Wave Height and Model Expectation of Maximum Wave Height and Its Standard Deviation

				Model Name and Parameter Set							
				Rayleigh (H_{rms})				modified Rayleigh (H_{rms},H_{rmq})			
			Obs. H_{max}	$E[H_{max}]$	diff.	σ[Hmax]	σ/E	$E[H_{max}]$	diff.	$\sigma[H_{max}]$	σ/E
Case	Date	Time	m	m	%	m	%	m	%	m	%
1	14 Sep 86	0700	1.28	1.35	4.87	0.11	7.98	1.30	0.89	0.10	7.59
2	21 Sep 86	1800	0.92	0.91	-1.52	0.08	8.45	0.90	-2.28	0.08	8.37
3	15 Feb 87	0100	1.17	1.23	5.28	0.10	8.04	1.19	1.69	0.09	7.66
4	16 Feb 87	0100	2.66	2.90	8.89	0.23	7.95	2.76	3.87	0.21	7.56
5	16 Feb 87	1900	4.00	3.98	-0.60	0.32	8.05	3.84	-4.16	0.30	7.72
6	16 Feb 87	2200	4.87	4.76	-2.21	0.39	8.12	4.68	-3.76	0.37	7.96
7	17 Feb 87	1600	5.71	6.05	6.03	0.51	8.35	6.14	7.62	0.53	8.55
8	17 Feb 87	1900	5.79	5.40	-6.77	0.45	8.28	5.34	-7.89	0.44	8.16
9	18 Feb 87	0100	4.15	4.50	8.40	0.37	8.30	4.47	7.69	0.37	8.24
10	18 Feb 87	0700	4.25	3.86	-9.06	0.32	8.26	3.82	-9.99	0.31	8.13
11	19 Feb 87	1900	1.64	1.77	7.59	0.14	8.09	1.69	2.85	0.13	7.68
	Mean |%|				5.57		8.17		4.79		7.97

				Beta-Rayleigh (H_{rms},H_{rmq},d)				Beta-Rayleigh (H_{mo},T_p,d)			
			Obs. H_{max}	$E[H_{max}]$	diff.	$\sigma[H_{max}]$	σ/E	$E[H_{max}]$	diff.	$\sigma[H_{max}]$	σ/E
Case	Date	Time	m	m	%	m	%	m	%	m	%
1	14 Sep 86	0700	1.28	1.29	0.52	0.10	7.43	1.41	9.58	0.10	7.05
2	21 Sep 86	1800	0.92	0.90	-2.43	0.08	8.31	0.90	-2.73	0.07	7.58
3	15 Feb 87	0100	1.17	1.19	1.39	0.09	7.58	1.25	7.01	0.09	7.30
4	16 Feb 87	0100	2.66	2.72	2.24	0.19	7.03	2.91	9.42	0.21	7.03
5	16 Feb 87	1900	4.00	3.74	-6.47	0.26	6.92	3.90	-2.70	0.26	6.76
6	16 Feb 87	2200	4.87	4.50	-7.45	0.31	6.87	4.58	-5.85	0.29	6.36
7	17 Feb 87	1600	5.71	5.62	-1.47	0.50	8.87	5.56	-2.50	0.28	5.03
8	17 Feb 87	1900	5.79	5.07	-12.39	0.35	6.80	5.16	-10.91	0.31	5.91
9	18 Feb 87	0100	4.15	4.30	3.55	0.31	7.16	4.33	4.22	0.27	6.25
10	18 Feb 87	0700	4.25	3.73	-12.23	0.27	7.36	3.78	-10.84	0.25	6.71
11	19 Feb 87	1900	1.64	1.68	2.31	0.13	7.49	1.77	7.90	0.13	7.32
	Mean |%|				4.77		7.44		6.70		6.67

waves observed in these tests and with the particular models being used, the variation about the expected H_{max} of the standard deviation is roughly 6 to 8 percent. With a few minor exceptions, the observations agree with the model expectations within that percentage range.

91. Typical percentage errors are shown as the mean (over 11 cases) of the absolute value of the percentage error at the bottom of the difference column for each model. Also shown is the mean of the standard deviations as percentages of the expected H_{max} . Because the model results are typically within one standard deviation of the observations, it can be said that the models agree adequately with observations. Because the models agree with each other to within comparable percentages, one cannot distinguish any model as superior to any other (in predicting H_{max}) from the data used in these tests.

92. Figure 13 is a correlation plot of expected H_{max} with observed H_{max} . The correlation coefficient of each model with the data is shown at the top of the figure. The correlation coefficients are reasonably high but not as high as for the less extreme characteristic heights of the previous section. The correlation coefficients are also all approximately equal, again

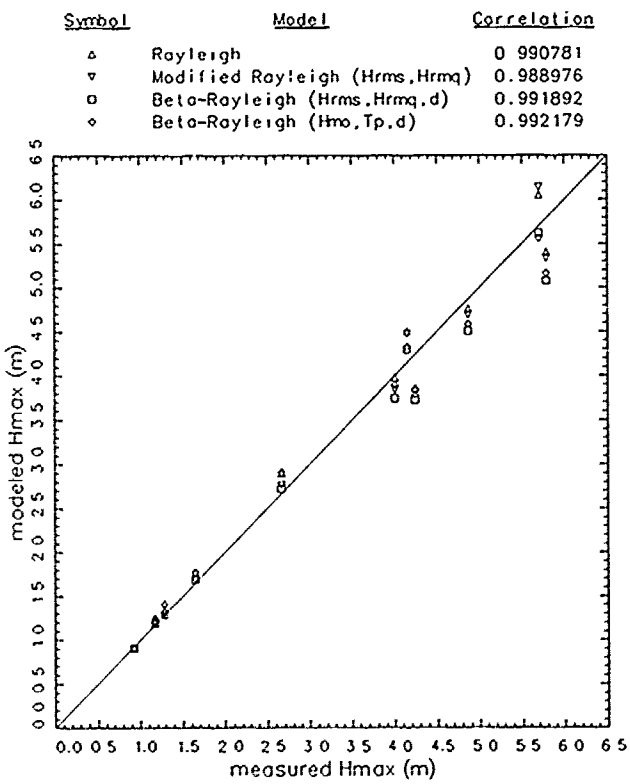

Figure 13. Correlation plot of observed and modeled H_{max}

suggesting that scatter in the data precludes distinction of a superior model (of H_{max}) at the statistical level of these tests.

PART V: CONCLUSION

93. The Beta-Rayleigh pdf given by Hughes and Borgman (1987) is a new and uniquely derived model for wave heights in shallow water. To see if it provides improved statistical descriptions of wave properties in diverse wave climates, it has been exercised, along with the classic Rayleigh model, to obtain results that have been compared with observations at the FRF. To establish an objective test, the models were constrained to be formulated exactly as published, and, further, no variation of model parameters (to improve comparison with data) was allowed. To this end, the tests simulated an application by a design engineer who must rely on model results without recourse to model or parameter variation.

94. The Beta-Rayleigh model was used in three forms. One was the complete, formal Beta-Rayleigh model in which was imposed the secondary model that breaking wave height is equal to water depth (as recommended by Hughes and Borgman 1987). A second was the deepwater asymptotic form of the Beta-Rayleigh distribution, called a modified Rayleigh model, which depends only on root-mean-square and root-mean-quad wave heights as parameters. The third form was again the Beta-Rayleigh model, as above, but another secondary model posed the two wave height parameters in terms of the frequency domain parameters H_{mo} and T_p as might be necessary if the only field data are smoothed processed wave frequency spectra, or spectral estimated derived from numerical models. This was referred to as the estimated Beta-Rayleigh model to distinguish it from the formal model. Along with the Rayleigh model, this made a total of four models to be tested.

95. Test data were time series from a Waverider buoy in 8 m of water about 1 km offshore. The time series were of 2 hr 16 min duration and contained typically 1,000 to 1,500 waves. Diversity of wave climate was established by selecting cases classified by energy level as well as broad and narrow energy spread in frequency and direction with diversity of directional distribution taking dominance. Directional information was obtained from the base of processed data from a high resolution, linear array directional wave gage, located at the FRF, also in about 8 m of water and slightly north of the Waverider buoy. Eleven test cases were selected. At low energy, $H_{mo} < 1$ m, directional spread varied from about 28 to 55 deg. At high energy, the spread

was more uniform, consistent with the directional wave climate of the FRF, but the energy-based wave height was as large as 3.1 m. This was high enough to test the effect of finite depth on the wave height distribution through the Beta-Rayleigh model.

96. The first test computed the RMS difference between modeled and observed exceedence probability curves. Curiously, the modified Rayleigh model showed the least diversion from the observations, with the formal Beta-Rayleigh only slightly worse. Both had differences of order 1 to 2 percent of the RMS wave height. The Rayleigh model was third, with differences typically 2 to 3 percent of RMS wave height. The estimated Beta-Rayleigh model had much more erratic results, with differences from 1 to 8 percent, typically 4 percent, of RMS wave height. This is due to the sensitivity of the Beta-Rayleigh model to the ratio H_{rmq}/H_{rms} and the uncertainty of up to 10 percent in estimating these two parameters from a simple model based on H_{mo} , T_p , and d . While this aspect of the applied model needs more work in order to compare in accuracy with the formal Beta-Rayleigh model, it is quite remarkable how small the differences are, given that no parameter fitting was employed.

97. This theme carried into the second test, which was an evaluation of the average of a given fraction of the highest waves. Here, again, the modified Rayleigh and formal Beta-Rayleigh were the best models overall with differences less than 1 percent for the averages all waves and of the highest one-third, one-tenth, and one-twentieth waves. The classic Rayleigh model was also very good but had differences typically twice those of the first two models. The estimated Beta-Rayleigh again suffered from uncertainties in estimated H_{rms} and H_{rmq} , with errors of 10 to 14 percent not uncommon.

98. At high energy and for the average of the highest 1 percent of the waves, there was an indication that the formal Beta-Rayleigh model may underpredict the true wave field. This may be due to the very simple model used for breaking wave height, but it should be investigated further. The statistics of high waves at high overall energy is most important for engineering design.

99. Curiously, the depth-independent modified Rayleigh curve gave the best estimates of these statistics. This suggests that further investigations regarding this simple, two-parameter model should also be conducted. This would be rather straightforward to do. Whereas the classic Rayleigh model has

all data collapse (ideally) to the same curve when normalized by H_{rms}, the modified Rayleigh would have the same data collapse to a family of curves for which the distinguishing parameter is H_{rmq}/H_{rms}. There is no shortage of data with which to conduct such a study.

100. Finally, all the models gave an adequate estimate of the maximum wave height to be expected from records of the given duration. As was computed, the uncertainties in sampling the maximum wave height made it impossible to ascribe superiority to any of the four models based on prediction of this parameter.

101. It is concluded, based on these simple tests, that the Beta-Rayleigh model, in the form of its deepwater asymptote, is the superior of the four models tested. The formal Beta-Rayleigh model is second, followed by the classic Rayleigh model and, at some distance behind, the estimated Beta-Rayleigh model. It is noted that all of the models behaved well and, depending on the level of accuracy required by the engineering designer, any of the models give reasonable results. There was no observable distinction in observed or modeled wave height distributions based on characteristics of frequency-direction energy spectra. All were reasonably close to the one-parameter Rayleigh model, which suggests that total energy (of which H_{rms} is a measure) is the overriding parameter of dominance. The fine tuning brought about by the modified Rayleigh model is most likely due to modifications of the ratio H_{rmq}/H_{rms} by subtleties of the frequency distribution of energy rather than directional effects. This could be investigated with the study recommended above.

102. The following recommendations are made for future studies:

a. Investigate the effect of filtering the time series from the full measured spectrum which goes from very low frequencies to a Nyquist cutoff to a spectrum confined by predefined wind-wave cutoff frequencies, especially in light of the new models considered here that have sensitive behavior due to parameters which surely are affected by such filtering.

b. See if an improvement can be made in modeling Beta-Rayleigh parameters in terms of spectral parameters. If these had been more finely tuned in the present study, the estimated Beta-Rayleigh model would have performed as well as the formal Beta-Rayleigh model (by definition).

c. Examine carefully the various models for breaking wave heights in shallow water to determine the effect in the tail region of the formal Beta-Rayleigh model. If all of them cause an

underestimation of wave height characteristics in shallow water outside the breaker zone, the model may have to be modified to compensate. This effect could also be investigated with longer, better resolved records from just outside the breaker zone than were used for model testing by Hughes and Borgman (1987).

d. Perform a proper statistical study of the modified Rayleigh model, as outlined above. This version of the Beta-Rayleigh formulation showed remarkable conformation with the observations and is deserving of further study.

103. In closing, it should be noted that this was the most cursory of examinations of a new model, intended to show indications rather than strong formal conclusions. Especially striking in this study was the close agreement of all the models with the data in the absence of any curve fitting or other model enhancing activity. Whether this was due to a fortuitous choice of test cases, the effect of very long, high-quality time series of sea-surface displacement, some artifact of the way the data were filtered or a truly improved model of wave statistics remains to be seen. The latter is strongly indicated in this brief study, suggesting the evolution of a much-improved tool for engineering design.

REFERENCES

Abramowitz, M., and Stegun, I. A. 1970. Handbook of Mathematical Functions, Dover, NY.

Battjes, J. A. 1972. "Set-Up Due to Irregular Waves," Proceedings of the 13th International Conference on Coastal Engineering, American Society of Civil Engineers, 10-14 July 1972, Vancouver, British Columbia, Canada, pp 1993-2004.

Birkemeier, W. A., Miller, H. C., Wilhelm, S.D., DeWall, A. E., and Gorbics, C. S. 1985. "A User's Guide to the Coastal Engineering Research Center's (CERC's) Field Research Facility," Technical Report CERC-85-1, US Army Engineer Waterways Experiment Station, Vicksburg, MS.

Cartwright, D. E., and Longuet-Higgins, M. S. 1956. "The Statistical Distribution of the Maxima of a Random Process," Proceedings of the Royal Society of London, Series A, Vol 237, pp 212-232.

Collins, J. L. 1970. "Probabilities of Breaking Wave Characteristics," Proceedings of the 12th Coastal Engineering Conference, American Society of Civil Engineers, 13-18 September 1970, Washington, DC, pp 399-412.

Earle, M. D. 1975. "Extreme Wave Conditions During Hurricane Camille," Journal of Geophysical Research, Vol 80, pp 377-379.

Forristall, G. Z. 1978. "On the Statistical Distribution of Wave Heights in a Storm," Journal of Geophysical Research, Vol 83, pp 2353-2358.

Goda, Y. 1975. "Irregular Wave Deformation in the Surf Zone," Coastal Engineering in Japan, Vol 18, pp 13-26.

_____. 1985. Random Seas and Design of Maritime Structures, University of Tokyo Press, Japan.

Hughes, S. A., and Borgman, L. F. 1987. "Beta-Rayleigh Distribution for Shallow Water Wave Heights," Proceedings of a Conference on Coastal Hydrodynamics, American Society of Civil Engineers, 28 June-1 July 1987, Newark, DE, pp 17-31.

Kuo, C. T., and Kuo, S. T. 1974. "Effect of Wave Breaking on Statistical Distribution of Wave Heights," Proceedings of Civil Engineering in the Oceans, Vol 3, pp 1211-1231.

Long, C. E., and Oltman-Shay, J. M. "Directional Characteristics of Waves in Shallow Water,' Technical Report in preparation, US Army Engineer Waterways Experiment Station, Vicksburg, MS.

Longuet-Higgins, M. S. 1952. "On the Statistical Distribution of the Heights of Sea Waves," Journal of Marine Research, Vol 11, pp 245-266.

_____. 1980. "On the Distribution of the Heights of Sea Waves: Some Effects of Nonlinearity and Finite Bandwidth," Journal of Geophysical Research, Vol 85, pp 1519-1523.

Shore Protection Manual. 1984. 4th Ed., 2 Vols, US Army Engineer Waterways Experiment Station, Coastal Engineering Research Center, US Government Printing Office, Washington, DC.

Thompson, E. F., and Vincent, C. L. 1985. "Significant Wave Height for Shallow Water Design," Journal of the Waterway, Port, Coastal, and Ocean Engineering, American Society of Civil Engineers, Vol 111, pp 828-842.

Thornton, Edward B., and Guza, R. T. 1983. "Transformation of Wave Height Distribution," Journal of Geophysical Research, Vol 88, pp 5925-5938.

APPENDIX A

FREQUENCY-DIRECTION SPECTRA FOR TEST CASES 2 THROUGH 11

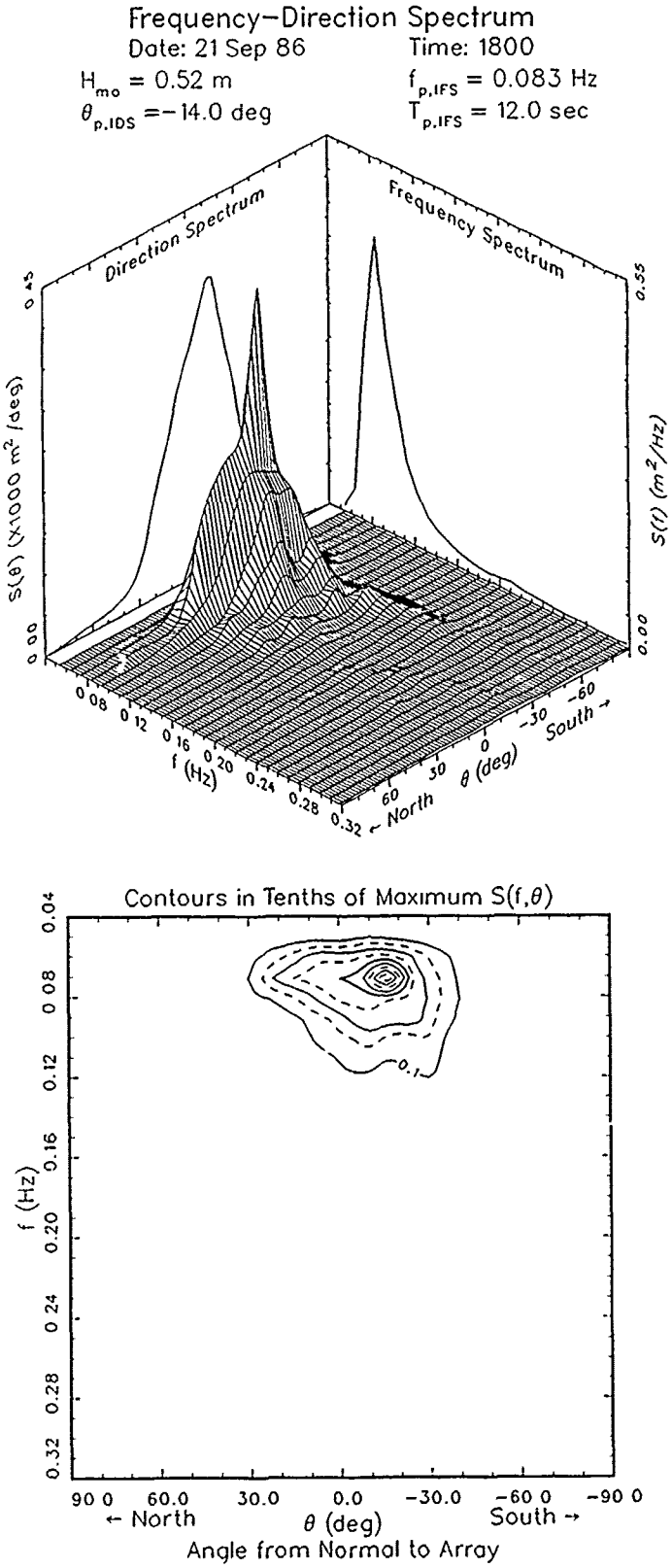

Figure A1. Case 2

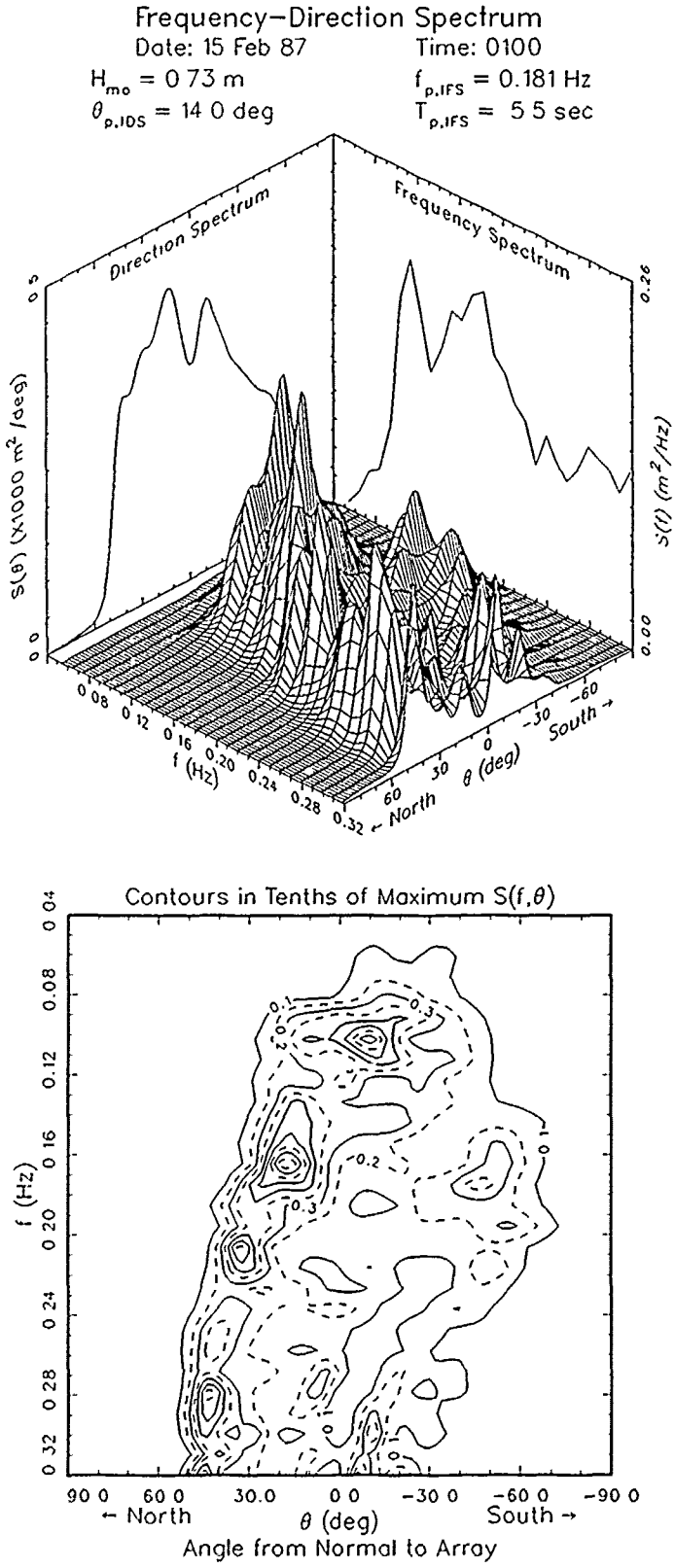

Figure A2. Case 3

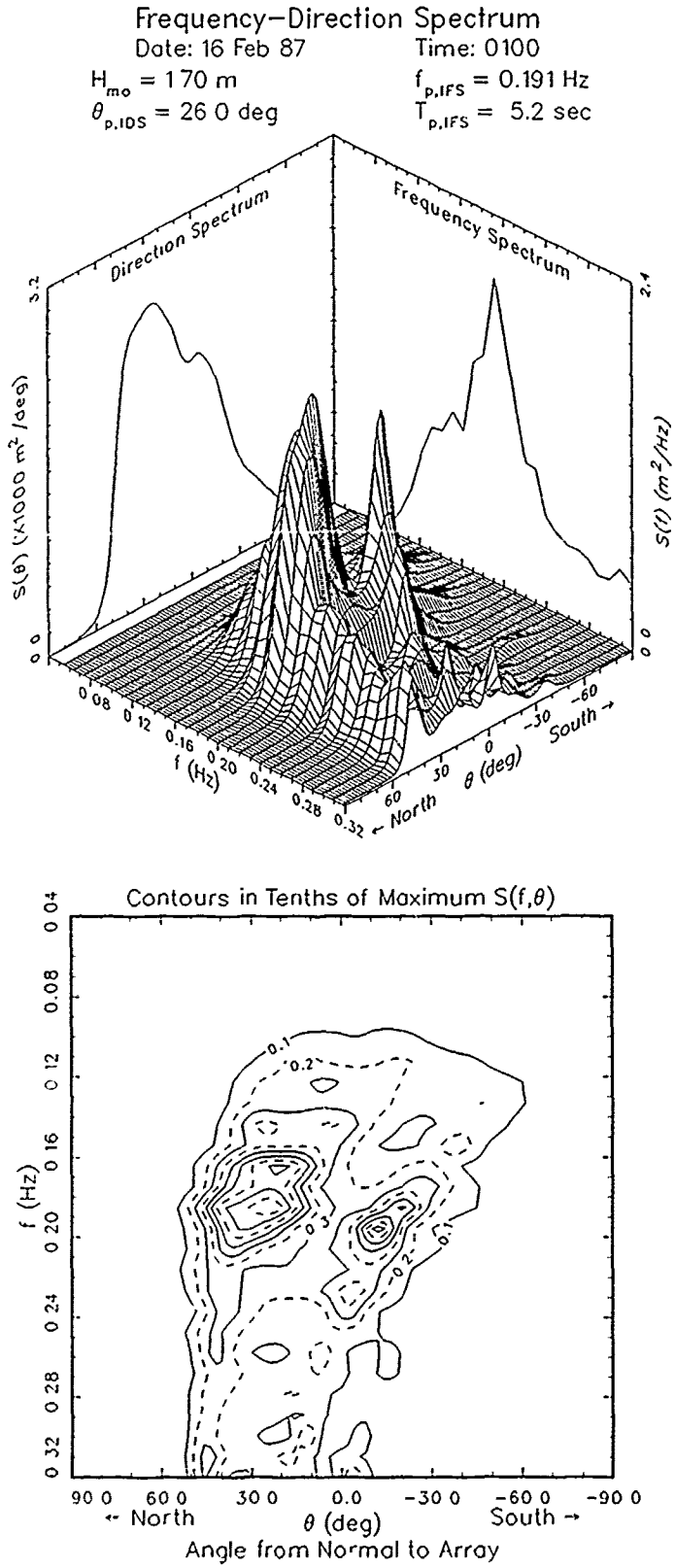

Figure A3. Case 4

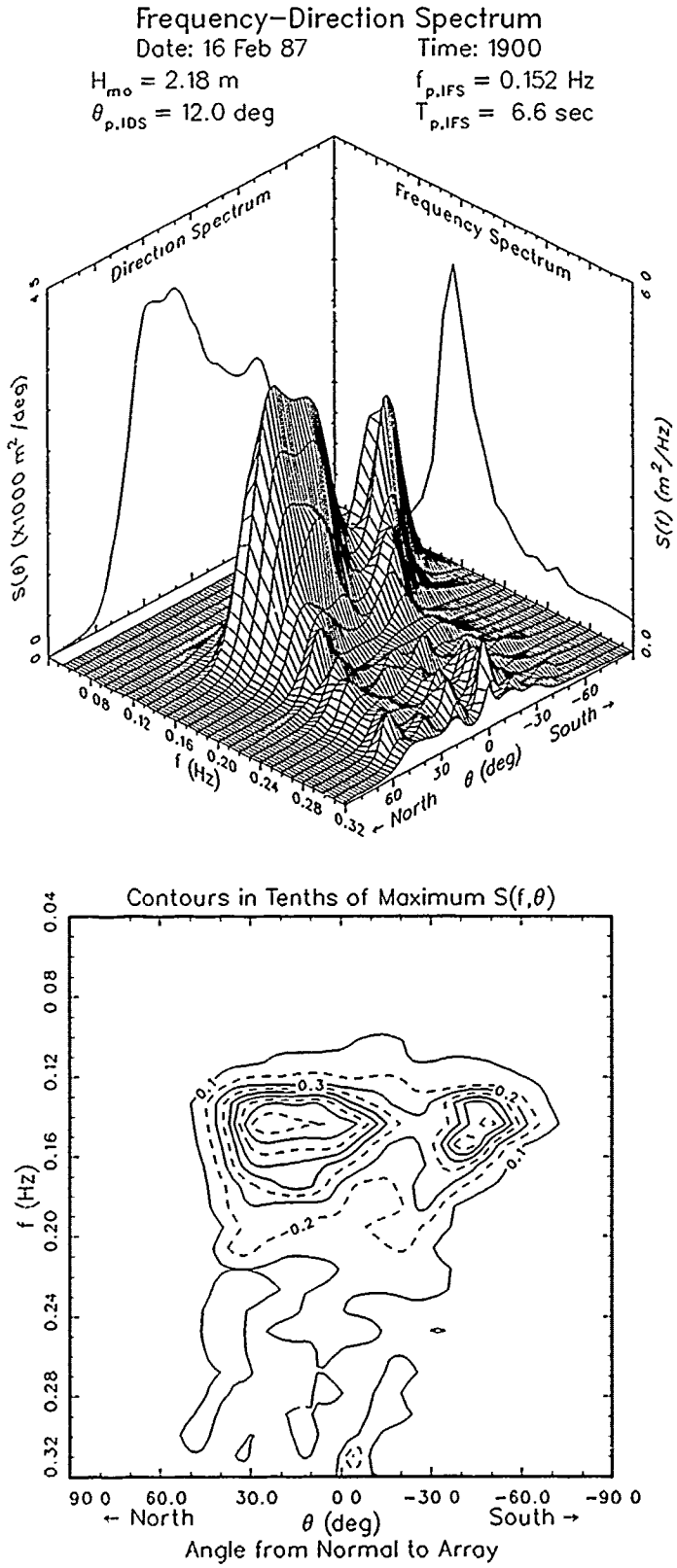

Figure A4. Case 5

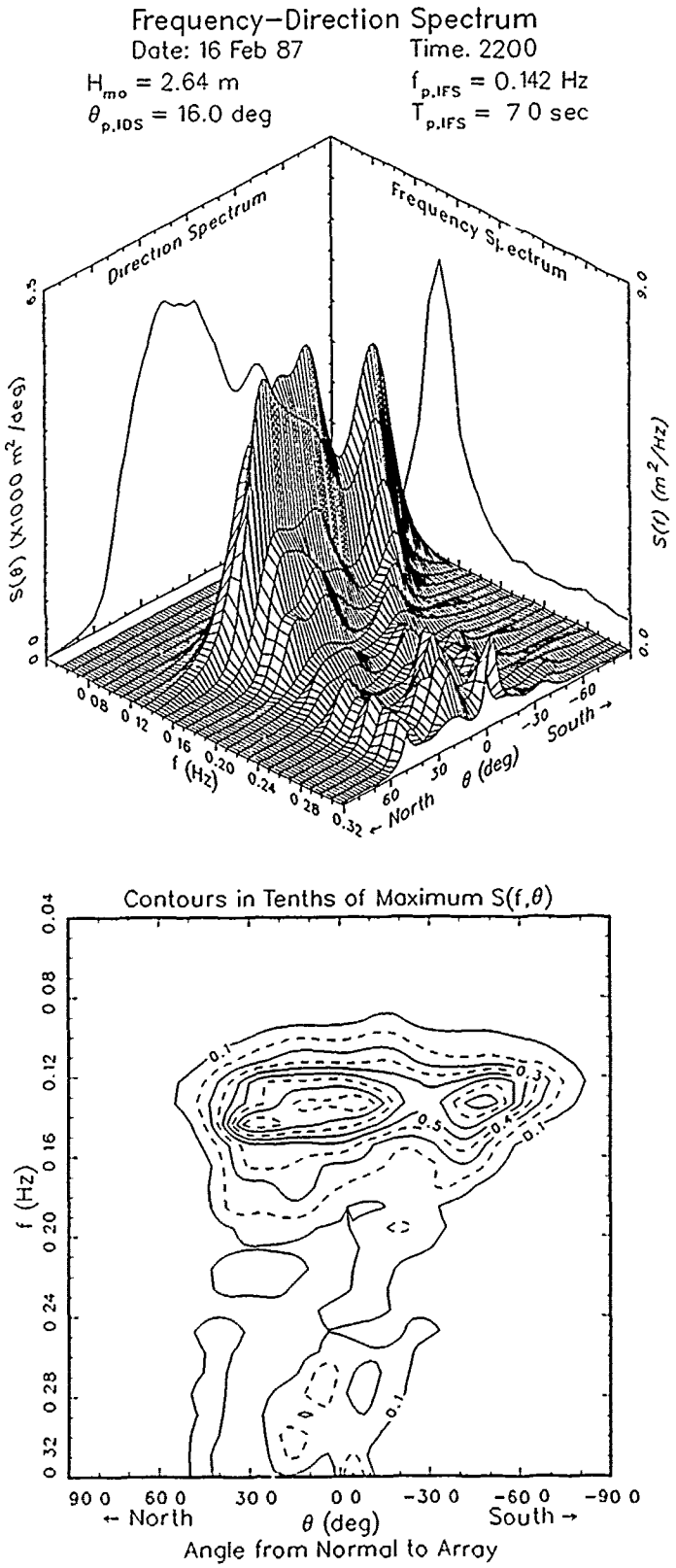

Figure A5. Case 6

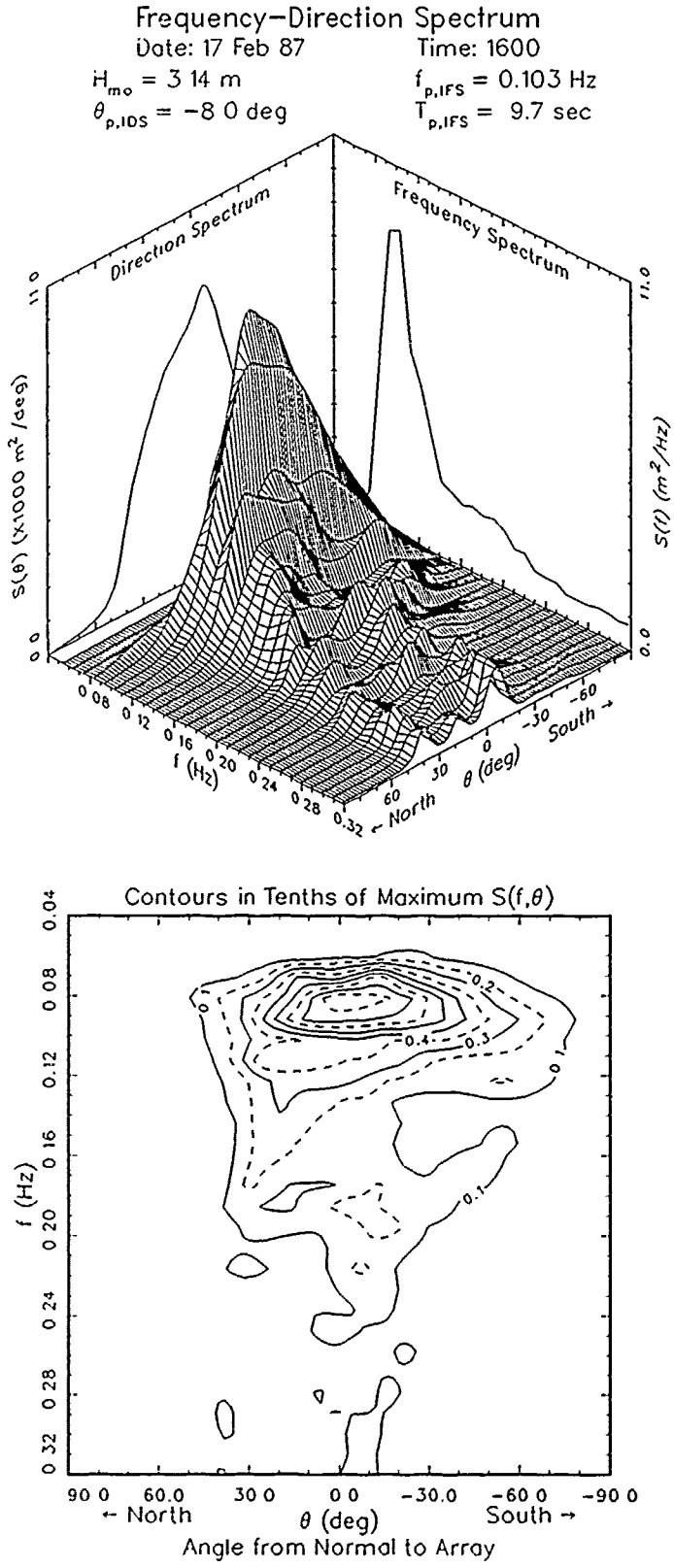

Figure A6. Case 7

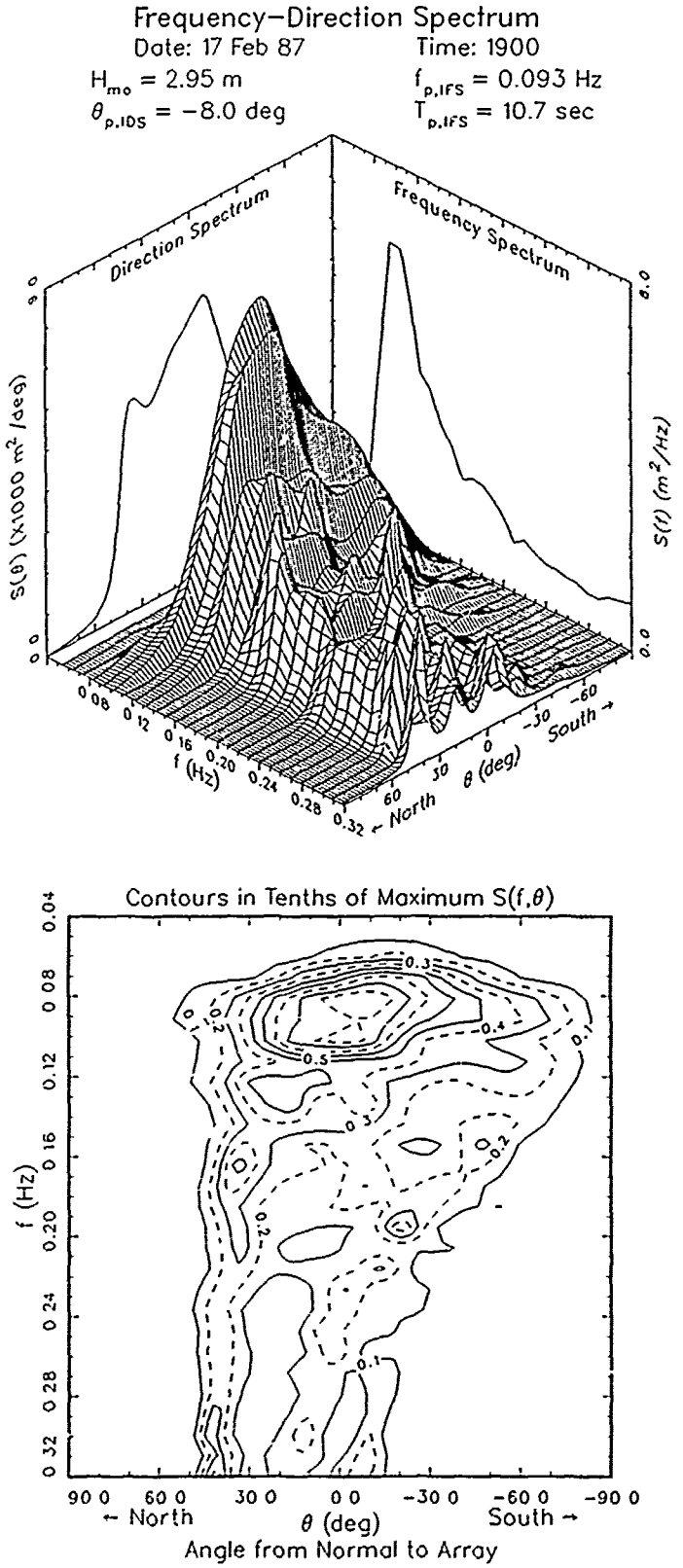

Figure A7. Case 8

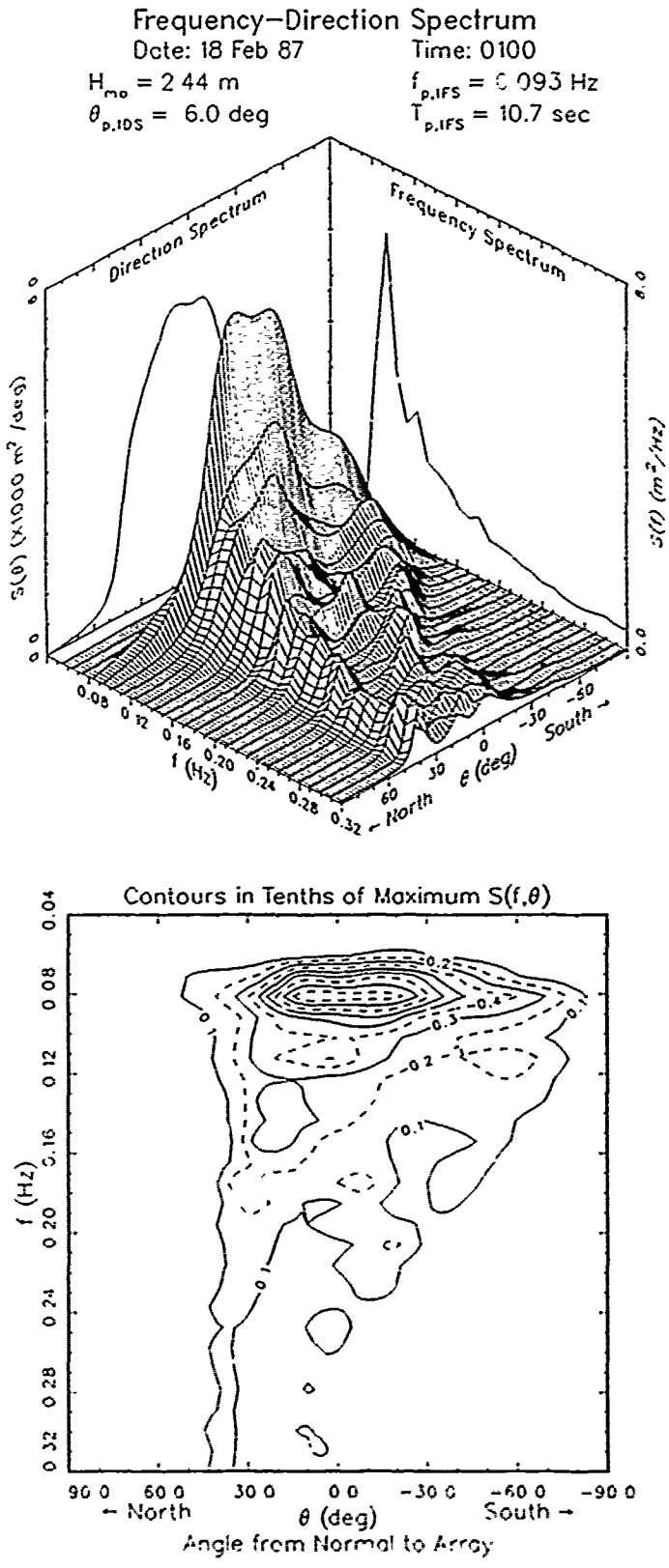

Figure A8. Case 9

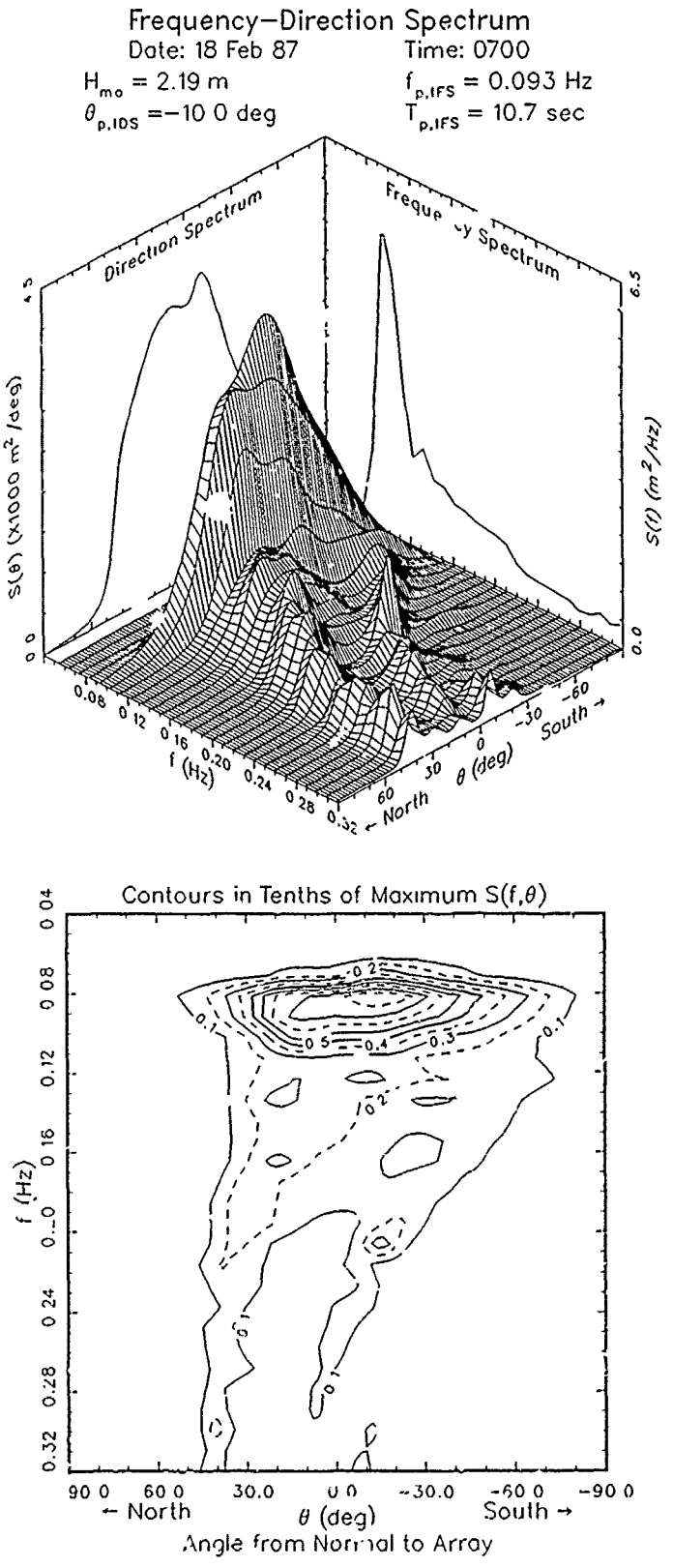

Figure A9. Case 10

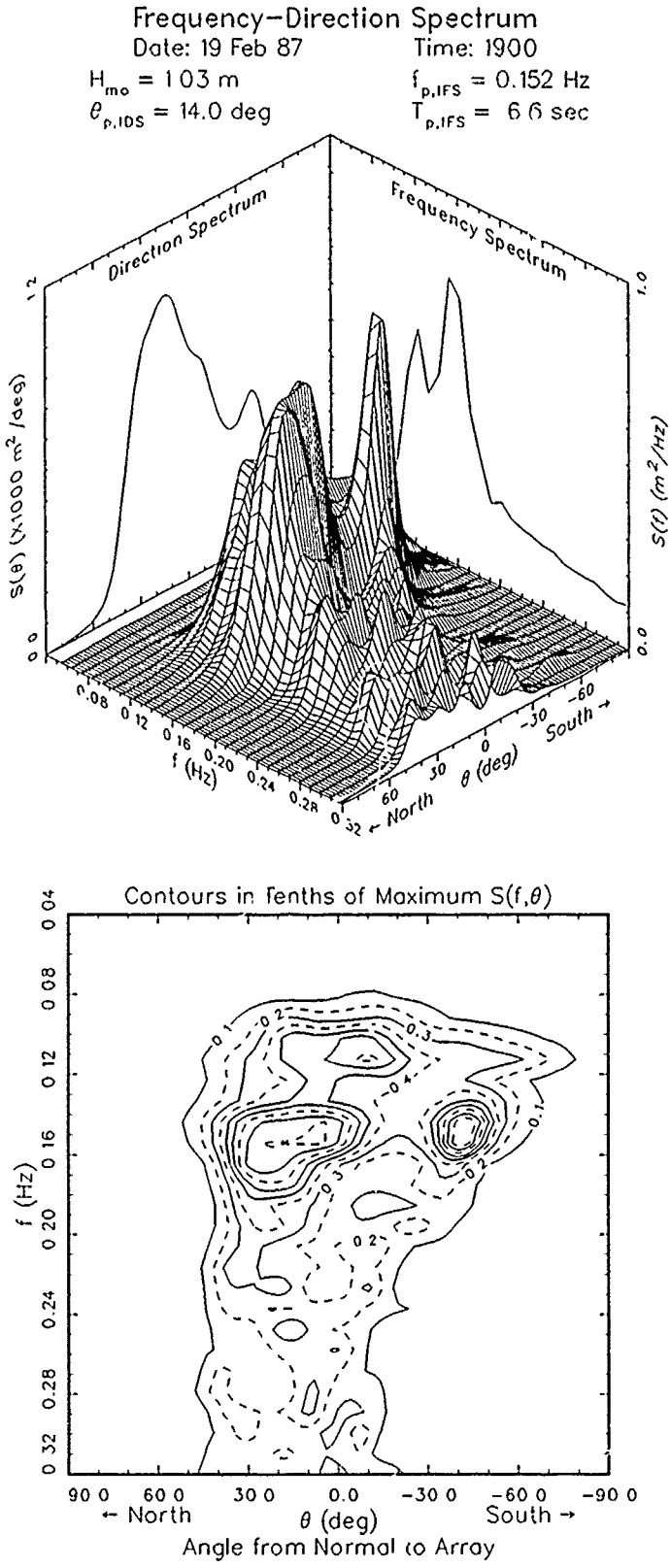

Figure A10. Case 11

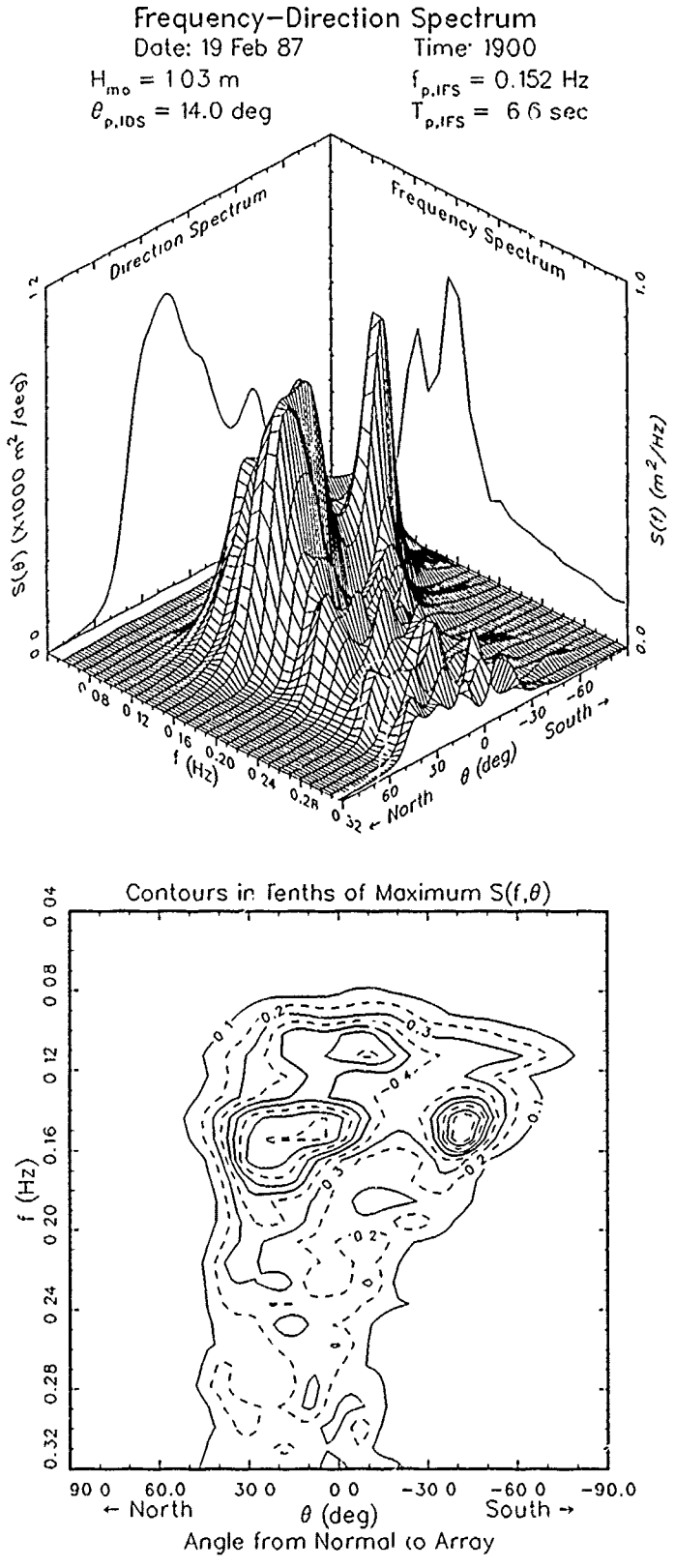

Figure A10. Case 11

APPENDIX B

WAVERIDER FREQUENCY SPECTRA FOR TEST CASES 2 THROUGH 11

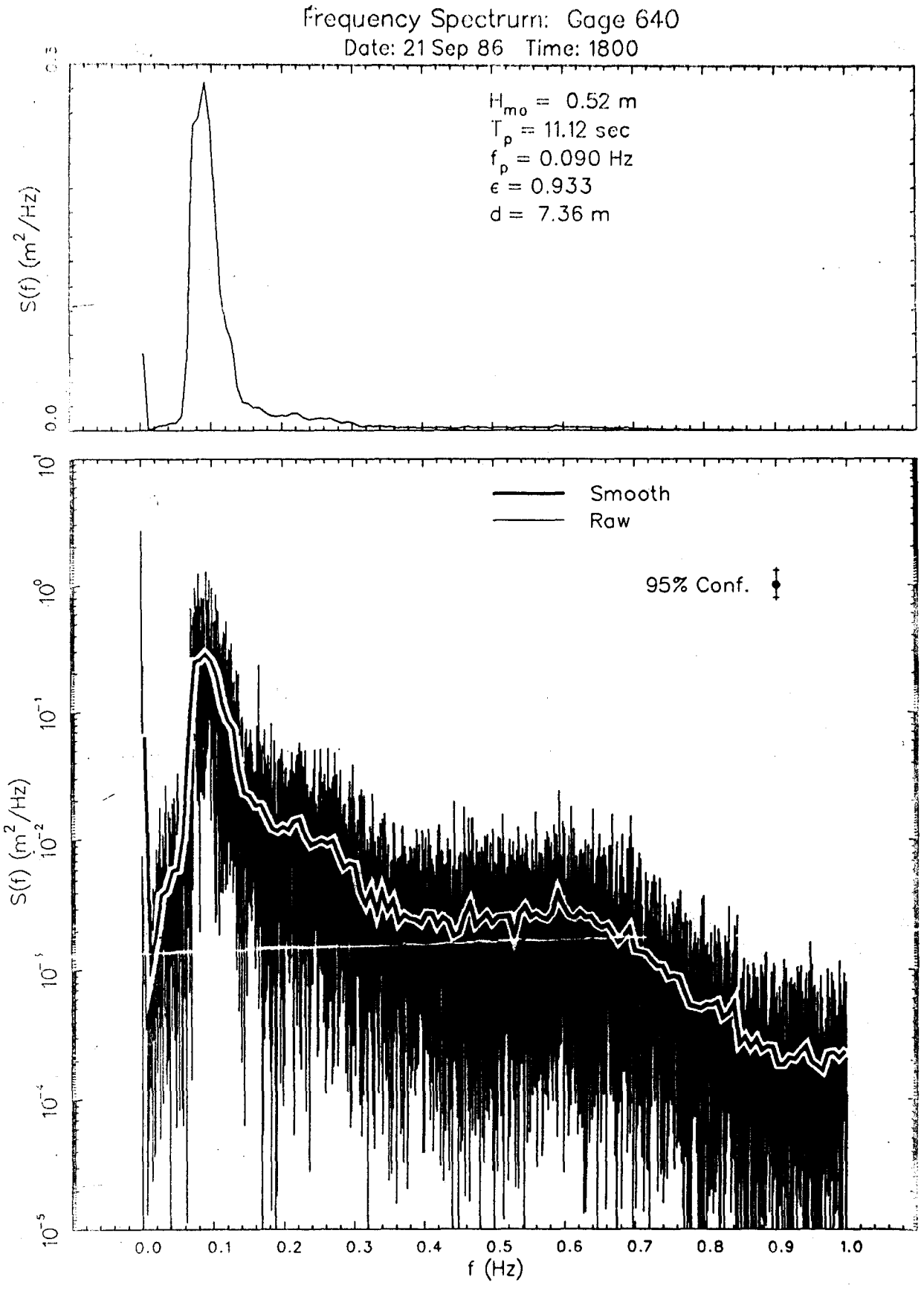

Figure B1. Case 2

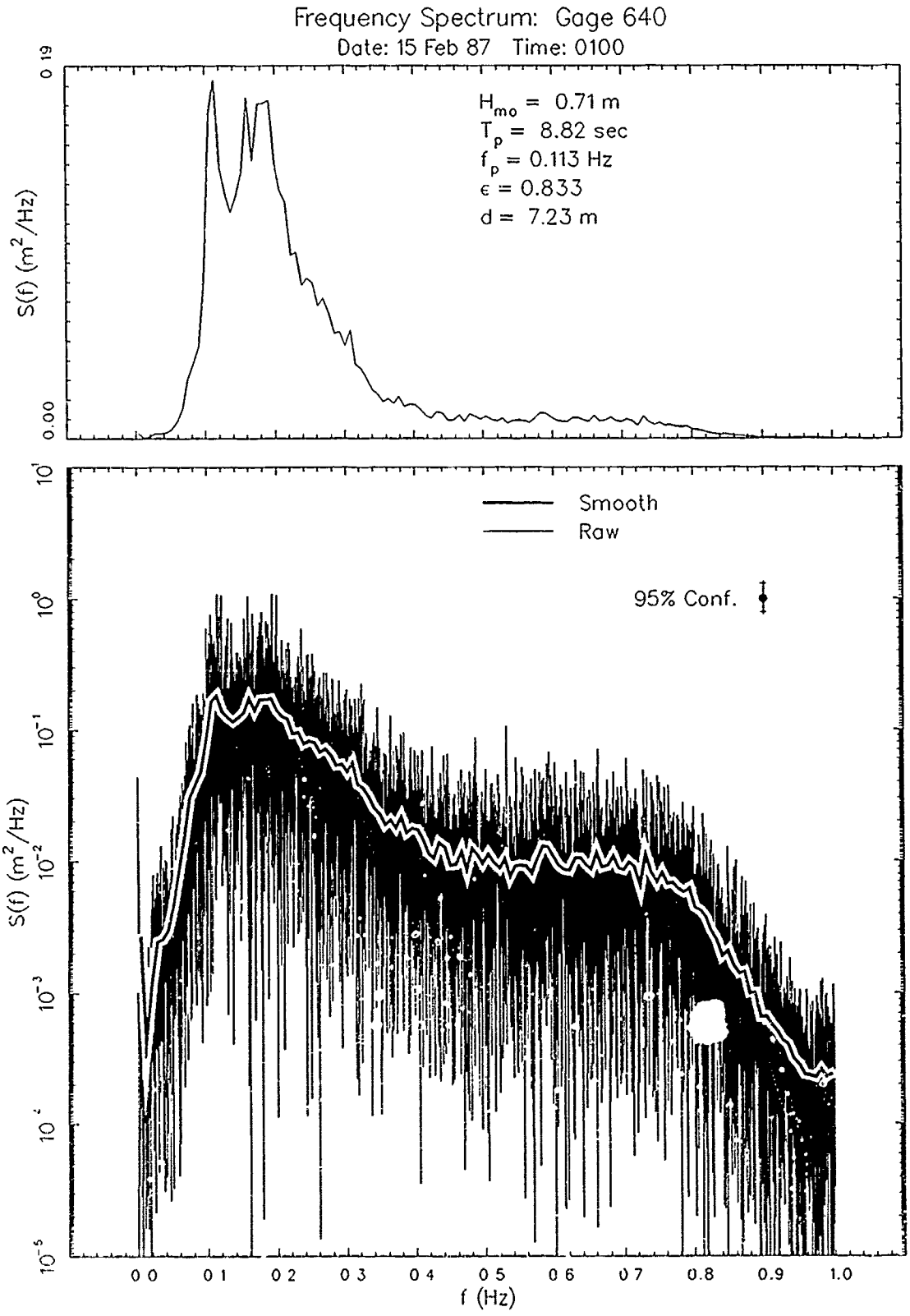

Figure B2. Case 3

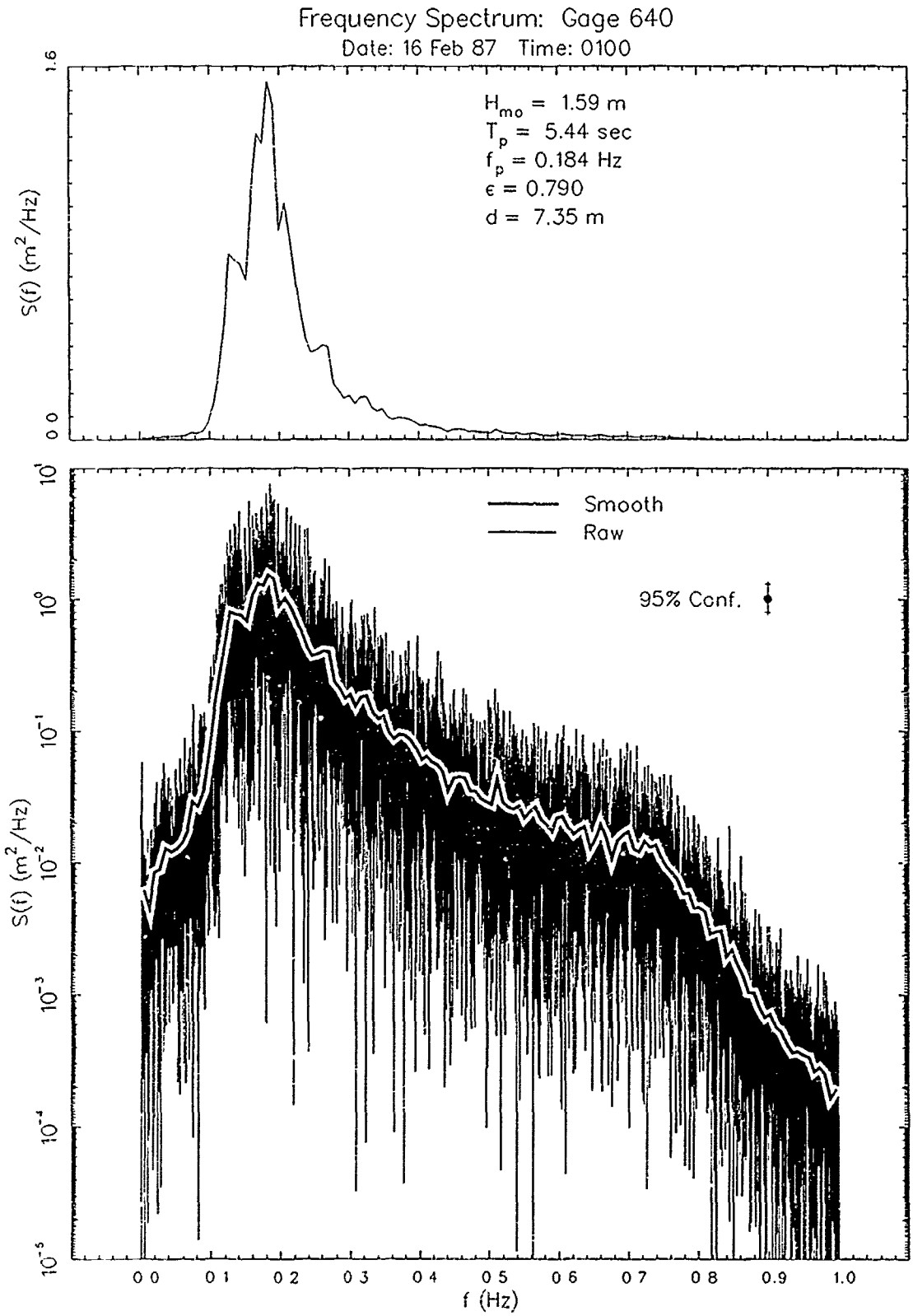

Figure B3. Case 4

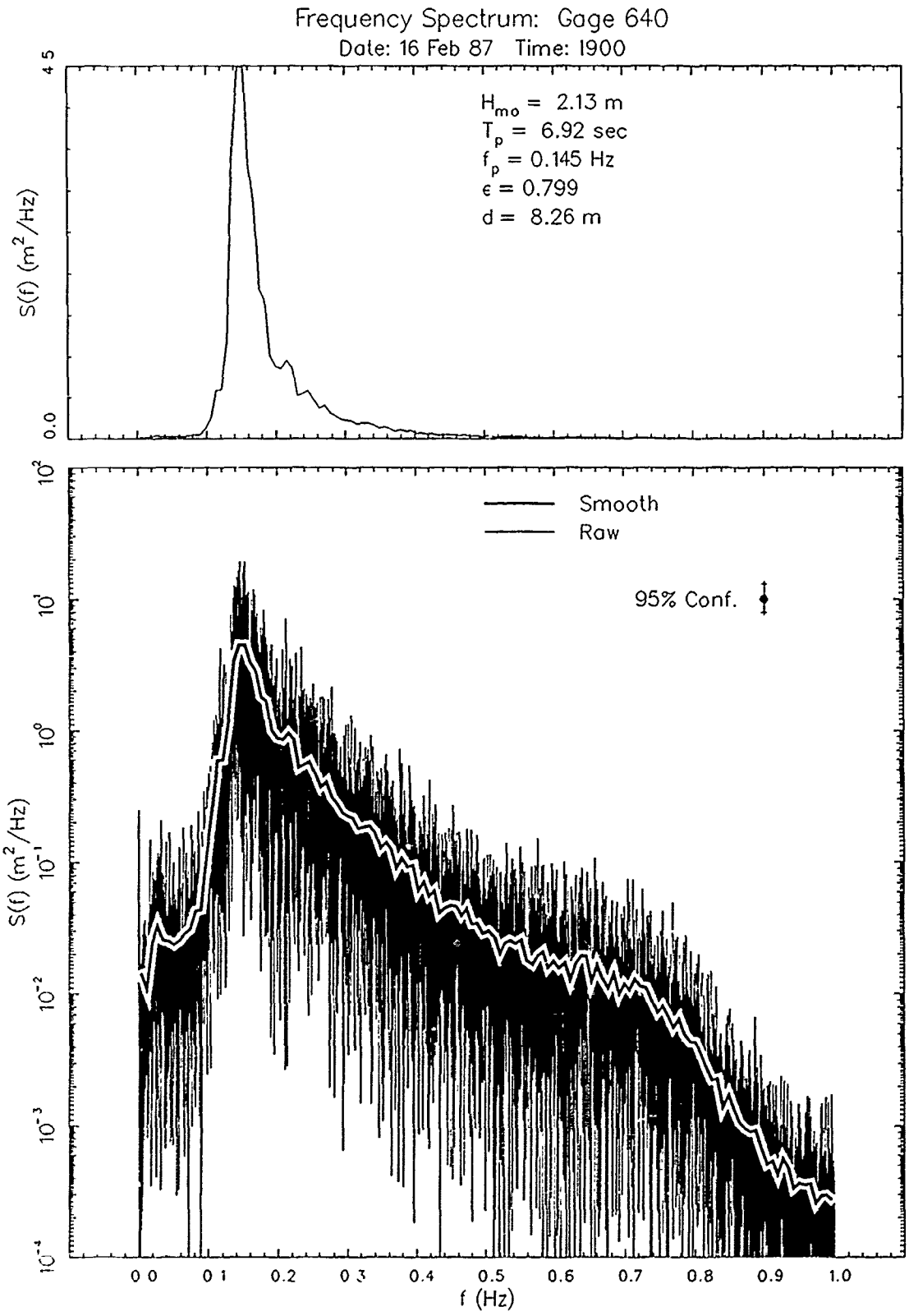

Figure B4. Case 5

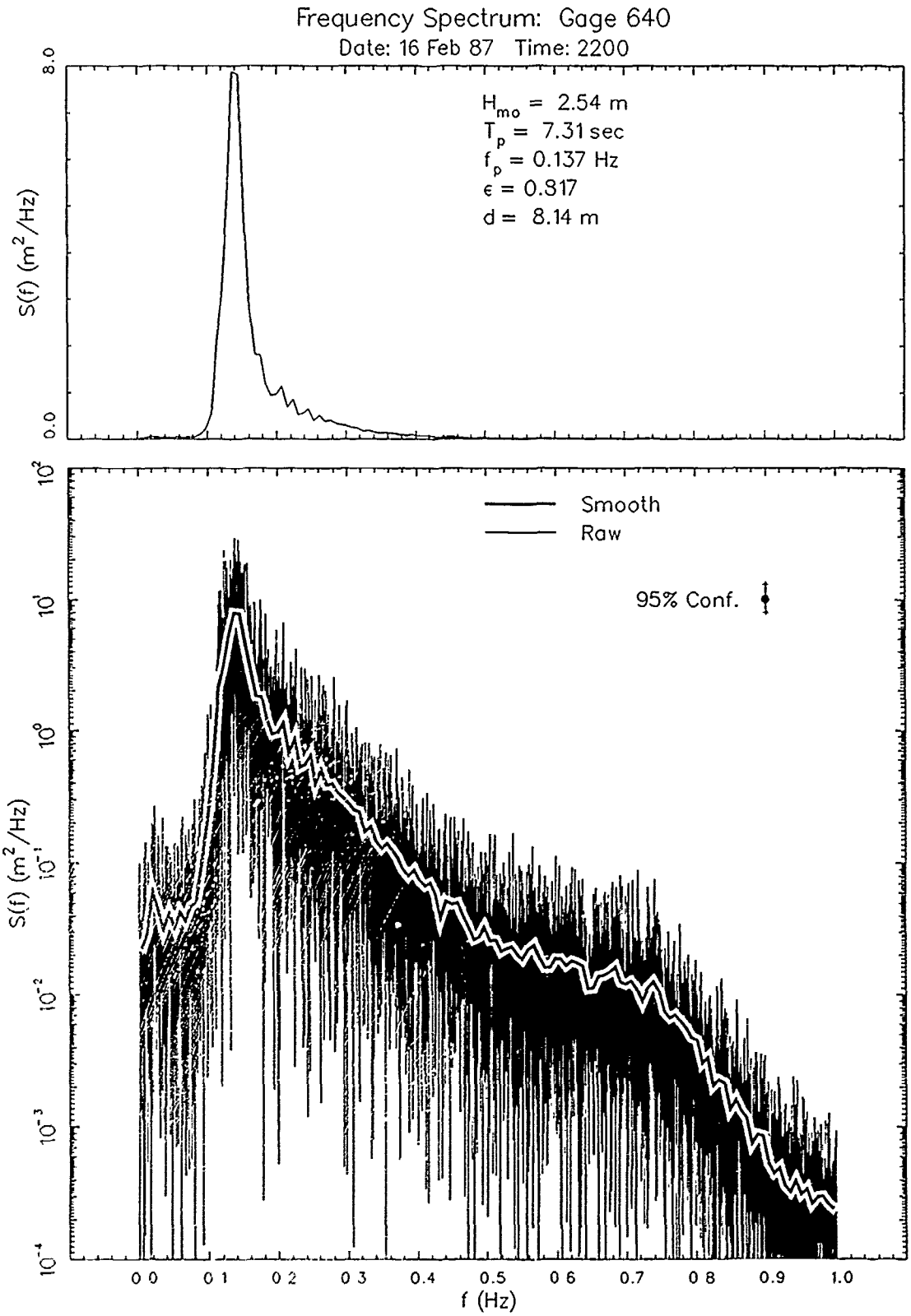

Figure B5. Case 6

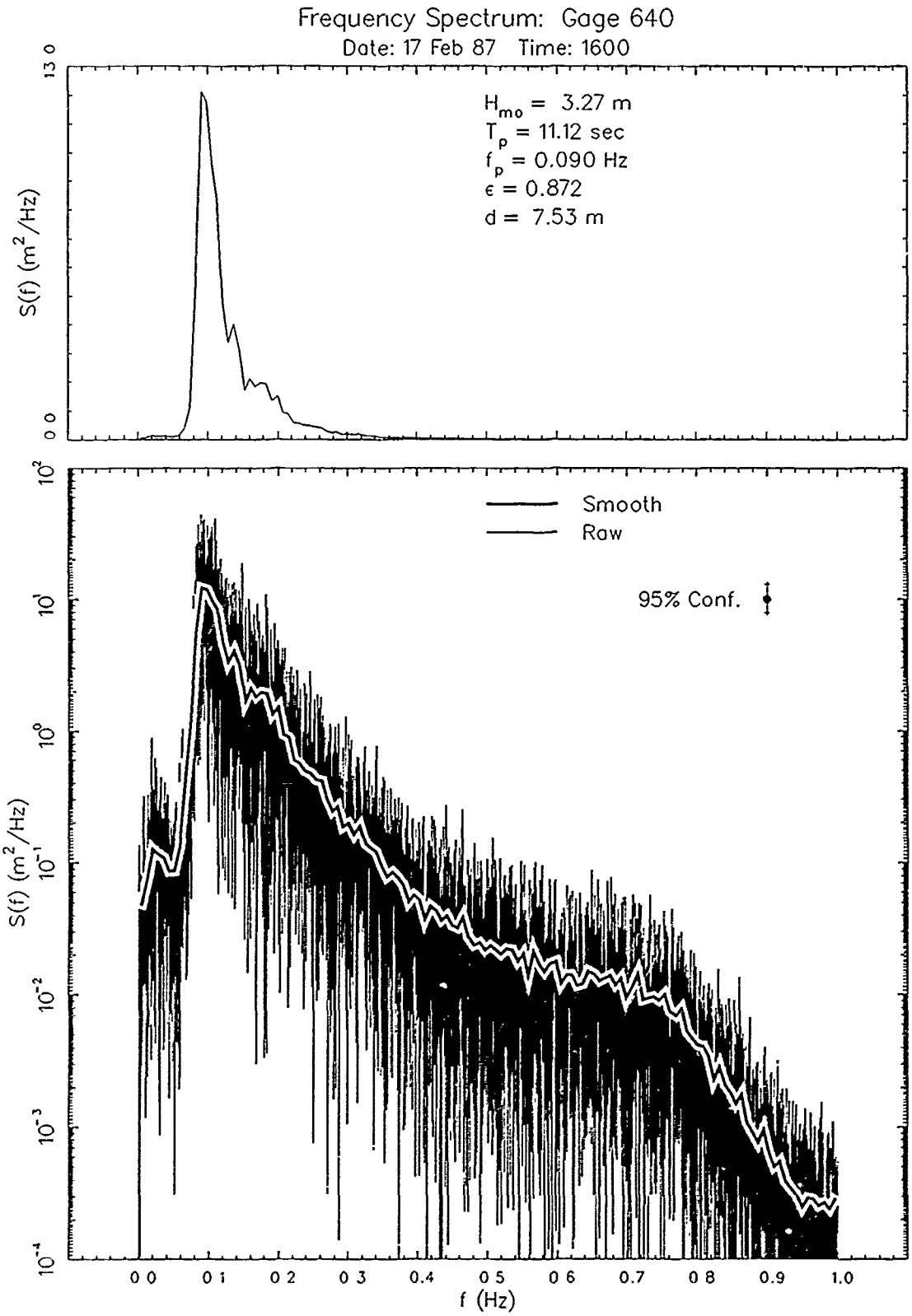

Figure B6. Case 7

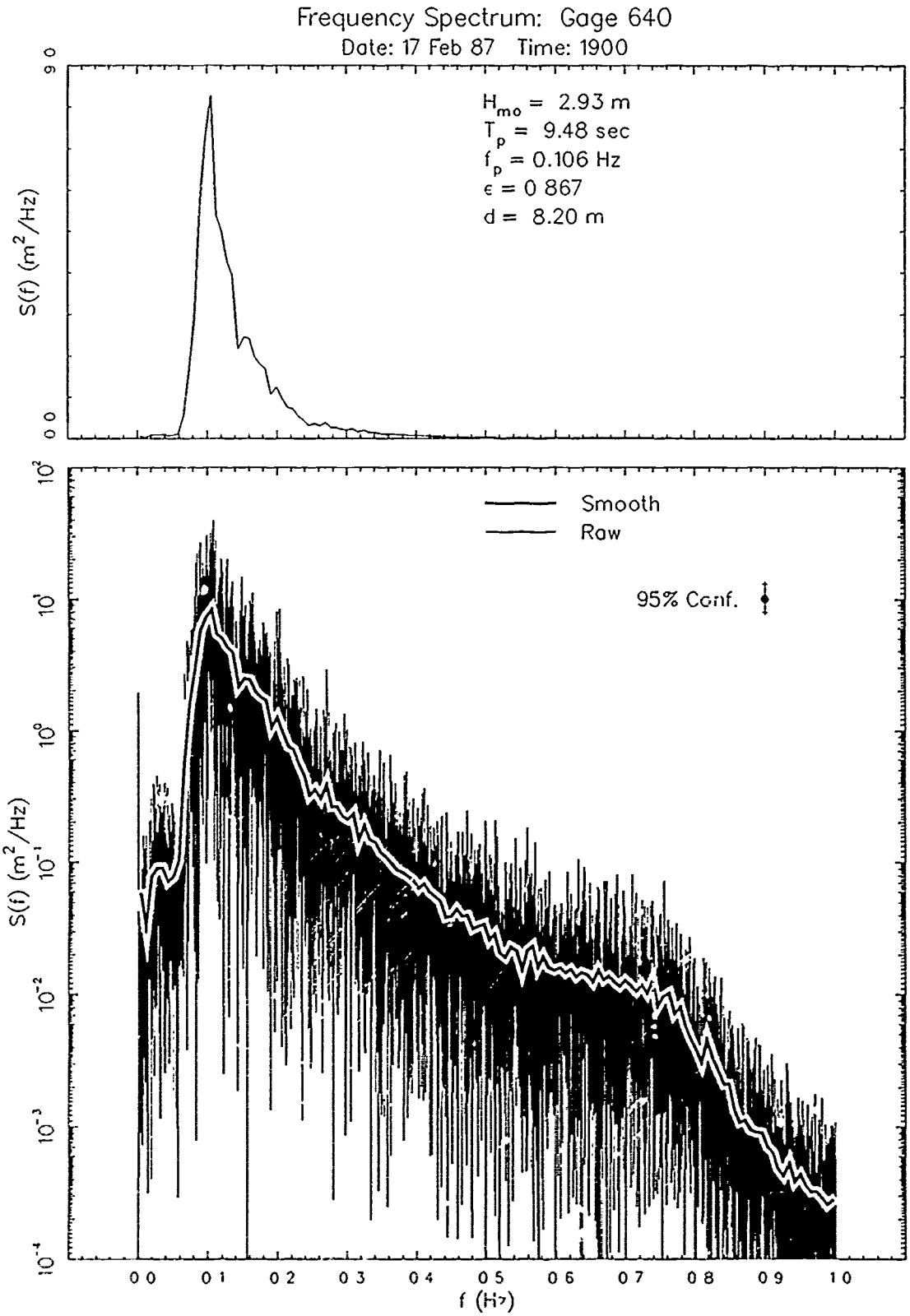

Figure B7. Case 8

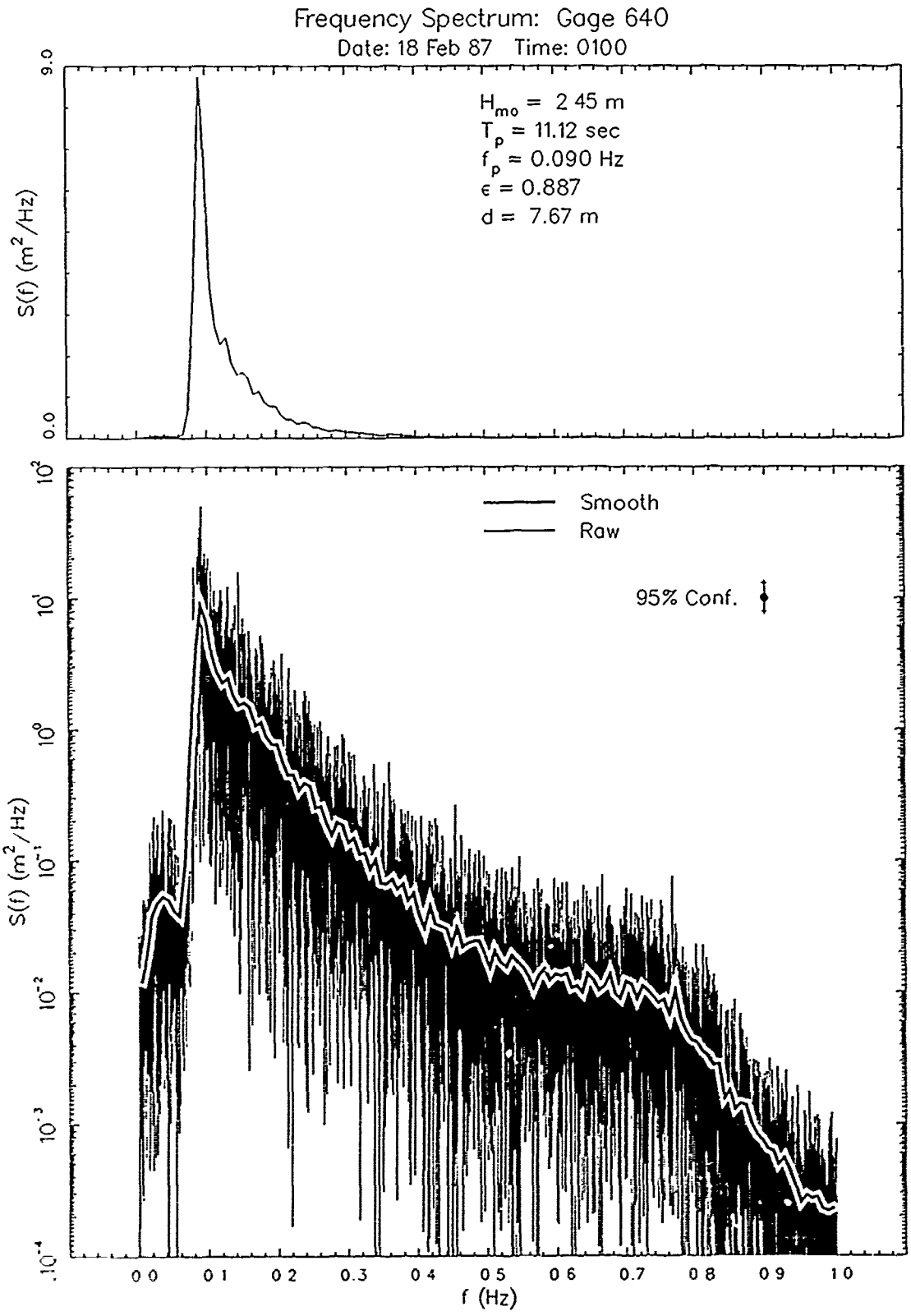

Figure B8. Case 9

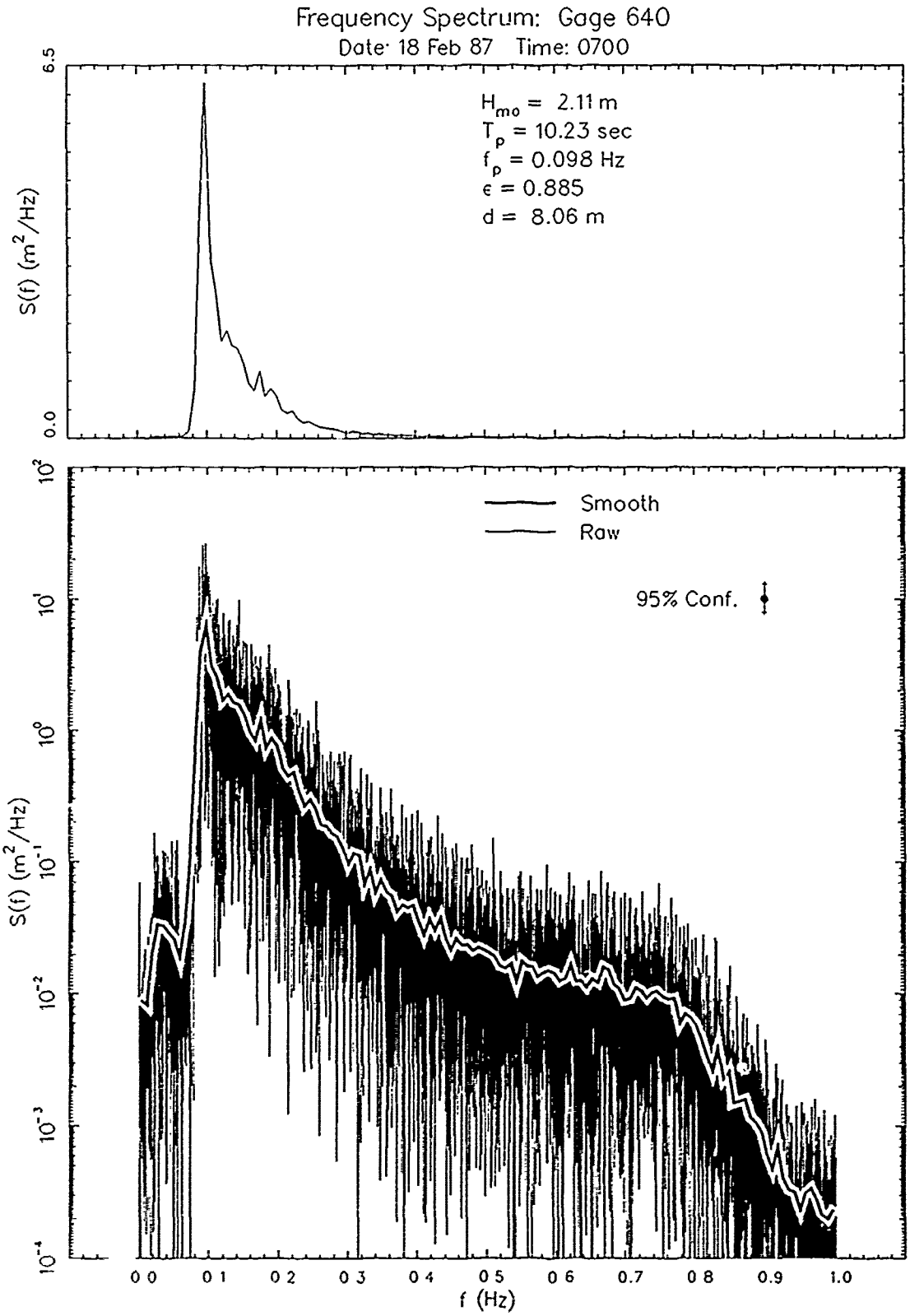

Figure B9. Case 10

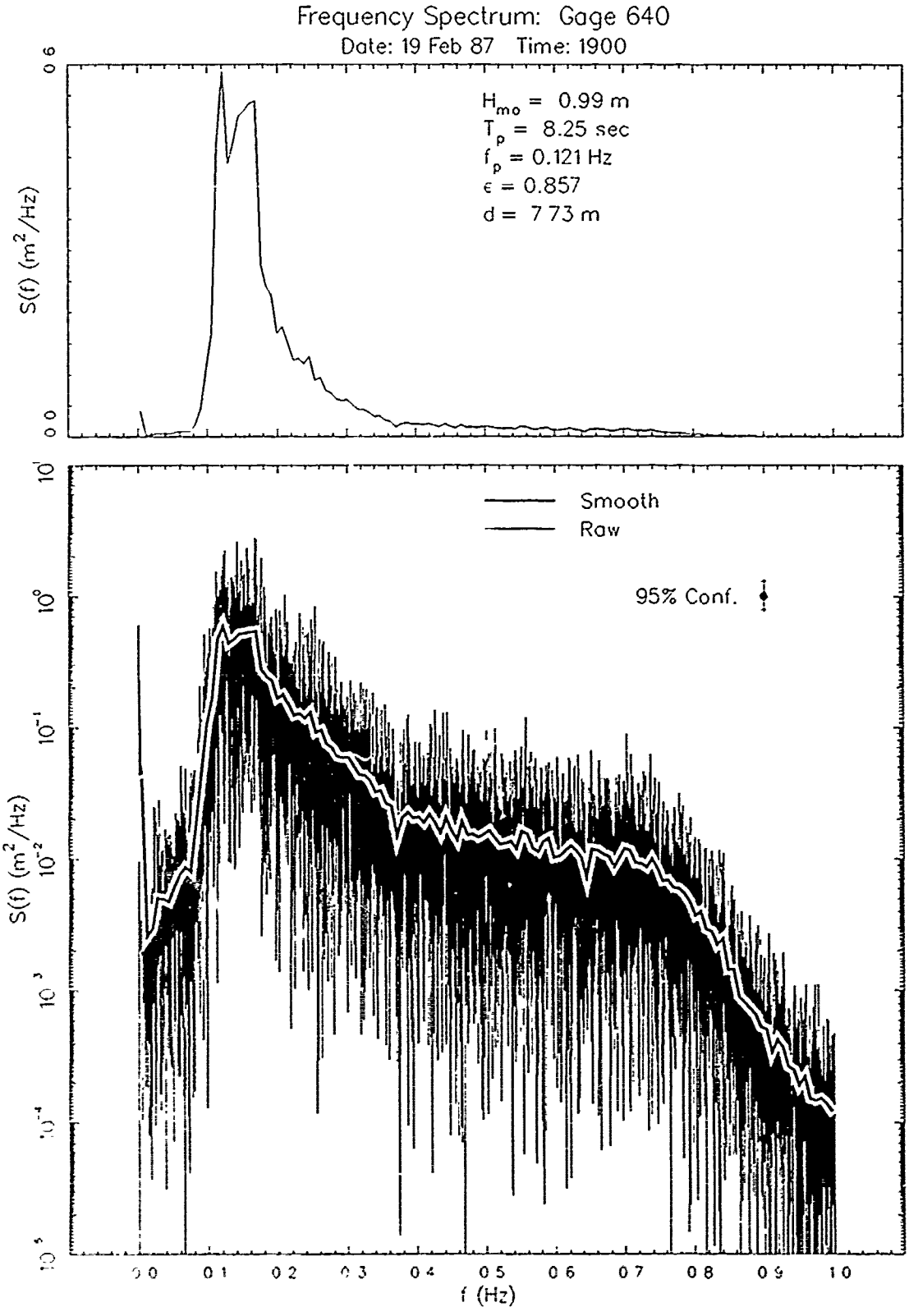

Figure B10. Case 11

APPENDIX C

WAVE HEIGHT DISTRIBUTIONS FOR TEST CASES 2 THROUGH 11

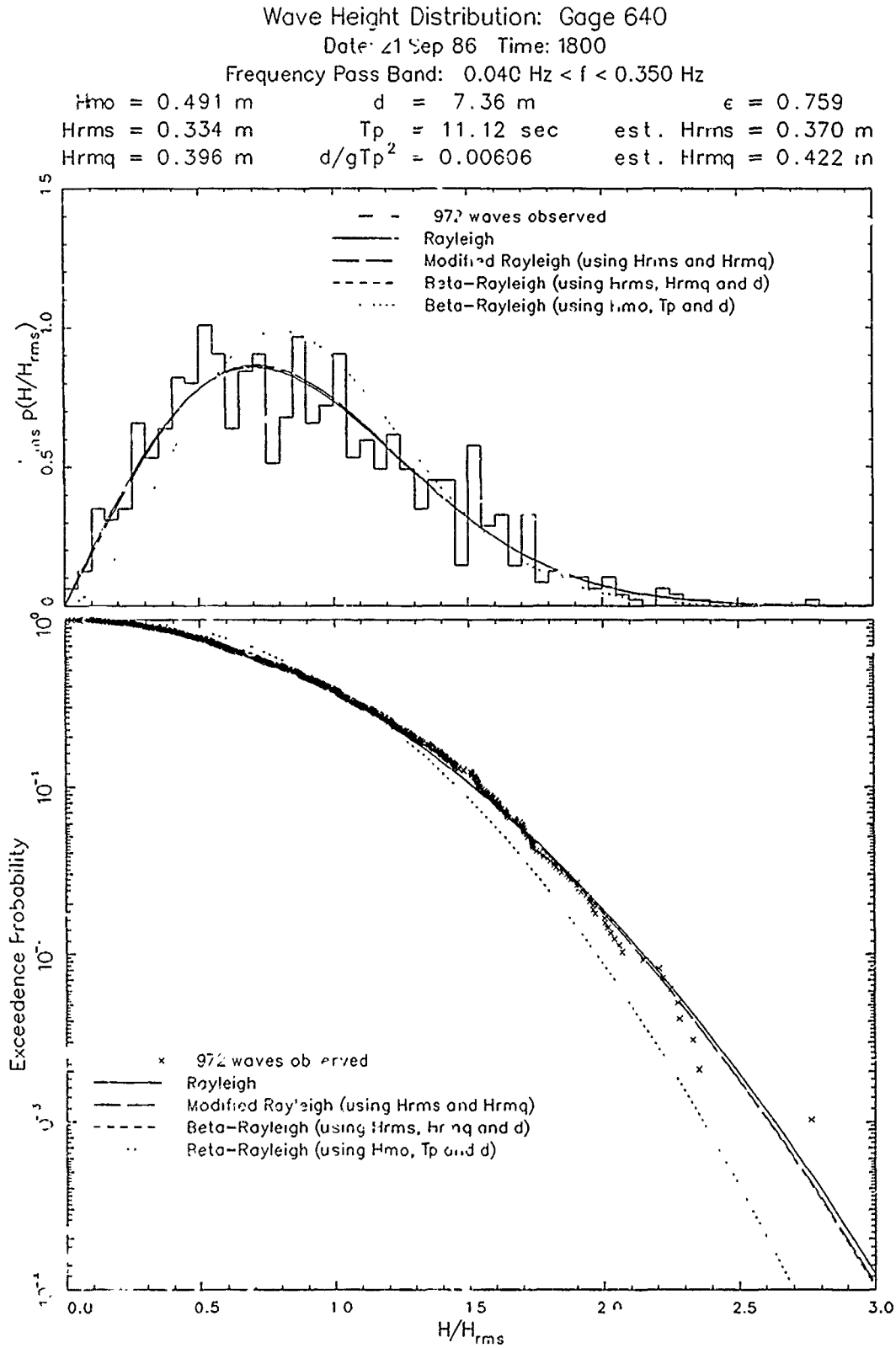

Figure C1. Case 2

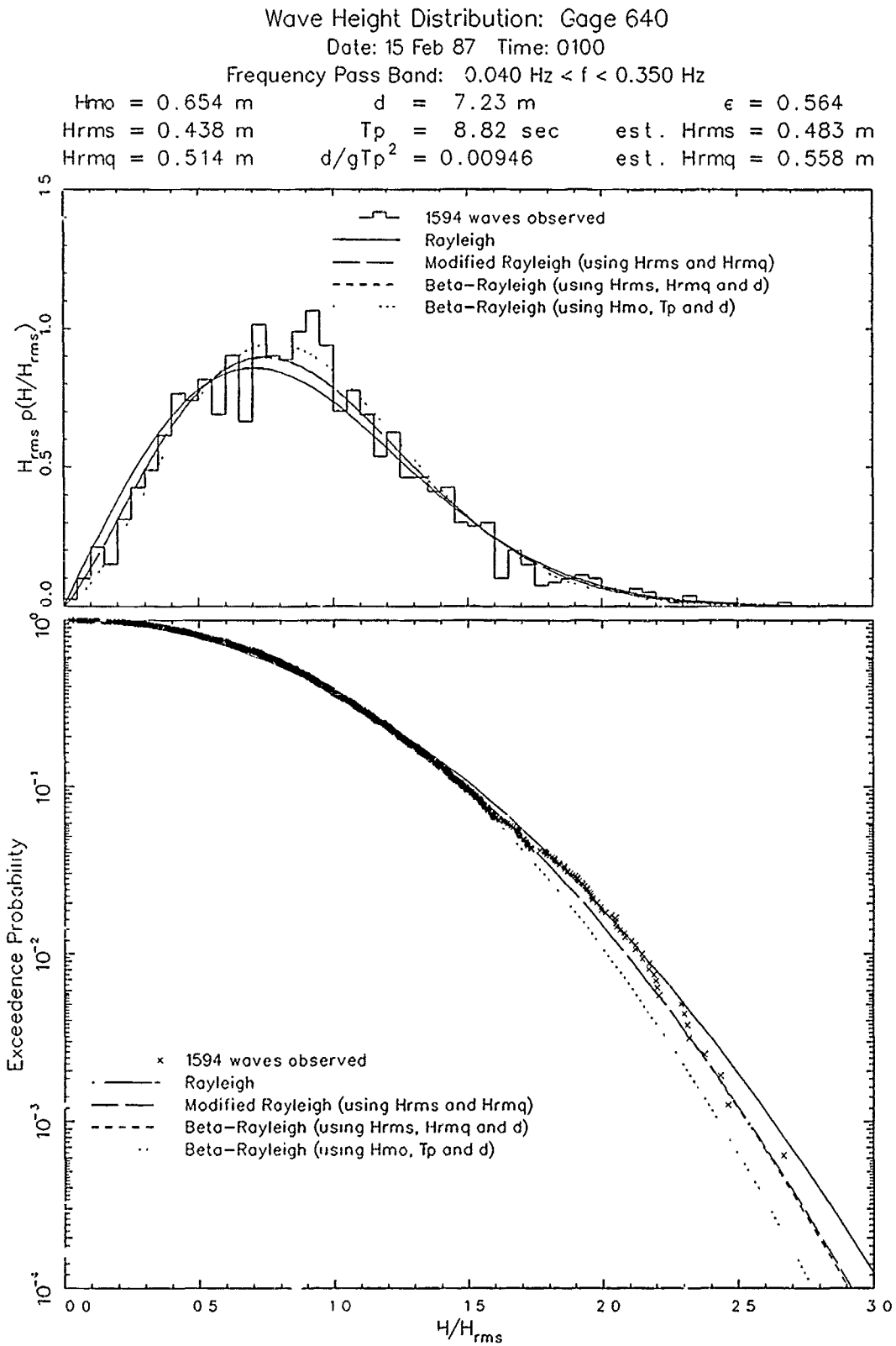

Figure C2. Case 3

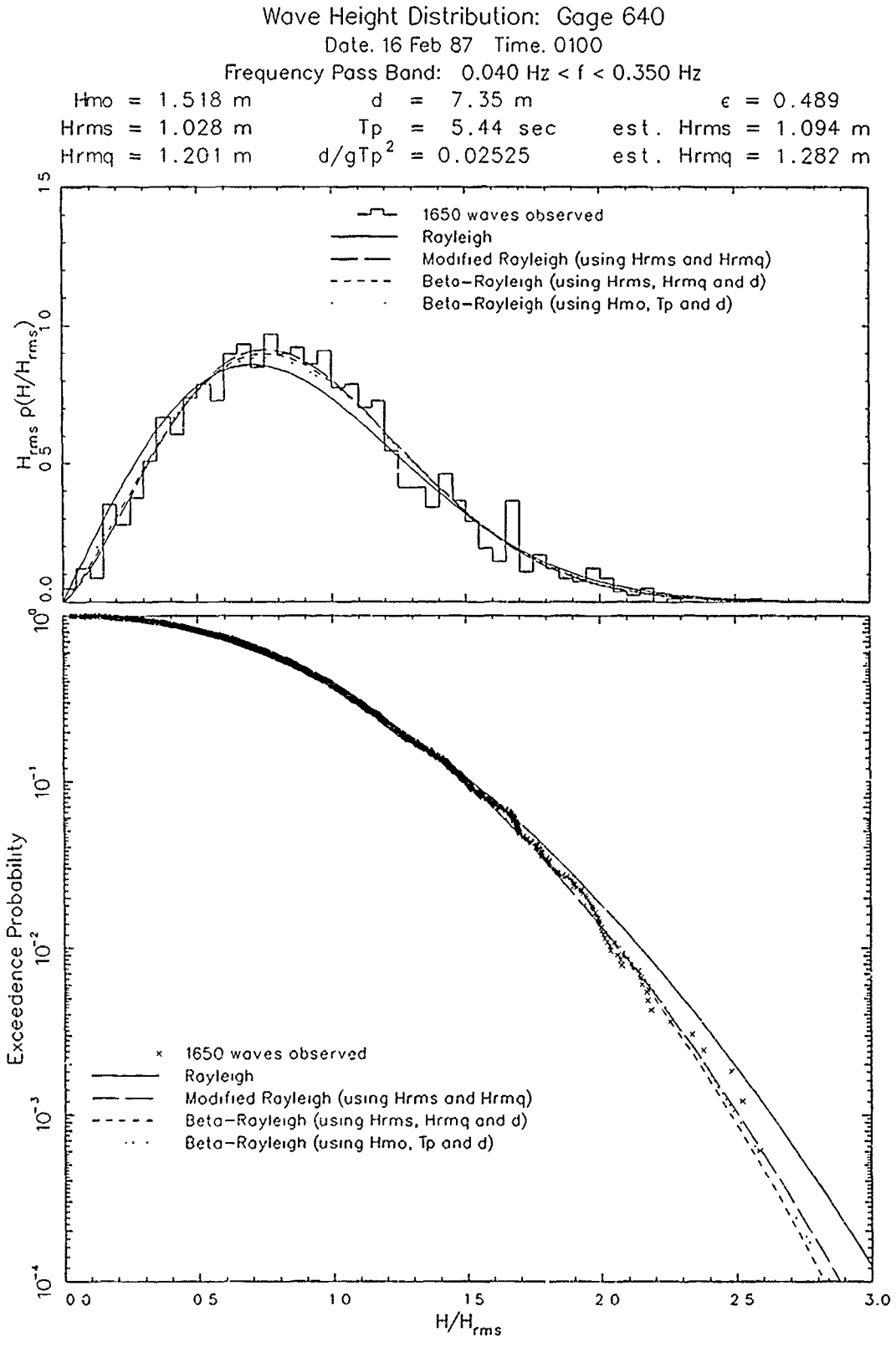

Figure C3. Case 4

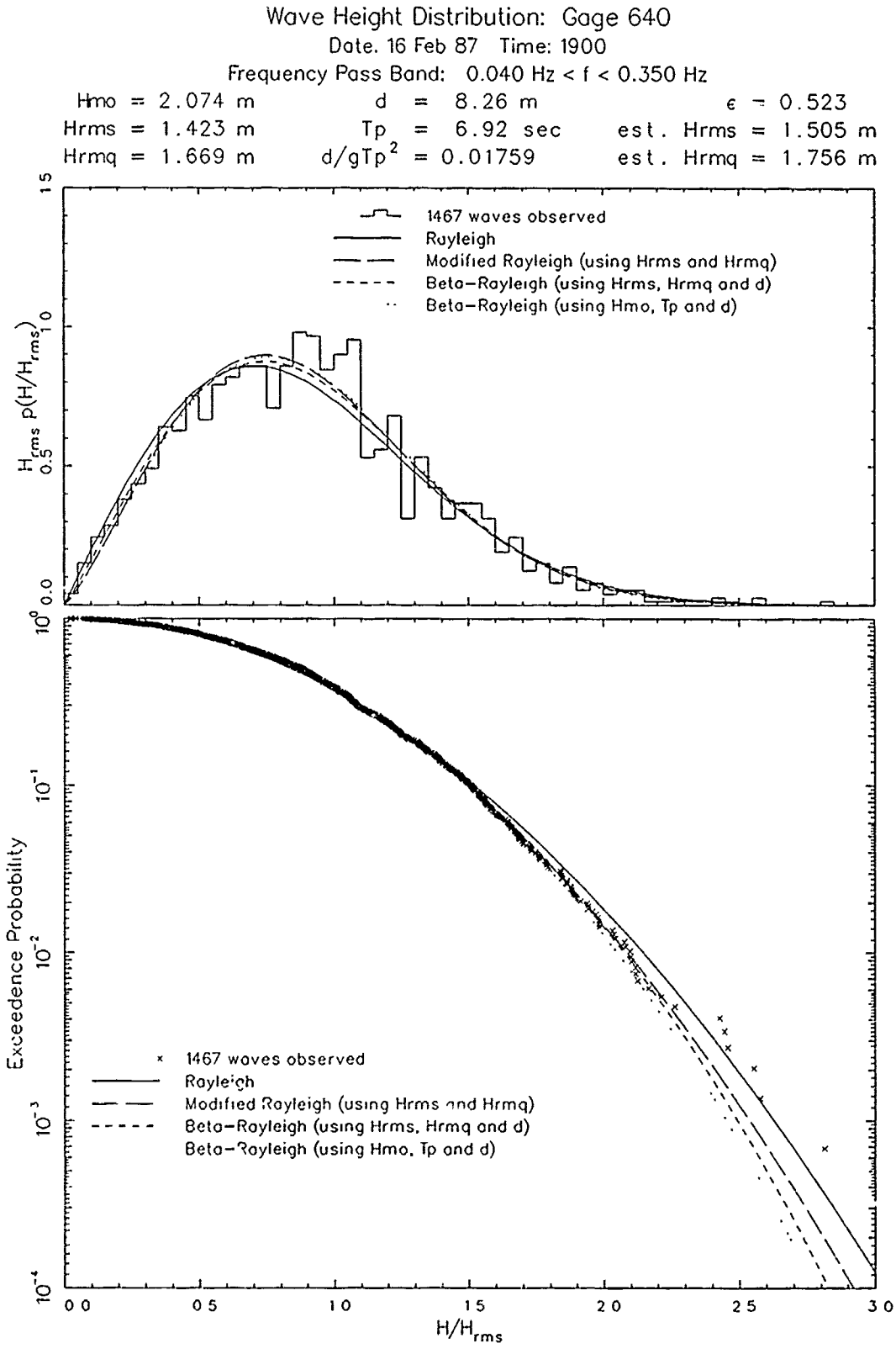

Figure C4. Case 5

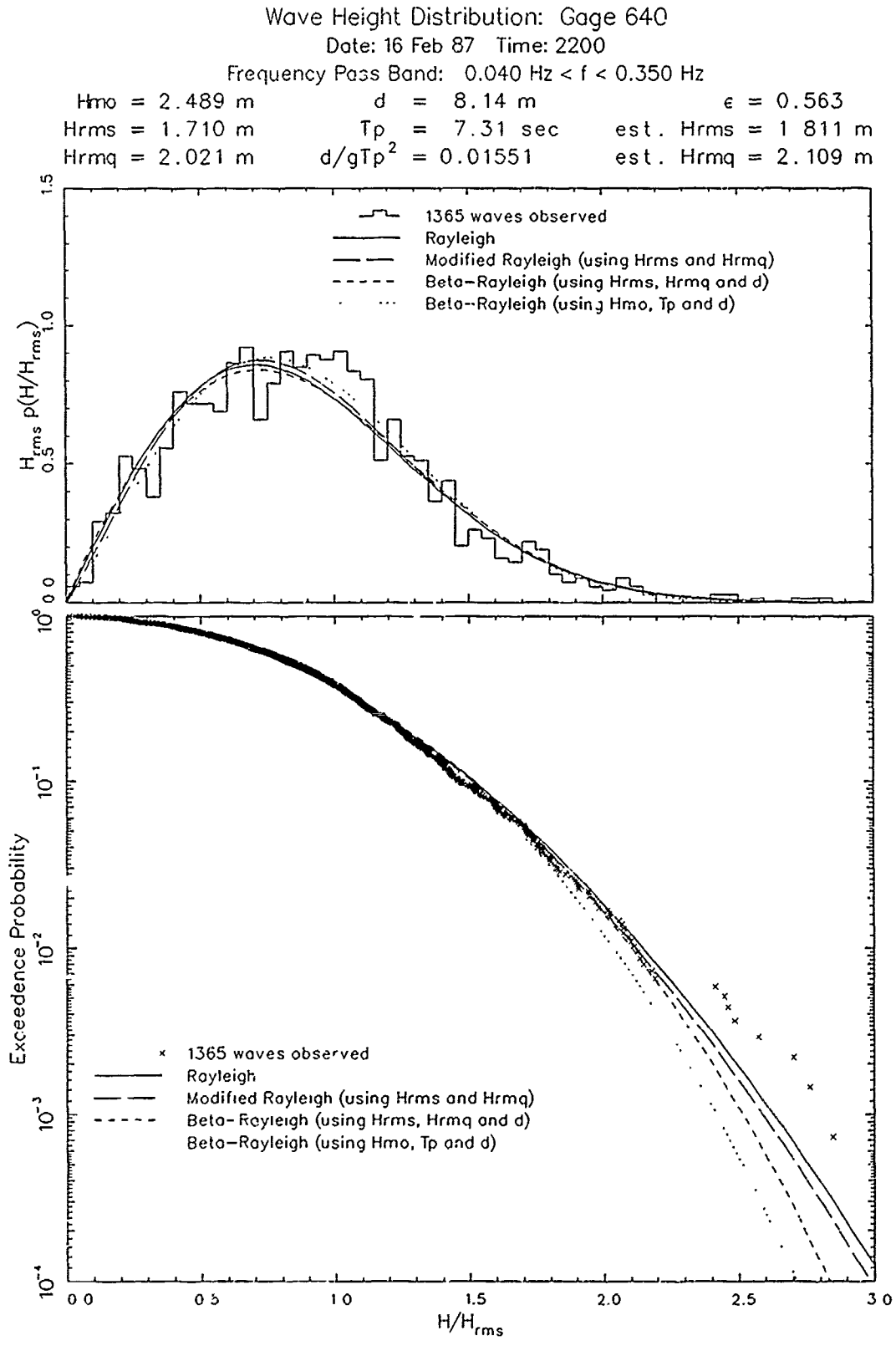

Figure C5. Case 6

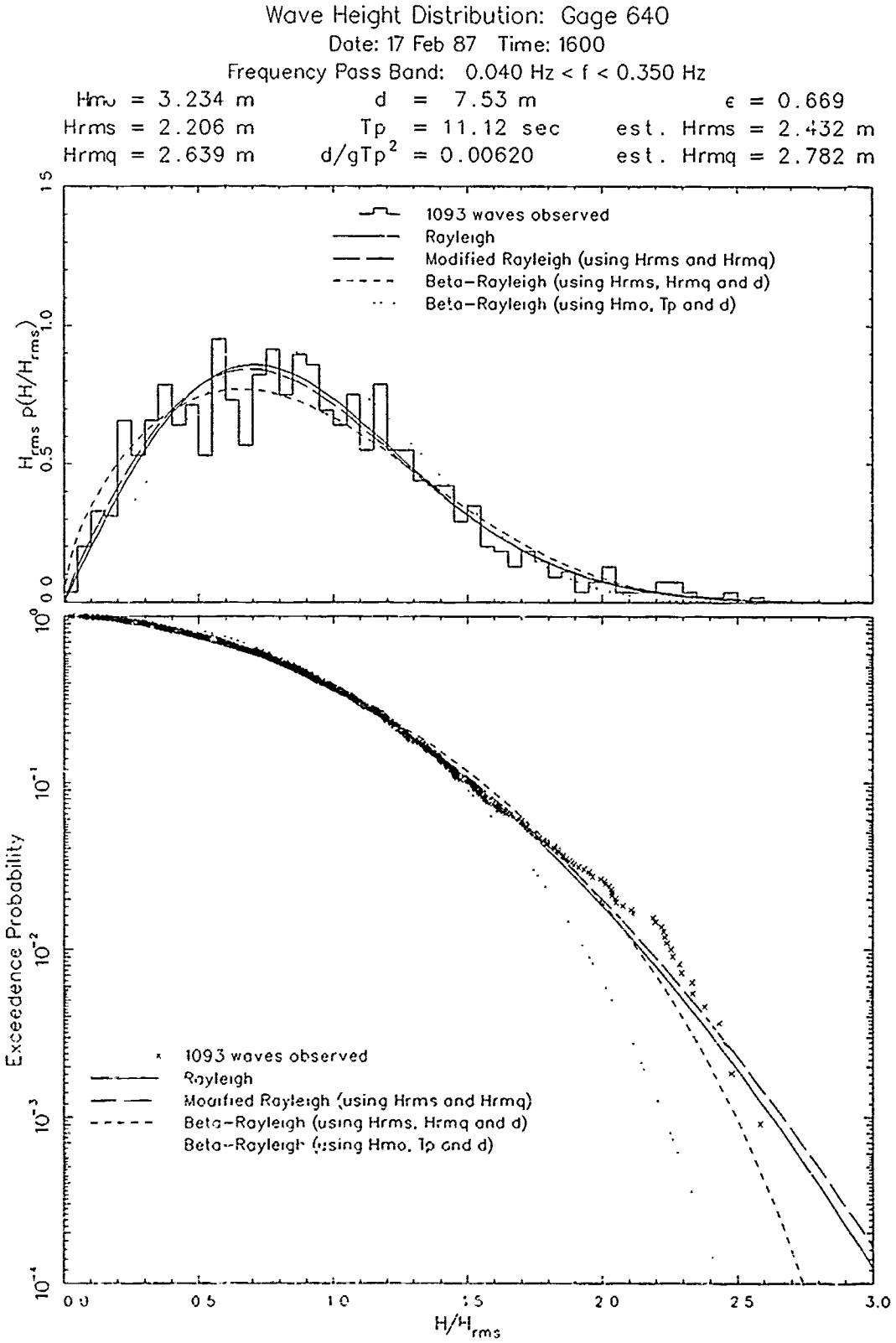

Figure C5. Case 7

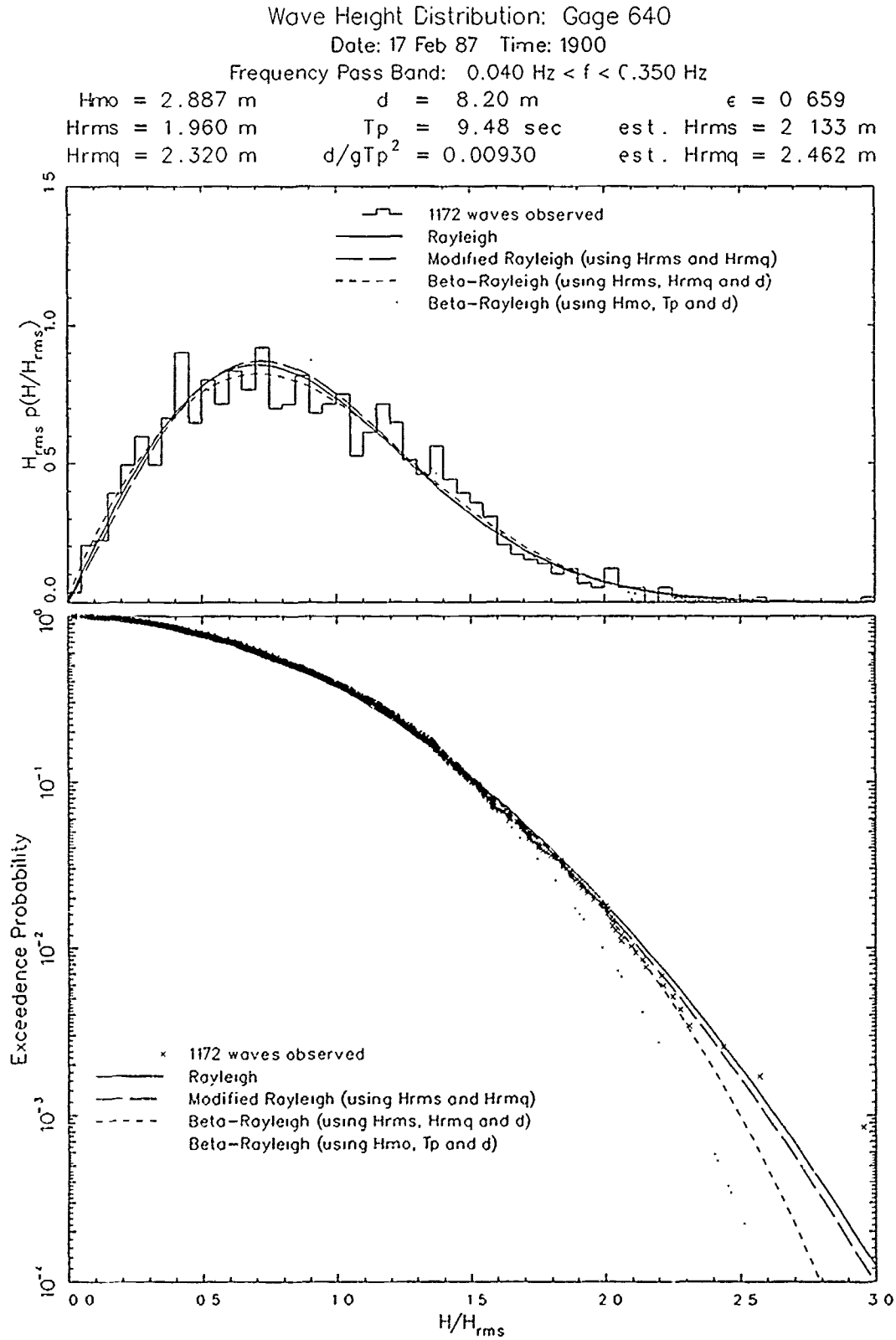

Figure C7. Case 8

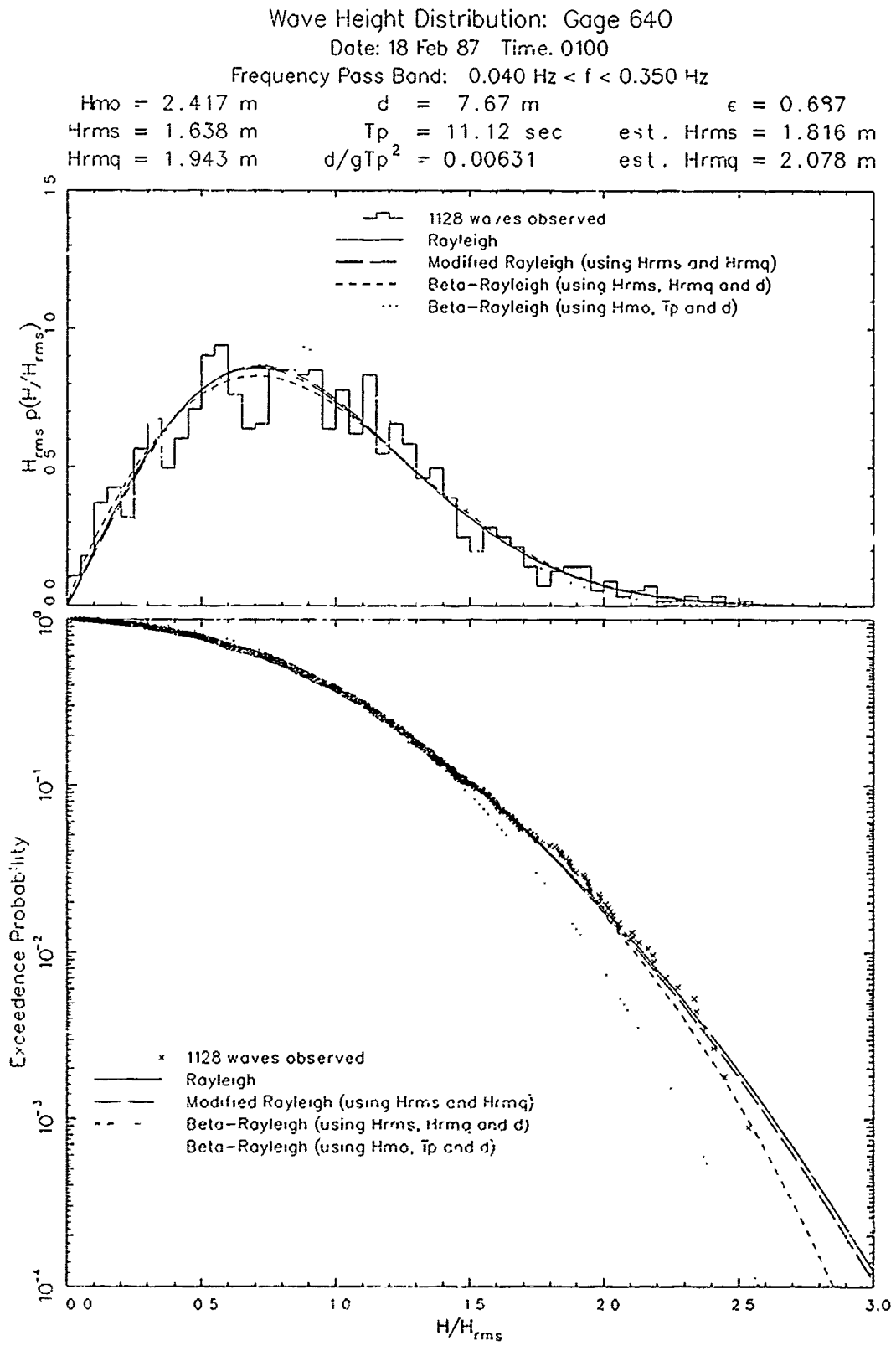

Figure C8. Case 9

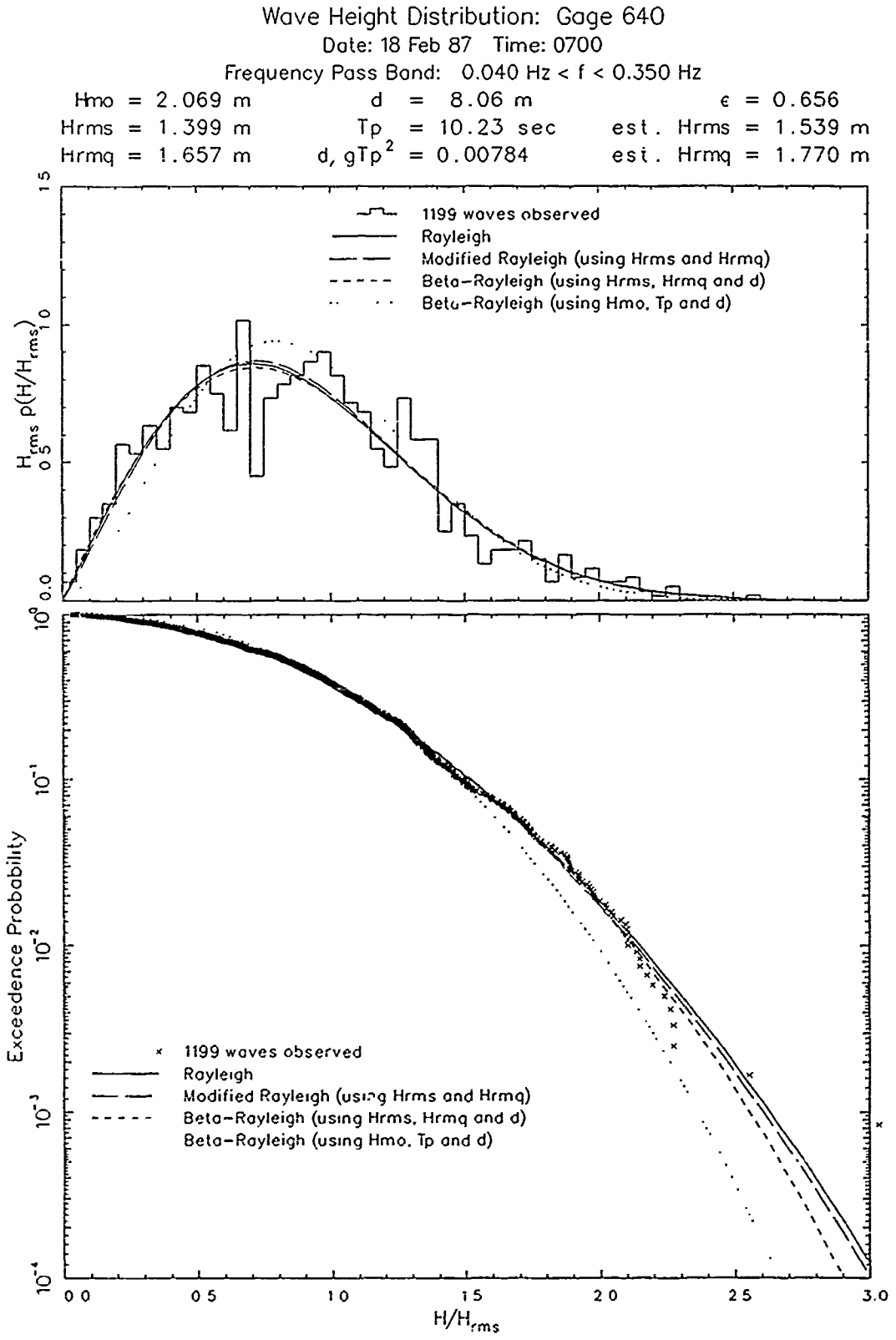

Figure C9. Case 10

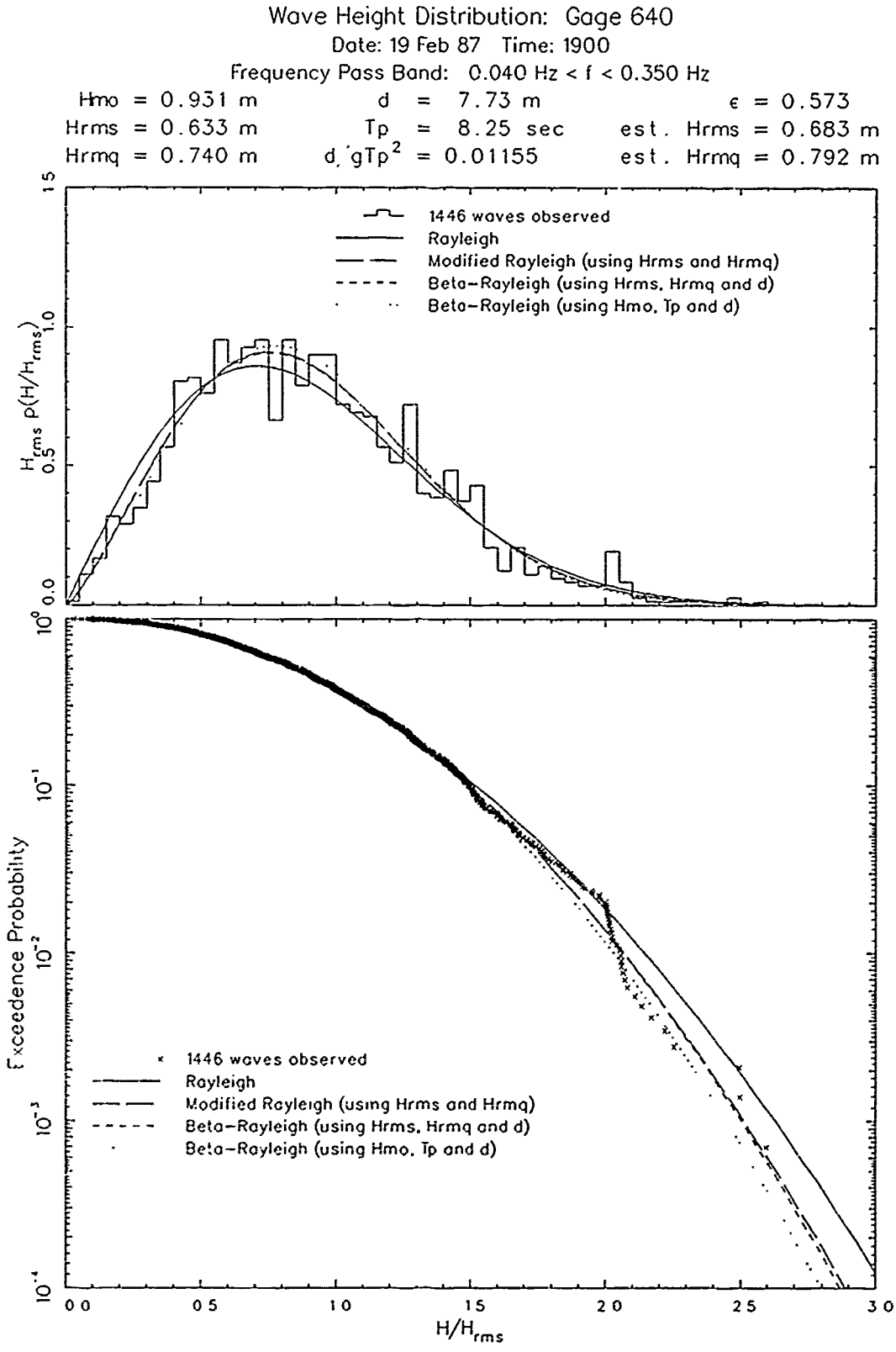

Figure C10. Case 11

APPENDIX D

WAVE HEIGHT AVERAGE DISTRIBUTIONS FOR TEST CASES 2 THROUGH 11

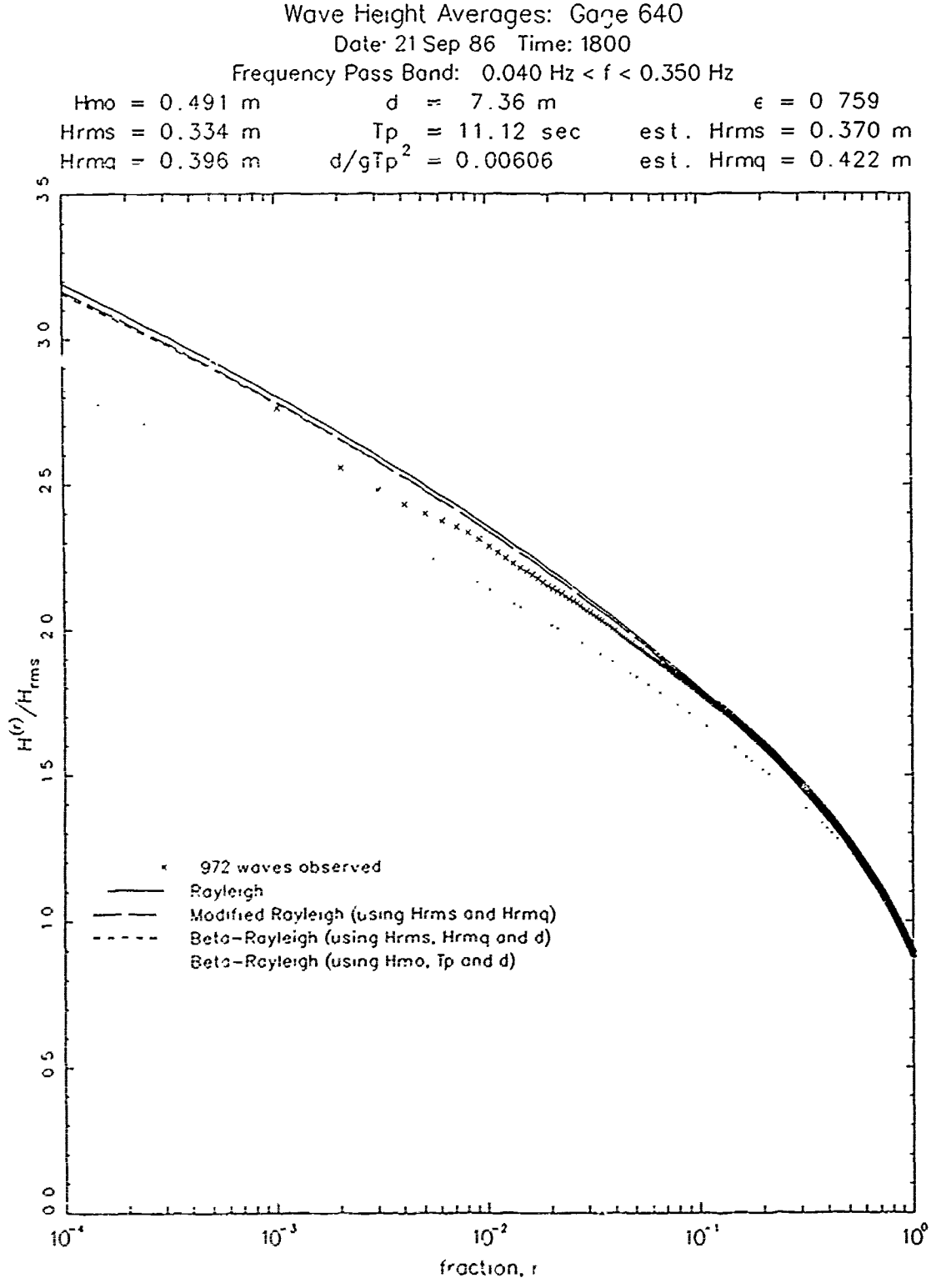

Figure D1. Case 2

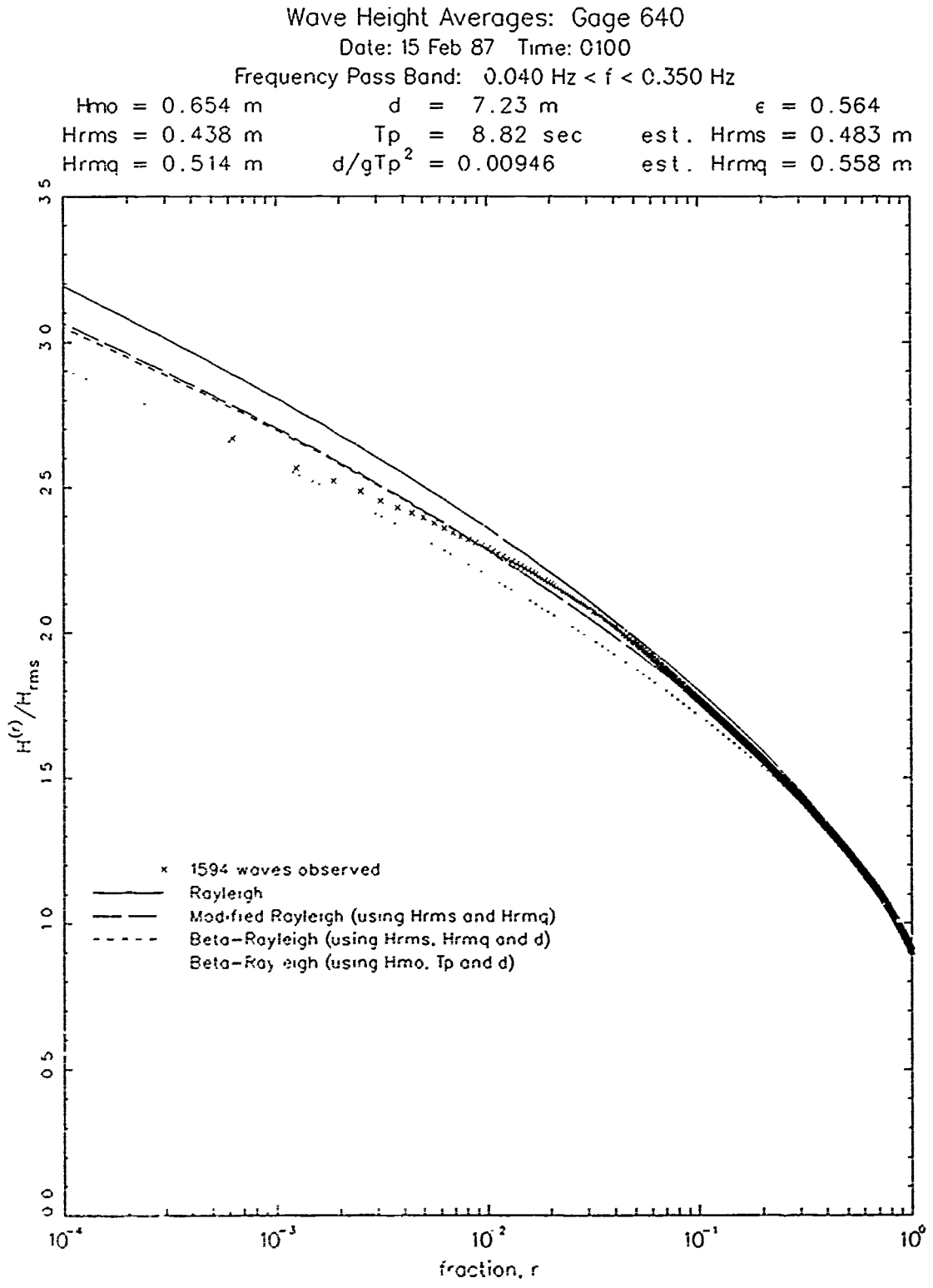

Figure D2. Case 3

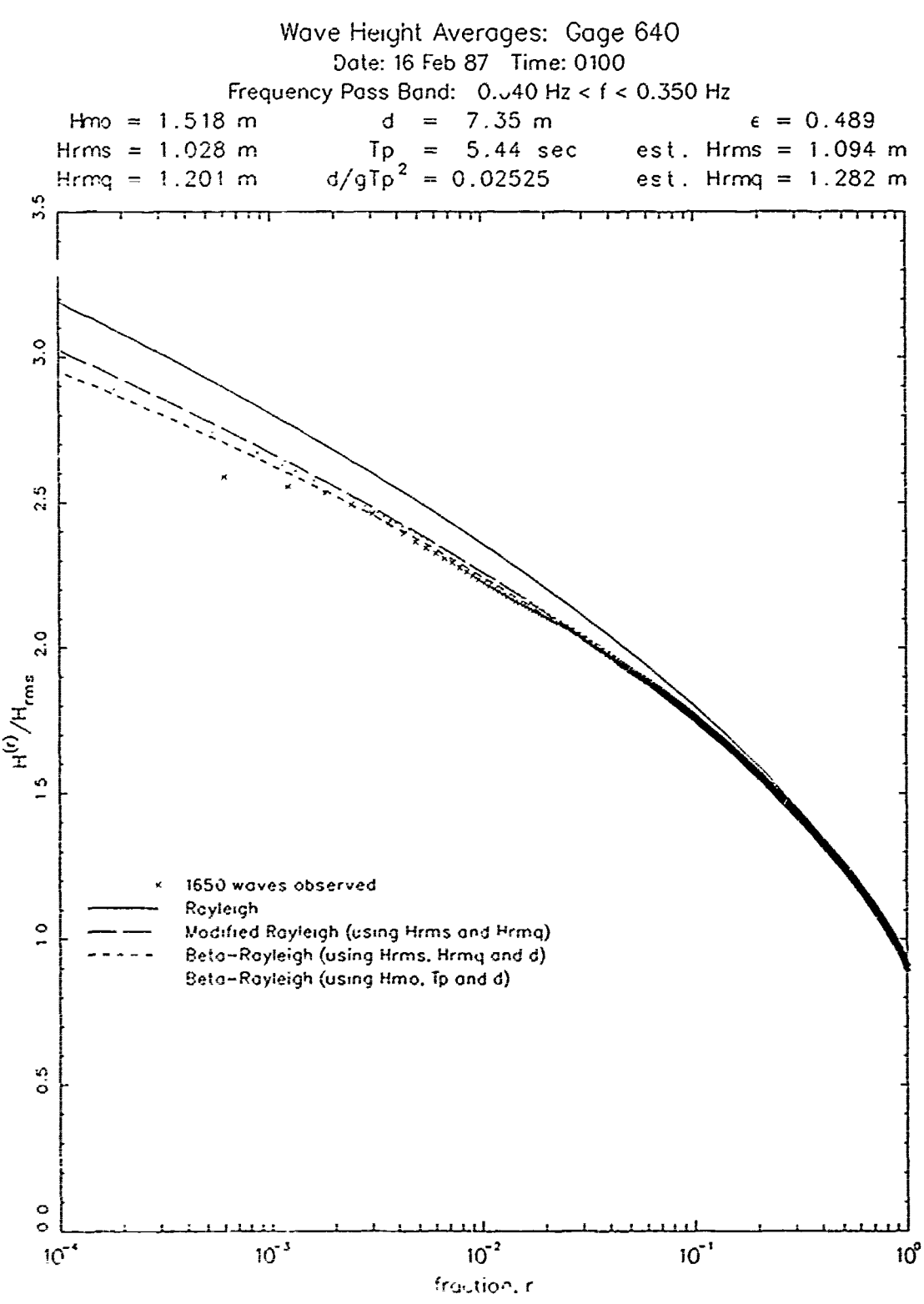

Figure D3. Case 4

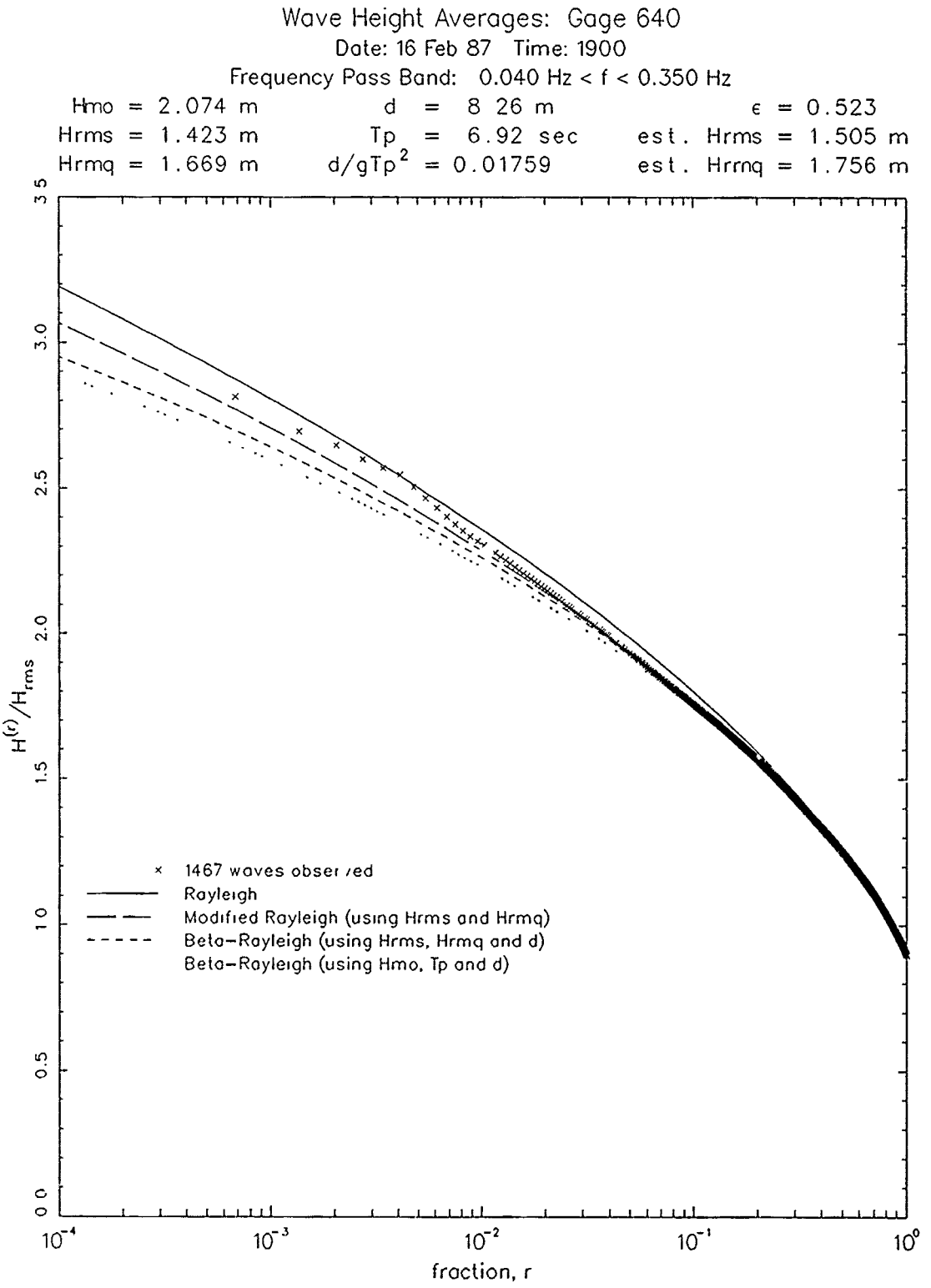

Figure D4. Case 5

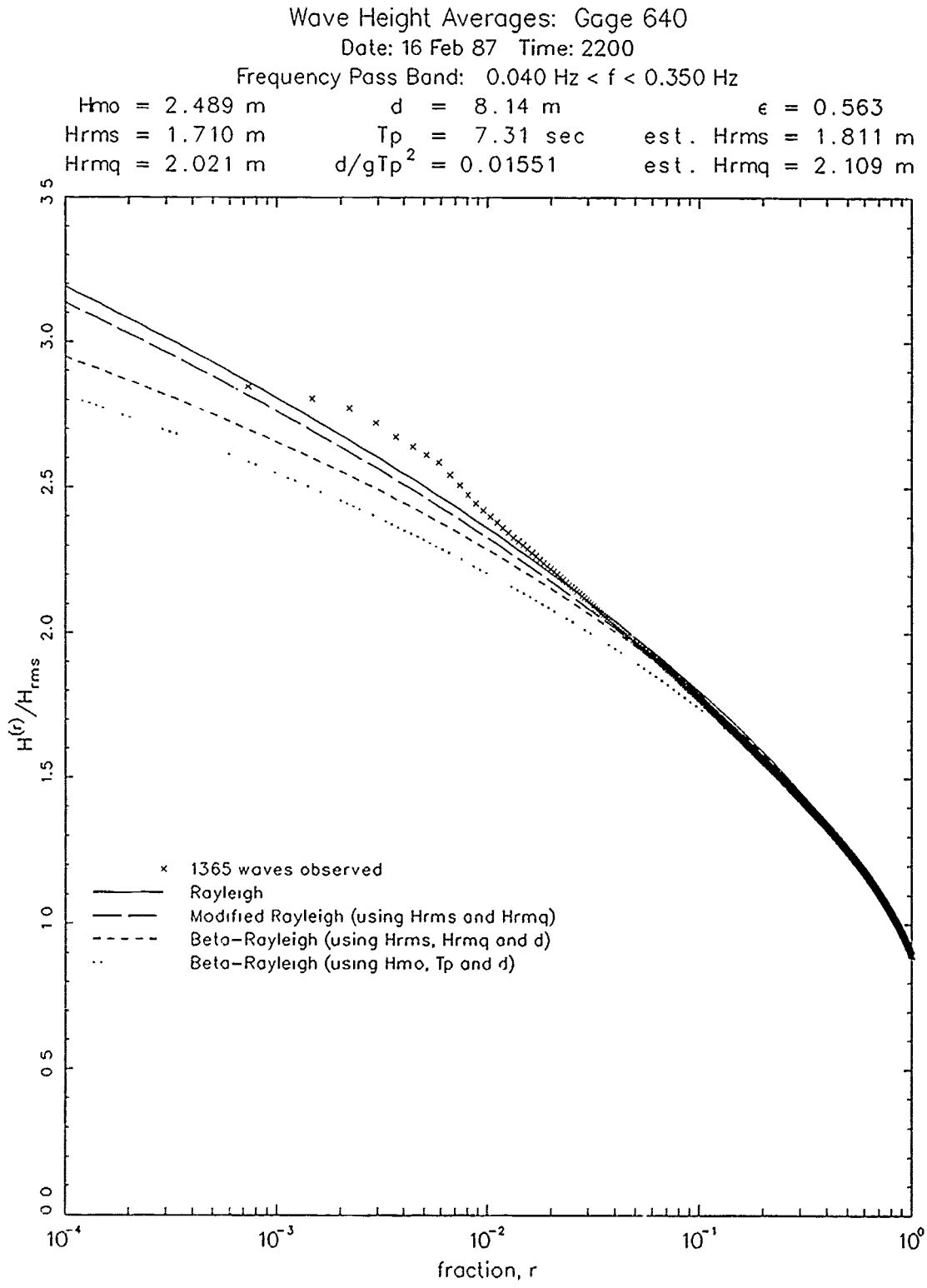

Figure D5. Case 6

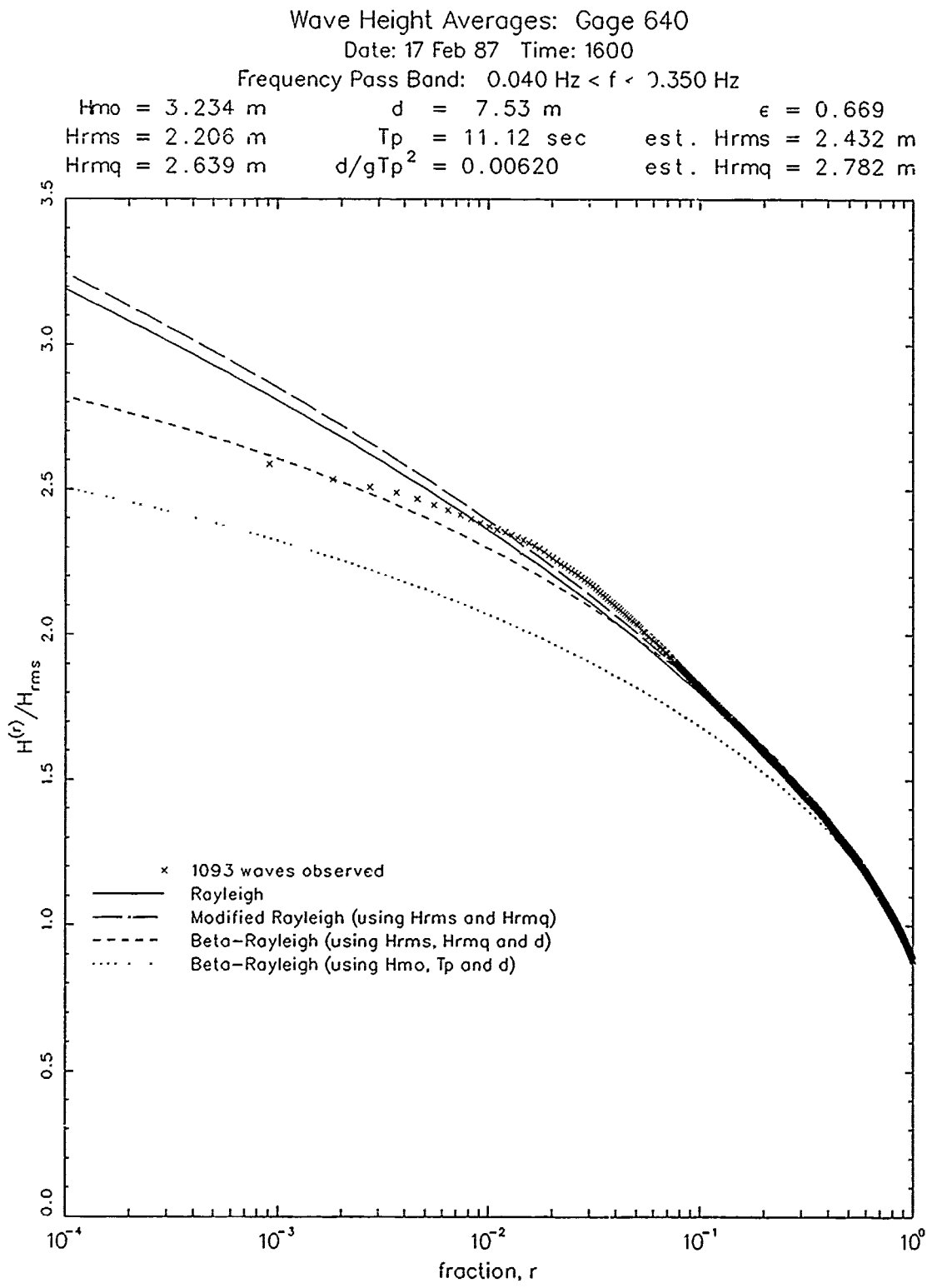

Figure D6. Case 7

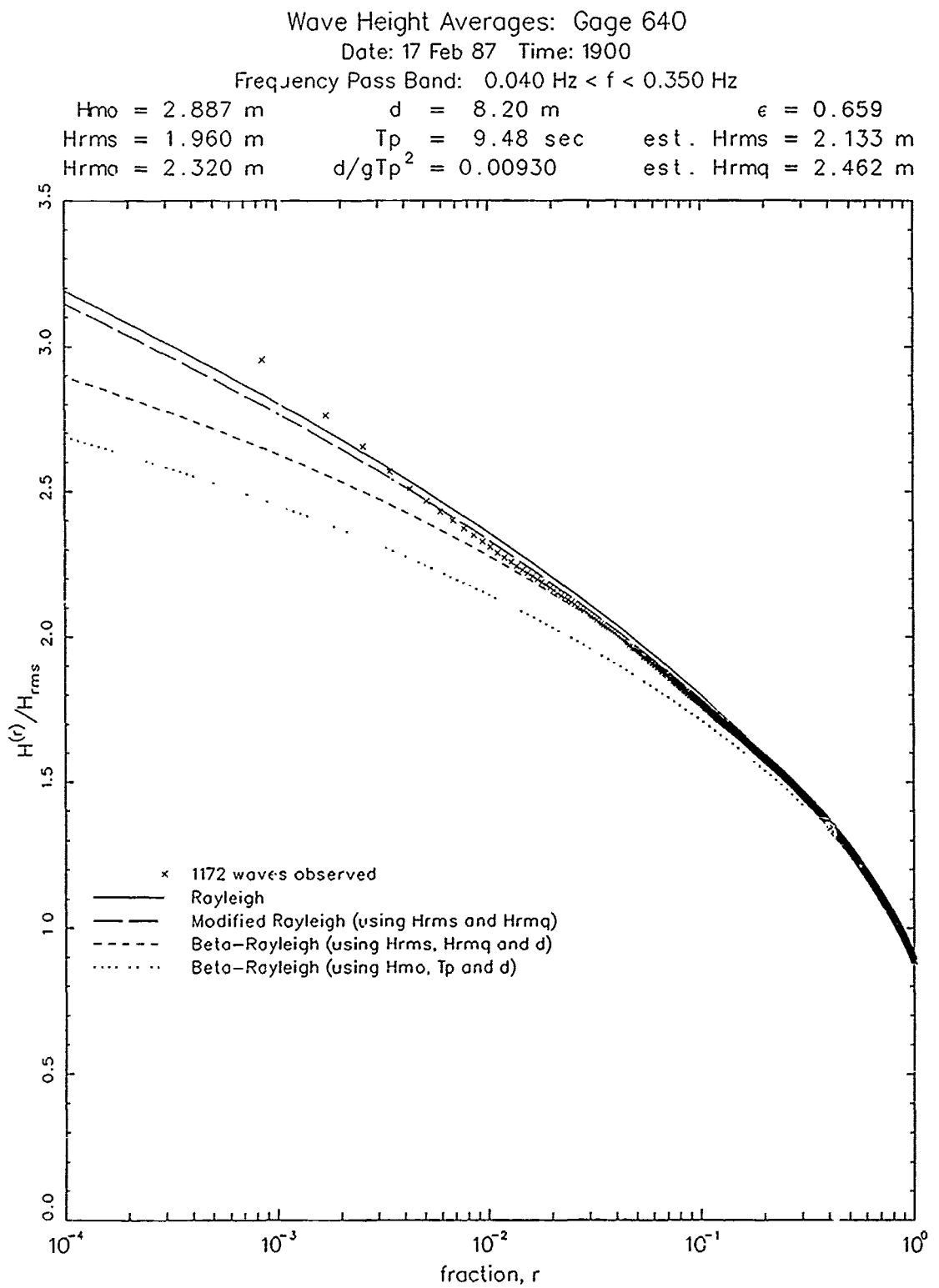

Figure D7. Case 8

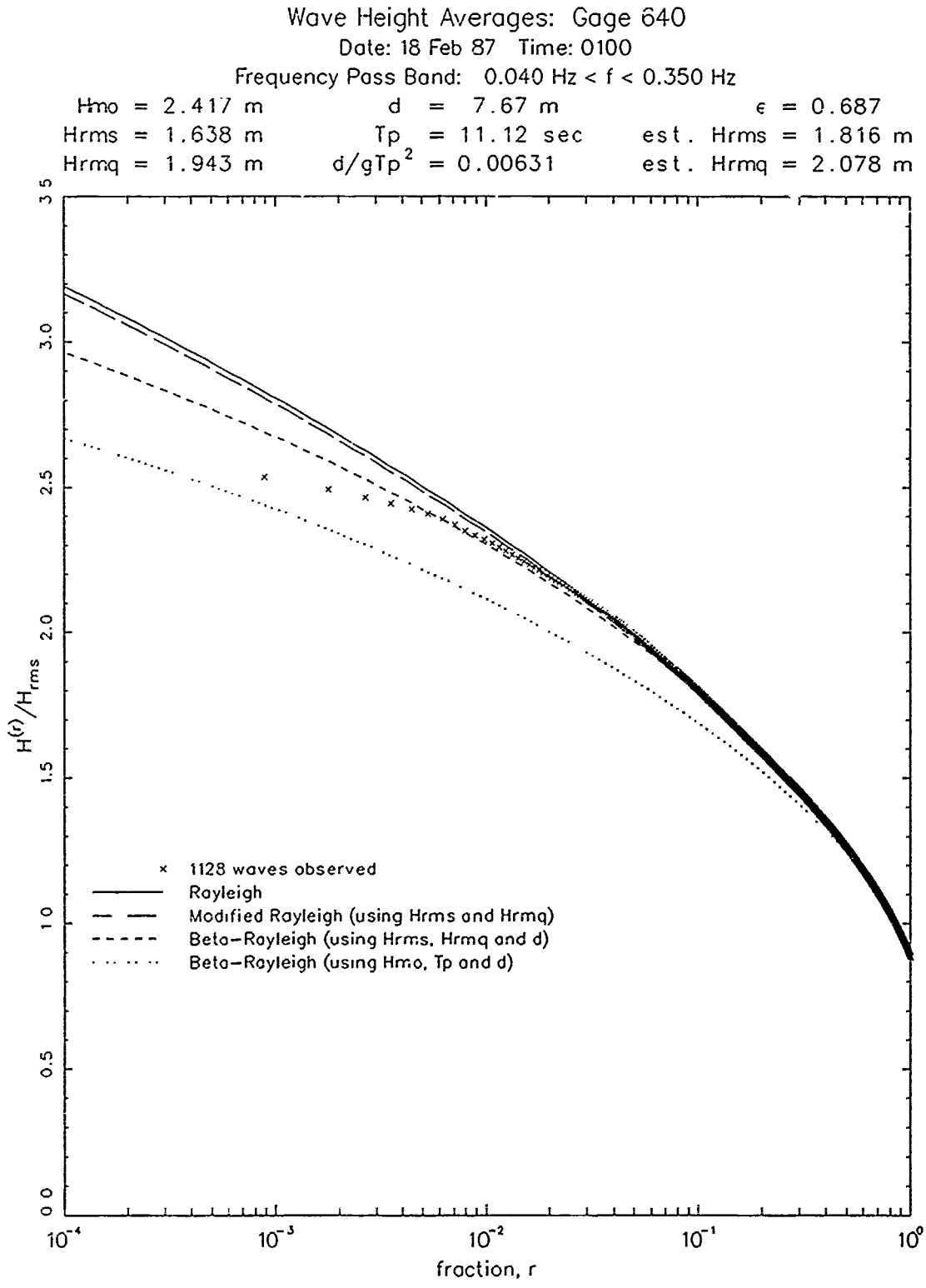

Figure D8. Case 9

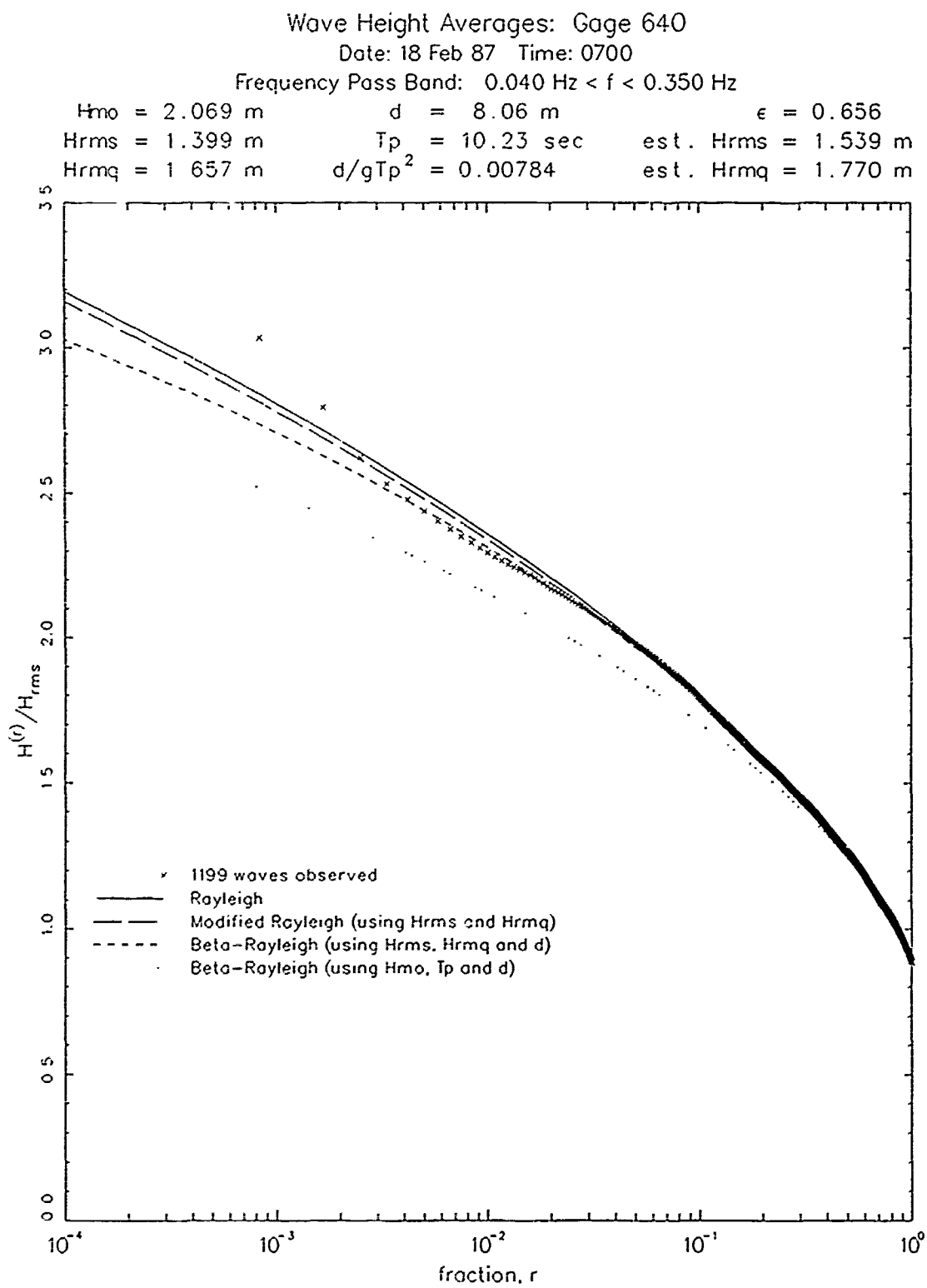

Figure D9. Case 10

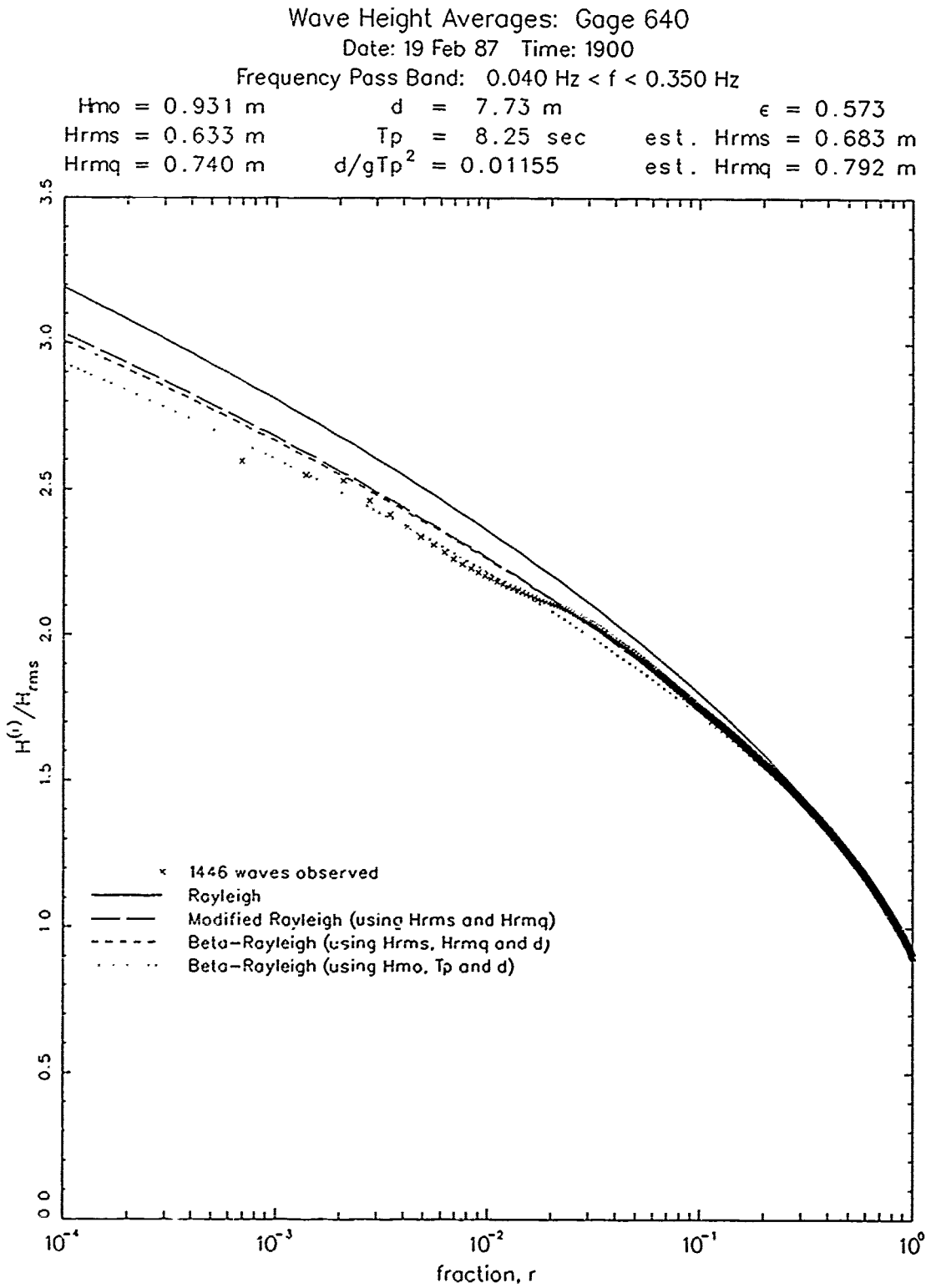

Figure D10. Case 11

APPENDIX E: NOTATION

APPENDIX E: NOTATION

a	Parameter of Beta-Rayleigh pdf
b	Parameter of Beta-Rayleigh pdf
d	Water depth
df	Infinitesimal increment of frequency
dH	Infinitesimal increment of wave height
$E[\ ]$	Expected value of quantity in [ ]
f	Frequency
f_p	Spectral peak frequency
$f_{p,IFS}$	Peak frequency of the integrated frequency spectrum
f_1 , f_2	Specific frequencies
g	Gravitational acceleration
H	Wave height
H_{max}	Maximum wave height
H_{mo}	Spectrum-based characteristic wave height
H_n	The n^{th} wave height in a set
$H^{(r)}$	Average of highest fraction r of all wave heights
H_{rmq}	Root-mean-quad wave height
$H_{rmq,e}$	Estimated root-mean-quad wave height
H_{rms}	Root-mean-square wave height
$H_{rms,e}$	Estimated root-mean-square wave height
H_1 , H_2	Specific wave heights
$H^{(1/3)}$	Average of highest one-third of all wave heights
$H_{1/3}$	Alternate notation for $H^{(1/3)}$
$\hat{H}$	Randomly chosen wave height
i	Summing index

j	Index of an observed wave height
J_u	Number of wave he ghts in accumulation bin u
m_n	The n^{th} moment of a frequency spectrum
m_0	Zeroth moment of frequency spectrum
m_2	Second moment of frequency spectrum
m_4	Fourth moment of frequency spectrum
n	Index of a set of discrete wave heights
N	Number of observed waves in a record
p	Probability density function
pdf	Probability density function
p_{BR}	Beta-Rayleigh probability density function
p_{max}	Probability density function of maximum wave height
p_{MR}	Modified Rayleigh probability density function
p_R	Rayleigh probability density function
P	Cumulative probability function
P_R	Rayleigh cumulative probability function
Prob[ ]	Probability that expression in [ ] is true
Q	Exceedence probability
Q_d	Exceedence probability estimated from d. ta
Q_R	Rayleigh exceedence probability
r	Fraction between zero and one
r_j	Fraction of highest observed wave of index j
RMS	Root-mean-square
S	Sea-surface variance spectral density
T_p	Spectral peak period
$T_{p,IFS}$	Peak period of integrated frequency spectrum
u	Bin index for histogram of wave heights

x	Dummy integration variable
α	Parameter of modified Rayleigh pdf
Γ	Gamma function
ΔH	Discrete increment of wave height
$\Delta\theta_{IDS}$	Directional spread parameter of integrated direction spectrum
ϵ	Frequency spectral width parameter
$\sigma[\ ]$	Standard deviation of quantity in [ ]
$\sigma^2[\ ]$	Variance of quantity in [ ]
θ	Wave direction
$\vartheta_{p,IDS}$	Peak direction of the integrated direction spectrum